Design, Optimization and Testing of Valves for Digital Displacement Machines

Nørgård, Christian

DOI (link to publication from Publisher):
10.5278/vbn.phd.eng.00013

Publication date:
2017

Document Version
Publisher's PDF, also known as Version of record

DESIGN, OPTIMIZATION AND TESTING OF VALVES FOR DIGITAL DISPLACEMENT MACHINES

BY
CHRISTIAN NØRGÅRD

DISSERTATION SUBMITTED 2017

AALBORG UNIVERSITY
DENMARK

Design, Optimization and Testing of Valves for Digital Displacement Machines

Ph.D. Dissertation

Christian Nørgård

Dissertation submitted October 17, 2017

Dissertation submitted: October 17, 2017

PhD supervisor: Associate Prof. Michael M. Bech,
Aalborg University, Aalborg, Denmark

PhD committee: Lektor, Peter Omand Rasmussen (Chairman)
Aalborg University

Adjunct Professor, Matti Olavi Linjama
Tampere University of Technology

Vice Business Area Manager Drives, Siegfried Silber
LCM GmbH

PhD Series: Faculty of Engineering and Science, Aalborg University

Department: Department of Energy Technology

ISSN (online): 2446-1636
ISBN (online): 978-87-7210-090-6

Published by:
Aalborg University Press
Skjernvej 4A, 2nd floor
DK – 9220 Aalborg Ø
Phone: +45 99407140
aauf@forlag.aau.dk
forlag.aau.dk

Printed in Denmark by Rosendahls, 2017

Preface

This dissertation has been submitted to the Faculty of Engineering and Science at Aalborg University in partial fulfillment of the requirements for the degree of Doctor of Philosophy and is submitted in the paper collection format. This work was carried out as part of the HyDrive research project which is funded by Innovation Fund Denmark.

I would like to extend my sincerest gratitude to Ph.D. Daniel Beck Roemer for countless, long and inspiring discussions on different aspects of digital pumps/motors.

I would also like to thank Professor Rudolf Schiedl for making my interesting research visit with him possible and for sharing some of his endless insights on engineering and life. Likewise, I would like to thank Bernd Winkler and his team at Linz Center of Mechatronics for good times and for their support and interest.

I also greatly appreciate the countless of motivating, educational and inspiring daily discussion with my supervisor Michael M. Bech. Thank you for always being involved and supporting me in this journey, I could not have asked for more.

Also, my sincerest gratitude goes to Jeppe H. Christensen for spending countless of fun and motivating (and sometimes demotivating) hours with me in the laboratory working on building test set-ups and testing valve prototypes. A special thanks also goes to the workshop staff at the Department of Energy Technology for good inputs during prototyping. Finally, I want to thank my family for their everlasting patience and support.

Christian Nørgård
Aalborg University, October 17, 2017

List of Publications

This dissertation has been submitted for assessment in partial fulfillment of the Ph.D. degree. The dissertation is based on the submitted or published scientific papers below. Parts of the papers are used directly or indirectly in the extended summary of the dissertation and referred to as e.g. Paper **A**. Co-author statements have been made available to the assessment committee through The Doctoral School of Engineering and Science. The main body of this dissertation is based on the contents of the following papers:

A **Christian Noergaard**, Daniel B. Roemer, Michael M. Bech and Torben O. Andersen, "Experimental validation of mathematical framework for fast switching valves used in digital hydraulic machines". In *Proc. of The 2015 ASME/Bath Symp. on Fluid Power and Motion Control*, Chicago, US, ISBN: 978-0-7918-5723-6, DOI: 10.1115/FPMC2015-9612.

B **Christian Noergaard**, Michael M. Bech, Daniel B. Roemer, and Lasse Schmidt,"Experimental Validation of Modelled Fluid Forces in Fast Switching Hydraulic On/Off Valves", In *Proc. of The 2015 International Conference on Fluid Power and Mechatronics*, Harbin, China, pp. 68-73, ISBN: 978-0-7918-5723-6, DOI: 10.1109/FPM.2015.7337087.

C **Christian Noergaard**, Daniel B. Roemer, Michael M. Bech, "Modelling of Moving Coil Actuators in Fast Switching Valves Suitable for Digital Hydraulic Machines". In *Proc. of The 2015 ASME/Bath Symp. on Fluid Power and Motion Control* , Chicago, US, ISBN: 978-0-7918-5723-6, DOI: 10.1115/FPMC2015-9593.

D **Christian Noergaard**, Michael M. Bech, Daniel B. Roemer and Henrik C. Pedersen, "Optimization of Moving Coil Actuators for Digital Displacement Machines". In *Proc. of Eighth Workshop on Digital Fluid Power*, Tampere, Finland, 2016, pp. 39-54, ISBN: 978-952-15-3757-8.

E **Christian Noergaard**, Lasse Schmidt and Michael M. Bech, "A Simple and Robust Sliding Mode Velocity Observer for Moving Coil Actuators in Digital Hydraulic Valves". In *Proc. of The 2016 ASME/Bath Symp. on Fluid Power and Motion Control*, Bath, UK, ISBN: 978-0-7918-5006-0, DOI: 10.1115/FPMC2016-1789.

F **Christian Noergaard**, Michael M. Bech and Daniel B. Roemer, "A Motion Observer With On-Line Parameter Estimation for Moving-Coil Based Digital Valves in Digital Displacement Machines". In *Proc. of The Ninth Fluid Power Net International Ph.D. Symp. on Fluid Power*, Florianópolis, Brazil, 2016, ISBN: 978-0-7918-5047-3, DOI: 10.1115/FPNI2016-1543.

G **Christian Noergaard**, Michael M. Bech, Torben O. Andersen and Jeppe H. Christensen, "Flow Characteristics and Sizing of Annular Seat Valves for Digital Displacement Machines", accepted for publication in *The Modeling, Identification and Control Journal*.

H **Christian Noergaard**, Jeppe H. Christensen, Michael M. Bech, Anders H. Hansen and Torben O. Andersen, "Test Rig for Valves of Digital Displacement Machines". In *Proc. of Ninth Workshop on Digital Fluid Power*, Aalborg, Denmark, 2017.

I **Christian Noergaard**, Jeppe H. Christensen, Michael M. Bech, and Torben O. Andersen, "Modeling and Validation of Moving Coil Actuated Valve for Digital Displacement Machines". Submitted Oct. 12, 2017 to *IEEE Transactions on Industrial Electronics*. Status: under review.

J Esben L. Madsen, Janus M. T. Joergensen, **Christian Noergaard** and Michael M. Bech, "Design Optimization of Moving Magnet Actuated Valves for Digital Displacement Machines". In *Proc. of The 2017 ASME/Bath Symp. on Fluid Power and Motion Control* , Sarasota, US.

K **Christian Noergaard**, Esben L. Madsen, Janus M. T. Joergensen and Michael M. Bech, "Test of a Novel Moving Magnet Actuated Seat Valve for Digital Displacement Fluid Power Machines". Submitted Aug. 30, 2017 to *IEEE Transactions on Mechatronics*. Status: under review.

In addition to the papers above, the following have also been published during the Ph.D. period:

- Daniel B. Roemer, **Christian Noergaard**, Michael M. Bech and Per Johansen, "Valve and Manifold Considerations for Digital Hydraulic Machines". In P*roc. of Eighth Workshop on Digital Fluid Power*, 2016, Tampere, Finland, pp. 213-227, ISBN: 978-952-15-3757-8.
- Michael M. Bech, **Christian Noergaard** and Saku Kukkonen, "A Global Multiobjective Optimization Tool for Optimal Design of Digital Fluid Power Components". In *Proc. of the 42nd Annual Conference of IEEE Industrial Electronics Society*, Florence, Italy, pp. 475-481, ISBN: 978-1-5090-3475-8.
- Niels C. Bender, **Christian Noergaard** and Henrik C. Pedersen, "Experimental Validation of Flow Force Models for Fast Switching Valves". In Proc. of *The 2017 ASME/Bath Symp. on Fluid Power and Motion Control*, Sarasota, US.

Abstract

The present thesis deals with design, modeling and testing of novel switching valves for an emerging class of variable displacement fluid power machines i.e. digital pump/motors also referred to as Digital Displacement Machines (DDMs)[1]. DDMs use several parallel configured pistons, each connected to a high- and low-pressure manifold through two electronically controlled switching valves. By controlling the switching sequence of the valves, each piston may be reconfigured on a stroke by stroke basis to perform motoring or pumping strokes, or the cylinder may be disabled by keeping the low-pressure valve open throughout the cycle also referred to as idling. This enables an effective method for controlling the displacement which may lead to a breakthrough in the achievable efficiency of variable displacement fluid power machines, especially at low displacement ratios.

Combining the improvement of efficiency with well-known benefits of hydraulics, such as high power density, robust operation and rugged design, digital pumps/motors are attractive candidates for several applications incl. hybrid vehicles, wind turbines, wave energy converters, mobile hydraulics etc. Depending on the application, different requirements exist to the electronically controlled valves. The present work focuses solely on high-speed applications where fast switching capability of the valves is essential.

The switching valves of digital pump/motors are key components and the nature of DDM operation set tough requirements to the valves, especially for high-speed applications. They must be fast switching to enable accurate and efficient switching, they must have large flow areas to ensure low flow losses, they must be electrically efficient and finally, they must endure billions of switching cycles in several of the potential applications. The objectives being multiple and conflicting make designing these valves relatively difficult and on-the-shelf components fully meeting all requirements do not yet exist.

[1]Digital Displacement® Technology is a registered trademark. In this thesis, the terms, digital displacement machines, digital pump/motors and digital hydraulic machines are used interchangeably.

The present research primarily revolves about two developed prototype valves for DDMs. Both prototypes use actuator topologies relatively new to hydraulics and certainly to the field of digital pump/motors. A model based optimization method is proposed for deriving a moving coil actuator for digital pump/motor valves using a multi-objective optimization algorithm. Evaluation of possible actuator candidates is carried out using several mathematical models representing a wide range of physical phenomena, to facilitate simulating a single digital displacement (DD) cylinder in operation. For each candidate, static axi-symmetric electro-magnetic finite-element-analysis (FEA) is initially carried out. Based on the results, parameters are derived for a fast executable lumped model describing the electro-magnetic dynamics of the moving coil actuator. The valve pressure drop and the induced axial forces acting on the moving valve member as a function of flow are modeled using lumped models with the coefficients derived from computational-fluid-dynamics (CFD) analysis. The proposed optimization method is applied to a 50 CC cylinder operating at 800 RPM and is shown capable of deriving actuators ensuring fast and efficient switching of the valves.

Based on the most suited candidate, valve prototypes are designed, built and rigorously tested to verify the simulated valve performance. The mathematical models used for virtual prototyping are compared against a series of measurements generally proving the models sufficiently accurate. Measurements show the valve to have switching times of 2-3.5 ms and a pressure drop of approximately 0.5 bar at the peak flow rate of 125 l/min. A test rig is built to test the valves in DD operation and to establish proof-of concept for novel switching valve and actuator concepts. Using the test rig, DD motoring and pumping operation at 100 bar and 800 RPM is accomplished. During operation, the valve related losses are approximately 1% of the output power demonstrating the developed prototype valve is a promising candidate for efficient DD operation.

Due to the valves of DDMs being compact and integrated units, implementation of direct methods for measuring the displacement of the moving member is impractical. To this end, methods for indirectly observing the valve movement based on the measurements of coil current and voltage waveforms, are presented. One method is proposed for moving coil actuator based valves in combination with an actuator parameter tracking scheme that gives both accurate tracking of the movement and important information of the health of the valve.

In collaboration with students, a moving magnet actuated valve have also been developed using an optimization method much similar to the moving coil actuator. Likewise, a valve prototype is designed, built and tested. Mea-

surements show the valve to have switching times around 6 ms and pressure drops of only 0.2-0.3 bar at the peak flow rate of 125 l/min.

In summary, the proposed model based optimization method is demonstrated capable of deriving optimal candidate valve designs satisfying the strict performance requirements set forth by DDM applications. In particular, the research documented in this dissertation concludes that valves actuated by moving coil and moving magnet principles are possible candidates for high-speed DDMs. Future research regarding e.g. wear and reliability will be of fundamental importance in order to mature the proposed valve concepts further.

Abstract

Resumé

Den foreliggende afhandling handler om design, modellering og afprøvning af ventiler til en ny klasse af hydrauliske maskiner med variabel fortrængning. Disse maskiner bliver oftest omtalt som *Digital Displacement Machnies* (DDMs). En DDM bruger flere parallelt konfigurerede stempler, der hver er forbundet til en højtryks- og lavtryksforsyning gennem to elektronisk styrede ventiler. Ved at styre ventilens skifte sekvens kan hvert stempel konfigureres, slag-for-slag, til at udføre motor- eller pumpeslag, eller cylinderen kan deaktiveres ved at holde lavtryksventilen åben igennem hele operationscyklussen, også omtalt som *idling*. Dette muliggør en effektiv metode til styring af olie fortrængningen, som kan føre til et gennembrud i den hidtil opnåelige effektivitet med konventionelle hydraulik maskiner, særligt ved lav last.

Forbedringen i virkningsgrad tilsammen med de øvrige fordele ved hydraulik, såsom høj effektdensitet, robust drift og design, gør digitale pumper/motorer attraktive kandidater til flere applikationer, blandt andet hybridbiler, vindmøller, bølgeenergiomformere og mobilhydraulik. Afhængigt af applikationen findes der forskellige krav til de elektronisk styrede ventiler. Dette arbejde fokuserer udelukkende på højhastighedsapplikationer, hvor det er afgørende at ventilerne er hurtigt skiftende. Ventilerne til digitale pumper/motorer er nøglekomponenter, og naturen af driften stiller strenge krav til ventilerne, særligt til højhastigheds applikationer. De skal være hurtigt skiftende for at muliggøre nøjagtig og effektiv omskiftning, de skal have store strømningsområder for at sikre lave strømningstab, de skal være elektrisk effektive, og endelig skal de kunne udholde milliarder af skifte cyklusser for flere af de foreslåede applikationer. Målene er flere og modstridende, hvilket gør det relativt vanskeligt at designe disse ventiler, og kommercielt tilgængelige komponenter, der fuldt ud opfylder alle krav, eksisterer endnu ikke.

Den nuværende forskning drejer sig primært om to udviklede prototypeventiler til DDMs. Begge prototyper er baseret på aktuator topologier, der er relativt nye i forhold til hydraulik og specielt i forhold til digitale pumpe/motorer. I denne afhandling foreslås en optimeringsmetode til udled-

ning af en bevægelig-spole aktuator til DDM ventiler. Evaluering af mulige design kandidater udføres ved hjælp af flere matematiske modeller, der repræsenterer en lang række fysiske fænomener, for at kunne simulere en enkelt cylinder i drift. For hver design kandidat udføres statisk elektromagnetisk finite-element-analyse (FEA) først. Baseret på FEA resultaterne er parametre afledt til brug i en hurtig eksekverbar analytisk model, der beskriver den elektromagnetiske dynamik i den bevægelige-spole aktuator. Ventilens tryksfald og de inducerede aksiale kræfter, som påvirker det bevægelige ventilelement pga. oile gennemstrømning, modelleres ved anvendelse af analytiske modeller (med koefficienter baseret på numerisk fluiddynamisk simulering). Den foreslåede optimeringsmetode anvendes på en 50 CC cylinder, der arbejder ved 800 slag/min., og er vist til at udlede aktuatorer, der sikrer hurtig og effektiv omskiftning af ventilerne.

På basis af den mest velegnede design kandidat, er ventilprototyper konstrueret, bygget og testet for at verificere den simulerede ydeevne og opførsel. Målinger viser, at ventilen har skiftetider på 2-3,5 ms, et trykfald på ca. 0,5 bar ved maksimal olie flow på 125 l/min. En testopstilling er bygget til at teste ventilerne i drift og demonstrere ventilenes egenskaber. Ved brug af testopstillingen demonstreres digital-motor og pumpe operationscyklusser ved 100 bar og 800 omdr./min. Under drift udgør tab relateret til ventilen ca. 1% af udgangseffekten.

Fordi ventilerne i DDM er kompakte of integrerede enheder, er det ofte højest upraktisk at implementere direkte metoder til måling af forskydningen af det bevægelige element. Til dette formål er metoder til indirekte at observere forskydningen baseret på målinger af aktuatorspolens strøm og spænding foreslået. En metode foreslås til DDM ventiler baseret på bevægelig-spole aktuatorer, i kombination med en aktuator parameter estimationsmetode, som muliggør både nøjagtig sporing af bevægelsen og vigtige oplysninger om ventilens tilstand. De foreslåede metoder testes ved simulering og ved brug af målte signaler.

I samarbejde med studerende, er en bevægelig-magnet aktueret ventil også blevet udviklet ved hjælp af en optimeringsmetode, der minder meget om metoden benyttet for den bevægelig-spole aktuator. På samme måde er en ventilprototype designet, bygget og testet. Målinger viser, at ventilen har skiftetider på 6 ms og trykfald på kun 0,2-0,3 bar ved maksimal strømningshastighed på 125 l/min.

Sammenfattende er et modelbaseret optimeringsproblem formuleret til udledning af optimale ventil og aktuator design, der opfylder de strenge krav til ydeevne, der er gældende ved DDM applikationer. Derudover er det vist, at ventiler aktiveret ved bevægelig-spole- og bevægelig-magnet-principper er mulige kandidater til hurtiggående digitale hydrauliske fortrængnings mask-

iner. I den videre forskning vil det være af afgørende betydning at undersøge for f.eks. slid og pålidelighed for de foreslåede ventilkoncepter for at forbedre disse yderligere.

Contents

Part I

Extended Summary

Chapter 1

Introduction

The thesis' main objective is exploring, designing and testing of novel valve concepts for an emerging class of variable displacement fluid power machinery, namely Digital Displacement Machines (DDMs), often also referred to as digital hydraulic pumps/motors. The potential of such a machine is great as it enables a breakthrough in the previously achievable efficiency of fluid power machinery. The applications are many and are still being explored. This chapter gives an introduction to the working principles of a Digital Displacement Machine, an overview of its development and valve candidates. Finally, the research objectives and the main contributions are outlined.

1.1 Fundamentals of Digital Displacement Machines

This section gives a brief introduction to the fundamental principles and advantages of DDMs. As most common conventional variable displacement fluid power machines operating at high pressures, DDMs employ reciprocating pistons connected to a main shaft through an eccentric, crankshaft or similar. The fundamental difference between DDMs and conventional fluid power machinery is that the connections to the high- and low-pressure manifolds are controlled by electronic valves opposed to being defined by the port-plate or camshaft geometries. This enables adjusting the timing of the valve switchings to obtain the maximum power output and efficiency under all operating conditions and more importantly, it enables a new, efficient and novel method for varying the machine displacement. The hydraulic layout of a DDM is illustrated in Figure 1.1.

By controlling the low-pressure valve (LPV) and high-pressure valve (HPV) accordingly to the motion of the piston each cylinder may be reconfigured — on a stroke-by-stroke basis — to perform motoring, pumping or idling operation cycles as illustrated in Figure 1.2. During idling strokes the LPV is

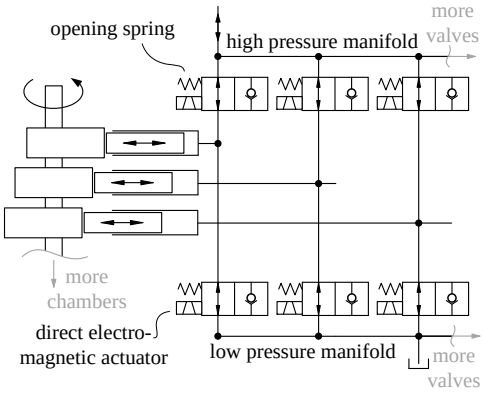

Fig. 1.1: Hydraulic layout of a DDM with normally opened check-valves.

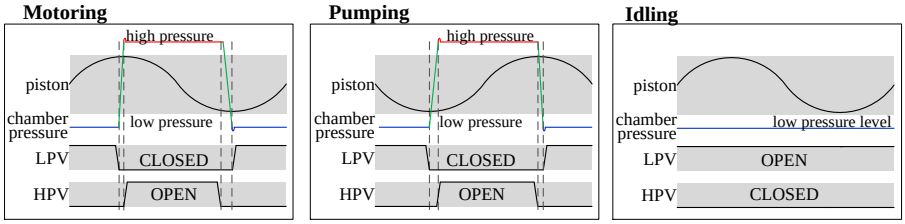

Fig. 1.2: Motoring, pumping and idling operation cycles.

kept open throughout the revolution resulting in a net displacement of zero and very low losses. This is an effective method of lowering the machine displacement since the machine losses in this case scales close to linearly with the number of active pistons [90]. This enables maintaining high efficiencies even at low displacement ratios where conventional fluid power machinery typically suffer [54], as can be seen from Figure 1.3 comparing the efficiency and losses of variable displacement fluid power machines.

State-of-the-art DDMs all rely on radially configured pistons as it offers the following advantages: friction losses are reduced since the sliding surfaces are located close to the shaft center where the surface velocity is low, the valves are furthest from the shaft leaving enough space for big valves with sufficiently large flow capacities and finally, the radial configurations permits multiple modules, or cylinder banks, to be placed side-by-side along the same shaft (often referred to as layer cake assembly). The latter permits relatively simple (and unconstrained) scaling of the machine power by using the appropriate number of modules and furthermore, radial loads on the main shaft bearings can be reduced by radially offsetting the eccentric of the indi-

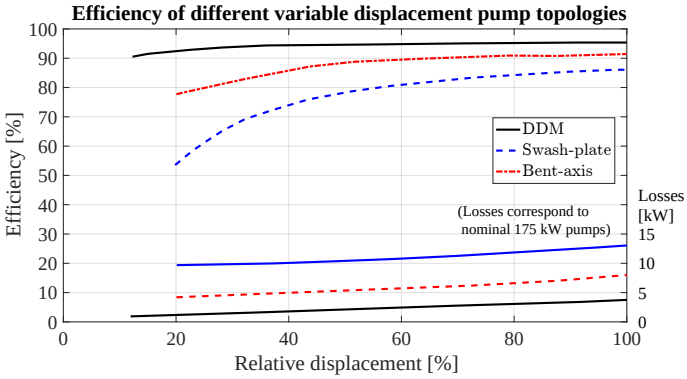

Fig. 1.3: "Comparison of measured efficiency of an automotive scale 175 kW DDM against the more developed Bent-axis and Swash-plate variable displacement type pump topologies, based on graphs published in [90]. The revolution speed is 1500 RPM." This figure is also shown in Paper **G**.

vidual modules and strategically selecting which cylinders should perform active strokes. Figure 1.4 shows pictures, taken from [2], of a state-of-the-art 12-piston 96 CC/rev Digital Displacement (DD) pump capable of operating at speeds and pressure up to 1800 RPMs and 350 bar (machine power approximately 100 kW), respectively. The pump made it market appearance in September 2015 and is the first and so far only commercially available pump based on DD technology [2]. As indicated in the figure, the machine casing is filled with oil which serves as low-pressure supply for the valves. The valves are situated directly above the pistons and only one valve body per cylinder is explicitly seen in the figure and only the low pressure bore is visible from the cut-away. Since the machine only is intended for pumping, only an active LPV is required since the task of the HPV in this case can be achieved using a passive check-valve (elaborated later in this introduction, cf. Section 1.3). The passive HPV is not directly visible, but it could be embedded into the LPV body for achieving a compact design. Such a LPV design has been patented in [36] and is revisited in Section 1.3.

The electronically controlled valves are key components and the nature of DD operation sets tough requirements both with respect to performance, efficiency and durability. For several of the proposed applications the valves are to endure billions of switching cycles, each involving rapid deceleration on impact at the extreme positions and loads from the cyclic pressure of the chamber. Furthermore, the valves must have large flow passages to ensure low flow losses, especially the LPV is important for maintaining high efficiencies at low displacements. The valves should be fast to allow for accurate execution of the valve switchings and to the amount of flow conducted with semi-opened valves. And finally, the valves must be electrically efficient in

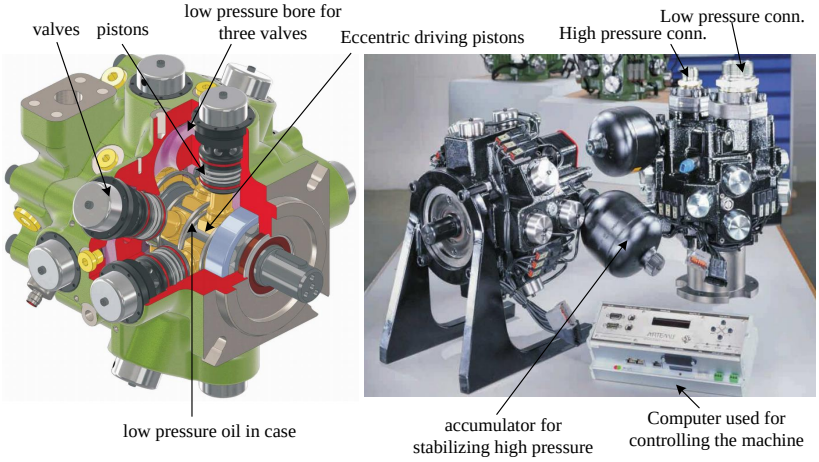

Fig. 1.4: Pictures taken from [2] showing the Artemis E-dyn 96 digital displacement pump.

order to maintain high efficiency and minimize the demands to the associated power electronics. On the shelf valves fully satisfying these requirements do not yet exist and therefore further research and development is needed to make a commercial breakthrough more viable. The work presented in this thesis' is aimed as a modest contribution to this purpose.

Terminology

Digital pump/motors are part of the digital fluid power branch based on hydraulics and part of the sub-branch based on parallel connected systems [45]. Digital fluid power is characterized by that discrete valued components are used to control the machine [45]. This is indeed the case as both the switching valves are discrete valued components which are used to control the machine displacement in discrete levels.

1.2 Development of Digital Displacement Machines

The following gives an overview of the research and development carried out with respect to digital fluid power pump/motor concepts. First, focus is turned towards the activities in industry and then academia.

The DD concept was conceived in the 1980s by a research team at Edinburgh University, which led to the founding of Artemis Intelligent Power Ltd. (AIP) in 1994 [69], which has developed and refined the DD technology ever

since. AIP has applied their revolutionary variable displacement technology to a wide range of different applications incl. wind turbine drive trains, commercial vehicles, wave energy recovery devices and excavators demonstrating the remarkable potential of the technology [3, 5]. In 2010 AIP was acquired by Mitsubishi Heavy Industries (MHI) with the main purpose of developing large scale hydro-static transmission systems for wind turbines [56].

Over the years, AIP has been involved with a number of highly reputable industry partners. In 2006, Bosch Rexroth overtook (from automotive components company Dana which became involved with AIP in 1999) licensing for the AIP technology for on-road vehicles but they have still not used the technology in any commercial products [69]. In May 2008, AIP demonstrated the DD technology deployed in a BMW 530i with up to 50% reduction in fuel consumption [1, 90]. Since the late 90's, AIP has been involved with Sauer Danfoss (today, Danfoss Power Solutions) in exploiting the technology for off-road vehicles and mobile equipment [69]. In [95] the new possibilities of using DDMs are outlined and experimental results show 25% decrease in fuel consumption compared to traditional hydrostatic transmissions even with using energy storage systems. But again, in spite of promising results, no products based on the technology have been introduced to the market. A more detailed walk-through of the developments done by AIP, based on published research, patents and engineering judgment, is given in [72] published in September 2014.

Since then, AIP have published their progress on a retrofittable hydraulic hybrid system for a city bus using a DDM and a hydraulic accumulator for storage of kinetic energy [89]. Based on validated models the system is predicted capable of reducing the fuel consumption by up to 27%. Also, earlier this year, AIP announced they are to test an alternative traction system for diesel powered rail vehicles comprising a diesel engine powering the mentioned E-dyn 96 CC pump which supplies axle-mounted DD motors [4]. The traction system also features energy storage enabling recapturing parts of the energy otherwise lost during braking. Tests are to commence December 2017 [80]. Finally, AIP and Quoceant (a marine energy and technology consultancy [68]) have been working towards using DD technology in the Pelamis wave energy converter power take-off. Lately, the duo were granted funds for carrying out full scale demonstration (power scales into the megawatt range) on a test-rig [98]. Commenting on the grant, the managing director of AIP, Dr. Niall Caldwell reports *"We believe our system is a fundamental advance in capturing the mechanical power generated by renewable sources"* and continues *"We have combined the established advantages of hydraulic power – controlling tremendous forces in harsh environments at comparatively low cost – with the latest in smart digital control, to enable dramatic improvements in efficiency and controllability of wave energy devices"* [4].

One of the key application areas of DDMs is the power take-off in renewable energies and especially wind turbines. As early as in 1984, Stephen published his paper [81] on the unseen possibilities fluid power can unlock, when used properly in wind turbines. He pointed many of the benefits of using a hydro-static transmission system out, such as mechanical decoupling of the rotor and generator, weight reduction and energy storage with high speed interface. He also points out that better fluid power machines are needed to achieve higher efficiencies making hydraulics viable for wind and has pursued realizing such machines (with AIP) since. In 2013 MHI announced plans for a 7 MW turbine with a first-of-it's-kind digital hydro-static transmission system [67]. In February 2015, MHI commenced testing at the SSE Hunterson test facility in Scotland [57, 58]. The transmission system is based on a large 7 MW slow-rotating digital pump connected to the main rotor shaft, and two fast-rotating 3.5 MW digital motors, each connected to synchronous generators running at 1000 RPM, however no experimental results have been published. Later the same year, MHI also erected a floating wind-turbine in Yukoshima, also with a digital hydrostatic transmission, but again, no results are published [18]. For more information on the 7MW transmission system, see [72, 82].

Besides the developments done in industry, or by private companies, DDMs have been explored by a few research groups in academia. A team at Purdue University has carried out research concerning digital pump/motor concepts, as reported in [26, 27, 53–55]. A part of this research is focused on partial displacement stroke operating strategies, such as Partial Flow Diverting (PFD) and Partial Flow Limiting (PFL). The PFD strategy is based on only using part of the stroke actively which is obtained by exiting the high-pressure state earlier (motoring) or entering the high-pressure state later (pumping). The PFL strategy for obtaining partial displacement strokes is based on deliberately cavitating the chamber during the down stroke which has the potential to increase the efficiency further since flow losses are avoided during chamber cavitation. Typically, cavitation is not provoked intentionally and is considered an extremely undesired phenomenon in fluid power systems due to the harmful consequences of the abrupt collapse of formed air bubbles. In addition to the possible complications associated with cavitation of the chamber, this operation mode does not permit the use of traditional check-valves for the LPV, as they would open passively due to the pressure difference across the seat/poppet during cavitation. In [27] two-stage bi-directional check-valves where explored for DDMs. The valve configuration facilitates the necessary functionalities for carrying out the mentioned operating strategies. Experimental results are presented and the authors conclude that both methods are promising for performing partial displacement

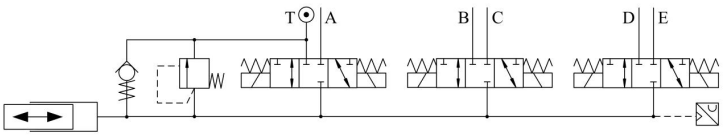

Fig. 1.5: Illustration taken from [23] showing the valve configuration used for each piston in the DHPMS prototype.

strokes. However, no information about efficiency is disclosed in [27]. The bi-directional check-valves are revisited later in this introduction.

The same group have developed a DD test-setup based on a commercial in-line three-piston check-valve plunger pump, fitted with commercial direct solenoid actuated normally closed poppet valves, as reported in [26, 53]. The machine has a total displacement of 28.5 CC/rev, corresponding to peak valve flow rates of 21 l/min at the maximum tested speed being 700 RPM. The used valves were the Sun Hydraulics DTDAXCN switching valve which according to the data sheet [87] has a pressure drop of 1.5 bar at 21 l/min (38 l/min at 5 bar) and a typical switching time of 50 ms which is much too slow for high-speed DDM operation. To improve the valve switching time advanced boosting and reverse current techniques, developed in [6], are used resulting in opening times of 8-10 ms and closing times of 16-20 ms (incl. delay) [26]. At full displacement, 103 bar and 700 RPM efficiencies of 86-89% were measured. The efficiency drops to 45-70% at 25 % displacement ratio, dependent on the operating strategy used for achieving variable displacement. The partial-stroke operating strategy PFL were found to be more efficient than the PFD strategy partially as a result of using normally closed valves [53].

Tampere University of Technology is currently also researching novel digital pump/motor concepts. The group has done substantial work on a Digital Hydraulic Power Management System (DHPMS), as reported in [20–23,44,46, 88]. A DHPMS system is basically a digital pump/motor with multiple independently controlled outlets. A second DHPMS prototype is introduced in [23]. It is a six piston unit with five independent outlets, enabling displacement control of two actuators leaving a residual outlet which can be used for energy storage. For each piston, three commercial 3/3 directional direct solenoid actuated control valves (Bosch Rexroth SEC type) are used in combination with the original check-valves of the machine to ease filling from tank (and a pressure relief valve for safety purposes), as shown in Figure 1.5. Each cylinder has a geometrical displacement of 1.8 CC (were originally 5 CC, but have been decreased to get better displacement resolution in the desired flow operation range), and at the maximum test speed of 1000 RPM, this lead

to peak flow rates of 5.7 l/min. At the peak flow rate, the pressure drop of the retrofitted valves is 3.3 bar (according to data sheet [10]) corresponding roughly to 2% of the maximum tested machine pressure span being 160 bar. The valves are poppet based making them leakage free which leads to smaller parasitic losses and the possibility of efficient energy storage. Measured characteristics show efficiencies above 85%, but lower efficiencies at high speeds, because of the flow rates and thereby the flow losses are greater. The efficiency also decreases at lower pressures since the valve losses remain constant as they are independent of the machine pressure span. Pumping is more efficient than motoring since the DHPMS cannot take advantage of the original check-valves during exhaust of low pressure oil (as the flow is reversed). This means that all flow is conducted by the retrofitted valves during motoring cycles, leading to larger throttling losses and lower efficiencies. To achieve better efficiencies over the entire operation range, better valves are needed with larger flow capacity, especially for high-speed, high power DDMs. In [23] the electrical power consumption of the control valves is the not included in the efficiency calculation, and the valve transition times are not mentioned either. In previous work [46], the authors state that *"The electric power consumption of the valves should be at maximum few percent of the maximum power of the pump in order to retain good efficiency"* and in [88] the authors report on a previous prototype digital unit that *"the electrical losses decrease the total efficiency significantly"*, partially since the valves require holding power. The electrical power consumption of each valve in [23] is 30 W, according the data sheet [10], constituting approximately 1% of the transferred power of each piston at the highest tested speed and pressure (1000 RPM and 160 bar). And since three valves are used for each cylinder, the electrical losses may be up to 3%. However, only one valve should be active at a time for one cylinder, hence the valve losses should not increase significantly when increasing the number of outlets. The dead volume, on the other hand, increases significantly, especially when using commercial valves, leading to a smaller power throughput as larger of the stroke is used for compression and decompression. The larger dead volume does not necessarily lead to lower efficiencies. In [32, 32] the DHPMS prototype is applied to directly control a two-degree of freedom system showing a 40% energy savings compared against conventional state-of-the-art systems.

Tampere University of Technology have since the early 2000s developed fast switching valves to be used in digital flow control units etc. [33,47,48,93]. However, to the knowledge of the author, no valves have been developed solely for the purpose of DDMs.

Also, recently Agder University has been active in the field of DDMs. In [61, 62] the potential and the feasibility of digital hydraulic winch drive systems are explored. The system is based on a digital hydrostatic trans-

mission having a fast rotating pump and a slow rotating motor. The studies concluded that DDMs are viable candidates for a hydro-static winch drive with the main advantages being fast control and efficiency improvement.

Different digital (or discrete) pump/motor concepts, not relying on fast switching electronically controlled valves for commutation, are also currently being explored in academia [24,70,91]. In [70] a digital pump/motor concept is studied which uses a two degree-of freedom pilot valve that rotates with the rotation of the shaft and can be translated axially to perform pumping, motoring or idling strokes (partial strokes are also possible). The rotary pilot valve actuates a 3/2 main stage spool valve which handles the commutation of the cylinder. No information about the flow vs. pressure characteristics for the main stage valve have been disclosed. Based on pressure measurements, the transition time of the main stage valve is estimated to be approximately 3 ms. The authors predict efficiencies of 85-95% displacement ratios above 0.5, however due to excessive leakage across the main stage spool valve, the efficiency was low (not directly mentioned). The proposed concept was proven capable of varying the displacement (in both a discrete and continuous manner) and the authors assess that non-electric digital pump/motors may be favorable in some situations, as lots of electro-magnetic valves having tough tasks are not required. Still, hydro-mechanical valve control mechanisms, as presented in [70] do not offer completely free valve timing leading to notable throttling losses under some operating conditions.

Aalborg University has been working with DDMs since 2010 and in 2011 the first experimental results were published on a 1-piston digital pump equipped with a prototype direct solenoid actuated seat valve for the LPV and a passive check valve for the HPV [73]. The most recent research is focused on electromagnetic valve actuation systems [50], verification of fluid-mechanical models [8], the reliability of fast switching on/off valves [9][1] closed loop control algorithms for system wide control [66] and modeling of tribodynamics (lubrication, friction and leakage conditions) [29,30]. The mentioned Ph.D. thesis [72] is titled *"Design and Optimization of Fast Switching Valves for Large Scale Digital Hydraulic Motors"* and, as the title suggests, it tackles several of the same issues as this work. Figure 1.6 presents a digital displacement machine concept developed in [72]. As the earlier AIP machines, the high pressure manifold enclosed the entire machine favoring low flow losses, but also making the valves harder to access (more recent developments use internal bores for both the high- and low-pressure manifold [72,78]). The suggested valves are of the annular seat type and actuated

[1] The paper presents an reliability analysis of the moving-coil actuated prototype valve developed in this work.

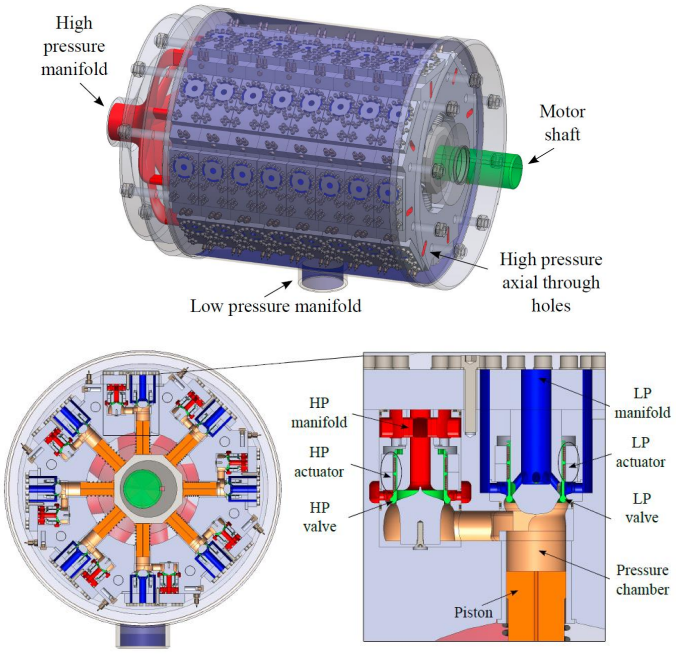

Fig. 1.6: Illustrations taken from [72] showing the layout of a DDM concept.

by moving coil actuators and the linear piston motion is connected to the rotating shaft using a polygon ring.

The research presented in [72] is primarily focused on modeling, design and optimization. A sequential optimization method is presented which involves a number of subroutines each dealing with different aspects and facets of the valve design. The method is based on iterations and arriving at optimal solutions appear difficult as the objectives are multiple and the interdependencies are many. Substantial effort is given to developing methods for evaluating stiction effects (resistance to separation of parallel lubricated surfaces [71]), and fluid-mechanical movement induced forces dampening the movement (more recent work on the same topic is found in [74]). Using the described method, the prototype valve shown in Figure 1.7 was developed for large scale DDMs, such as the DDM shown in Figure 1.6. The valve is of seat-type, it is normally opened (spring not shown in figure), it is moving coil actuated and has a simulated pressure drop below 0.5 bar at 600 l/min and a measured switching time of 1.8-2.9 ms, as shown in Paper **A**. Closing the valve at this speed requires approximately 500 N and 10 J. The valve plunger is made from carbon-reinforced PEEK which proved to be difficult to

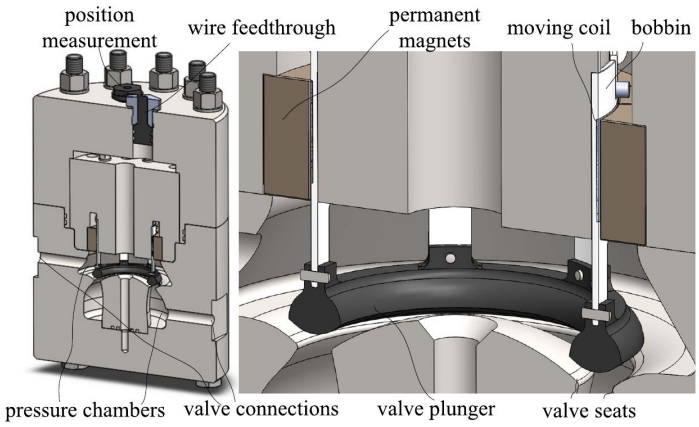

Fig. 1.7: Prototype valve developed in [72].

machine leading to inaccurate test specimens. Early in the present work, experimental tests were carried out on this prototype resulting in publications **A** & **B** concerning validation of models used for designing the valve.

The principles of electronic valve actuation for piston machines do not only enable new possibilities in fluid power. Experimental results have shown that variable valve timing actuation systems can reduce fuel consumption by 23% and increase power output by 11% while also significantly reducing emissions [40]. Camless combustion engines have been investigated for long by several major car companies, but still, no vehicles based on the technology have been introduced to the market. Different mechanical mechanisms for obtaining variable valve timing have long been used, such as helical camshafts. However, they do not offer complete freedom of the valve timing and typically involve additional moving parts. The company Koeningsegg Automotive AB has a long tradition of developing high-end leisure cars and has for more than a decade, through their sister company FreeValve AB, focused on developing and refining camless combustion engines for cars using novel valve technology [19]. To achieve maximum performance, the valves combine electric, pneumatic and hydraulic actuation principles [15, 19]. This technology appears promising and an impressive 47% increase in power, 45% increase in torque and 15% fuel savings is reported for the newest Qoros Qamfree camfree car (motor is done by Koeningsegg and FreeValve) debuted in 2016 [19]. At this time, no concise performance specifications have been published for the valves to the best knowledge of the author.

The engineering design company LaunchPoint Technologies has developed an electro-magnetic valve actuator for camless combustion engines [63].

The actuator is based on the moving coil principle which has superior transient performance compared to traditional electromagnetic actuation principles [12, 79]. Using an integrated sensor for closed-loop position control, the actuator system achieves fast transition times and low landing speeds (for durability purposes). An example of the system performance is given on the company website i.e. for a 3.2 ms transition time the electrical energy consumption is 3.34 J [37]. For the valves of high-speed, high-power DDMs, the requirements with respect to switching time and energy consumption are of similar magnitude[2].

Besides these similarities, the requirements to the valves of DDMs are widely different. During intake and exhaust, the working medium of combustion engines is on gas state meaning both the viscosity and the density is much lower than that of oil used in fluid power systems. This leads to much larger demands in terms of valve flow area and additionally if using seat-type valves, axial flow forces acting on the moving member may be of considerable magnitude during peak flow rates. To accommodate these circumstances, the valves of DDMs are typically larger in physical size (incl. moving member) which again increases the demands to the valve actuation system.

The milestones in the development of DDMs are summarized in the timeline shown in Figure 1.8. As can be seen, the major commercial activities done by AIP, and lately also by MHI (through ownership of AIP). In academia, the major contributors have been; Edinburgh University in the early days where the fundamental ideas of the technology were conceived, and more recently Tampere University of Technology, Purdue University and Aalborg University. Other academic institutions who recently published research related to DDMs are Jilin University [41] and Shanghai Jiao Tong University [42], both from China. Other commercial activities also exist, such as Dinef AS which recently published a paper on a digital distribution valve for high-torque low speed digital pump/motors [43].

The success of any digital hydraulic application is dependent on the capabilities of the deployed switching valve(s). This is much similar to switched power electronics which only became possible after the invention of force commutated fast power-electronic devices [52, 84]. In this regard, Johannes Keppler University of Linz and Linz Center of Mechatronics have been ma-

[2] Assuming a valve transition time of 5% of the revolution time [77], this roughly suits 1000 RPM DDM operation, and with a 1% electrical power consumption this corresponds to a 1.4 kW cylinder (corresponding to a 2.4 CC cylinder operated at 350 bar) which is approximately 16 times lower than the pressure chamber valves are developed for in this work (50CC chamber running 800 RPM at 350 bar). However, the switching time is approximately the same and the power consumption is less.

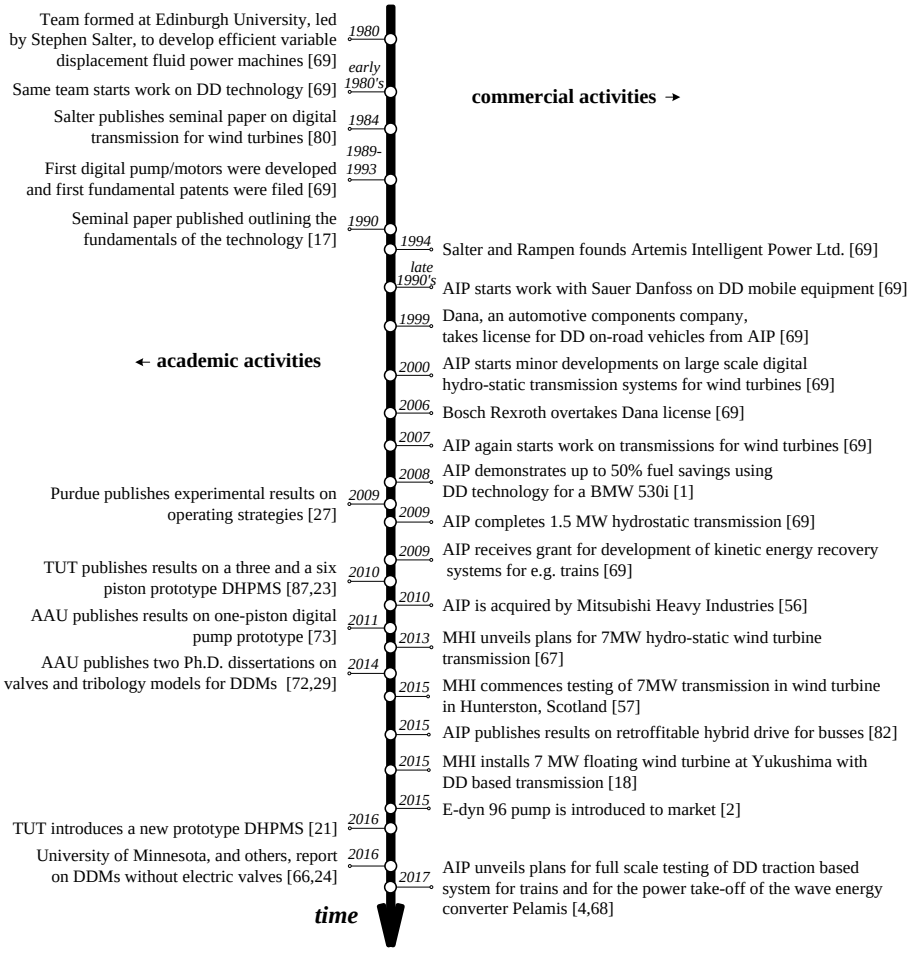

Fig. 1.8: Time-line giving an overview of the seminal developments and activities concerning DDMs.

jor contributors as both long have been involved with fast switching valve research pushing the limits of the technology.

1.3 The Valves of Digital Displacement Machines

In this section, further details are presented for the valves needed in DDMs. First, the suitability and possibilities when using different valve configurations and valves have different functionalities and capabilities are discussed. This is followed by a brief discussion of valves possibly used in the state-of-the-art AIP/MHI machines of today. Then, attention is turned to novel

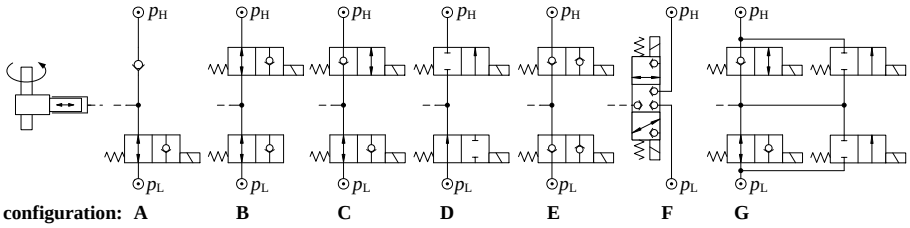

Fig. 1.9: Selected valve configurations enabling different variants of DD operation.

switching valves, used in other digital fluid power applications, in pursuit of potential candidates for DDMs followed by a discussion of other valves and actuators that could possibly be of relevance to DDMs.

Valve Configurations and Functionalities

This section discusses the pros and cons of different valve configurations or valves having different functionalities. Figure 1.9 shows some selected valve configurations.

The HPV of configuration **A** is a passive check-valve. When using a passive HPV, motoring is not possible but pumping and idling still is. The drawn LPV is a direct actuated normally open check-valve, as this type of valve seems to be the most appropriate in applications only requiring pumping/idling operation.

Configuration **B** & **C** use actively controlled check-valves. Using check-valves have the major advantage that only the timing of the valve closings need to be executed accurately since the subsequent valve opening occurs passively from pressure/flow (aided by passive element for the normally open case, and by the actuator for the normally closed case). A disadvantage is that opening against high pressure differentials typically is not possible disallowing the mentioned Partial Flow Limiting operating strategy and motoring self-start. This is elaborated later in this section.

If using valves without check-valve capability, as is the case for configuration **D** & **F**, both the closings and especially the valve opening must be carried out with great accuracy. In this case, the opening does not occur passively, and inaccurate timing leads to excessive throttling losses, and possibly a pressure relief valve is also needed for safety purposes (in case of the HPV failing to open). An advantage of using configuration **D** & **F** is that the valves are capable of opening against pressure differentials. This enables performing all of the discussed DD operating strategies (and motoring self start). Furthermore the valve configuration **F** only uses one valve which possibly can enable a more compact design.

The valve configuration **E** was studied in [27] and uses two bi-directional check-valves. Using such a valve configuration, all the discussed DD operation strategies are possible, but with lower demands to the valve timing. By switching the state of the bi-directional check-valves while they are closed passive valve opening may be achieved. Such bi-directional check valves were in [27] realized using a prototype main stage valve and a commercial electrically controlled directional 4/2 valve for a pilot stage. By controlling the 4/2 valve the check-valve direction of the main stage valve can be controlled.

The final valve configuration **G** shown in Figure 1.9 involves two LPVs and two HPVs. One of the HPVs and LPVs would have a large flow capacity ensuring low flow losses during peak flows. The other HPV and LPV would have a much smaller flow capacity, but also much rapider switching capability. Since valve switchings (for full strokes) are conducted closely to the dead centers the flow rates occurring are relatively small. This leads to the timing of the larger valves being less critical and can be closed well in time and opened late without significant increase in flow losses if the timing of the smaller valves is carried out accurately. A disadvantage is cost increase as a larger number of valves are needed.

In addition to the pros and cons of using check-valves discussed above, another advantage is that leakage is avoided which is extremely important for retaining high efficiencies. Especially leakage across the HPV is undesired as it would increase the parasitic losses during idling, and deteriorate the machine efficiency at lower displacement ratios.

As mentioned, (direct actuated) check-valves are typically incapable of opening against pressure differentials. For instance, the moving coil actuated check-valve prototype valve developed in this work has a shadow area (effective area the valve pressure difference acts on) of 4.7 cm^2 leading to a pressure force of 47 N/bar, making it impossible to open the valve at more than a couple of bars pressure difference using direct electro-magnetic actuators (taking the available size and power into consideration). This short coming limits possible DD operation cycle variants, such as the partial flow limiting operating strategy investigated in [26, 27, 55], but more importantly, it also prohibits motoring self start, unless other measures are taken to circumvent this limitation. At stand-still (and unloaded), none of the pistons are pressurized meaning that the LPVs are open and the HPVs are closed. In order to produce torque, the pistons must be pressurized, either by opening the HPV or by piston movement. Using check-valves incapable of opening against pressure results in that motoring start-up depends on an external torque source for rotating the shaft.

A novel, direct solenoid actuated normally closed poppet HPV which offers the outlined advantages of using check-valves and also permits motoring self-start is disclosed in the AIP patent [85] filed September 2006 (published June 2014). Based on the schematics included in [85] the working principle

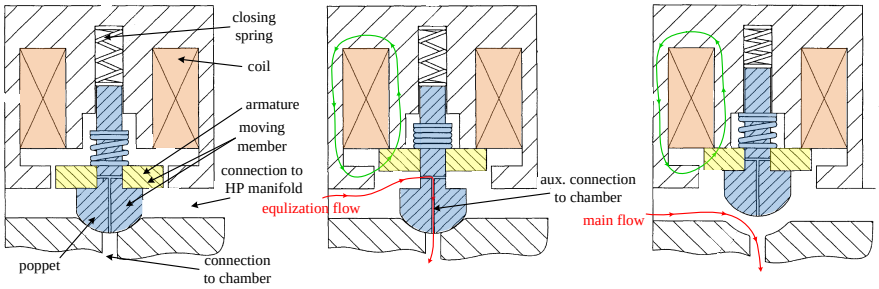

Fig. 1.10: Drawings taken from [85] modified to illustrate the working principle of the valve.

of the valve is illustrated in Figure 1.10. As can be seen, the moving valve member has two bodies which can move relative to one and another, denoted as poppet and armature in the figure. If energizing the coil while a pressure difference is present, the poppet cannot open, instead the armature moves which opens a small auxiliary connection to the pressure chamber enabling equalization. When the pressure difference across the poppet is sufficiently low, the poppet opens. Using such a concept appears attractive, but leakage occurring across the axillary valve may be an issue degrading the efficiency.

Another method that possibly can enable motor self-start, even when using check-valves incapable of opening against pressure is briefly discussed in the following. The high pressure manifold of a DDM is typically connected to an accumulator for stabilizing pressure and flow. If having the possibility to disable the accumulator and to throttle the pressure of the remaining oil of the high-pressure manifold it should be possible to open the appropriate HPVs (and close the appropriate LPVs). When the valves are switched to the desired states, the high-pressure accumulator is again enabled which pressurizes the desired pistons, making motoring self start possible. However, further investigation is still needed to determine if using such a method is viable.

As discussed, the electrical power consumption of the valves should be as low as possible to enable high efficiencies and to lower the requirements to the associated power electronics driving the valve. Ideally, the valve would only require electrical power for switching the state of the valve, but no electrical power for holding the valve in any state (often referred to as holding power). Such functionality is possible using normally opened check-valves for both the LPV and HPV as in this case for configuration **B**. In this case, the valves would only need electrical power for switching, as the closed position is maintained due to pressure difference across the valve and the opened position is maintained by the passive opening element which balances the axial flow/pressure forces acting to close the valve during flow conduction (when flow direction is against the check-valve). Using such a valve con-

figuration furthermore enables having identical LPVs and HPVs, or at least having LPVs and HPVs with identical functionality.

While such configuration appears attractive from the perspective of energy efficiency and valve design effort, having normally opened HPVs also comes with a major disadvantage. If the HPV actuator fails during operation, the HPV would open and the chamber would remain pressurized. Such an operation mode is referred to a high-pressure idling and considered extremely undesired as the leakage and friction losses occurring at the sliding surfaces of the piston assembly are increased.

This problem is circumvented if using a normally closed HPV as done for configuration configuration **C**. In this case, if the HPV actuator fails the low pressure idling operation mode is entered. However, as discussed, holding power is needed to keep the HPV open during motoring. Pumping operation is possible even if the HPV actuator fails, however, the flow losses would increase as the valve is opened by pressure/flow forces alone.

State-of-the-Art AIP/MHI Valves

Naturally, since the valves are key components of DDMs, AIP or MHI have not disclosed any concise information about the performance specifications or the working principles of the valves used in their state-of-the-art machines. Based on patent applications filed by AIP, this section presents a relatively recent LPV and HPV design to familiarize the reader with the capabilities and possible limitations of state-of-the-art DDM valves (patents are filed in combination with collaborators) .

In a patent filed by AIP/MHI December 2015 (published in December 2016) [60], relatively detailed technical drawings are disclosed showing a valve design which could resemble state-of-the-art HPVs used in large scale AIP/MHI machines. The technical drawing from [60], modified for easier interpretation, is shown in Figure 1.11 (*left*). The valve is of annular seat type with direct electro-magnetic solenoid actuation. The valve is normally closed, as can be seen by the extending spring situated above the moving valve member. The valve is solenoid actuated and relies on the steel of the surrounding manifold for completing the flux path which can be seen by the non-magnetic material otherwise open-circuiting the flux path. In the fully opened position, the moving member is partly shielded from the flow as indicated in the figure. This is supposedly done to reduce the axial flow force acting to close the valve, similarly to the method for axial flow force reduction explored in [50]. The outlet holes leading to the pressure chamber are shaped as circular sectors (normal to the axial direction of the valve) to maximize the flow capacity of the valve. In Figure 1.11 (*right*) a valve manifold block is shown, also from [60]. The drawing is clearly severely simplified,

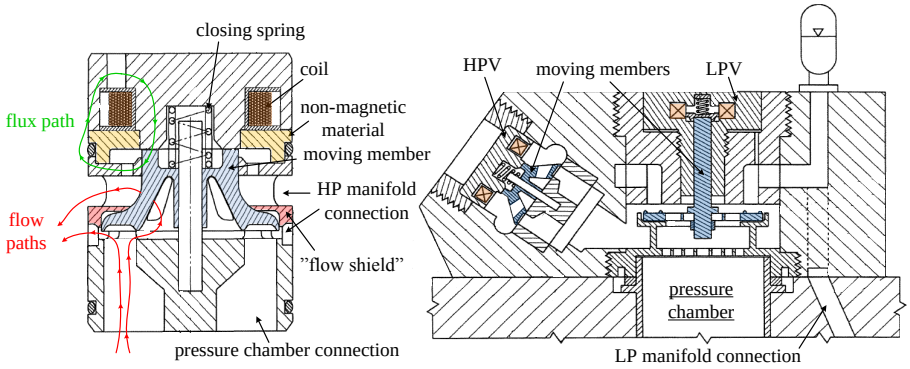

Fig. 1.11: Schematics taken from [60] showing a normally closed annular seat valve (*left*) and a manifold arrangement incl. much simplified valve drawings (*right*).

but worth noticing is that the LP manifold connection is directed (roughly) towards the machine center, and that the pressure chamber extends into the LPV. As pointed out in [72], this also appears to be the case for 3.5 MW AIP/MHI motors of the 7 MW digital hydrostatic wind turbine transmission.

In 2008, AIP (and Sauer-Danfoss Aps) filed a patent application for a fluid distribution LPV [36] (published in 2010). In the patent application, several schematics are disclosed showing different valve designs. Common is that the pressure chamber extends into the LPV and that the designs has multiple flow ports enabling distributing the flow to the LPV and the HPV. Some designs have a passive check-valve embedded directly into the LPV as can be seen from the modified schematic shown in Figure 1.12 (as discussed, a similar valve concept may be utilized for the E-dyn 96 CC pump). As can be seen, the actuator comprises two coils and a permanent magnet. The lower and bigger coil is used for generating the closing actuator force. The permanent magnet is used to aid the spring in keeping the valve open and the upper coil is used to cancel the flux of the permanent magnet making it possible for the lower coil to close the valve. An advantage of using this concept is that the demands to electro-magnetic closing force can be reduced. Since the permanent magnet aids the spring, a weaker spring may be selected. This is very beneficial, especially when using solenoids being based on the variable reluctance principle typically having non-linear force vs. position characteristics. At the fully opened position, the air gap of the closing coil flux path is the largest leading to the smallest force (even though the inclined surface helps to attenuate this effect, also referred to as pole shaping [16]) making it important to reduce the closing force demands, especially for valves operating at large flow rates having large stroke lengths.

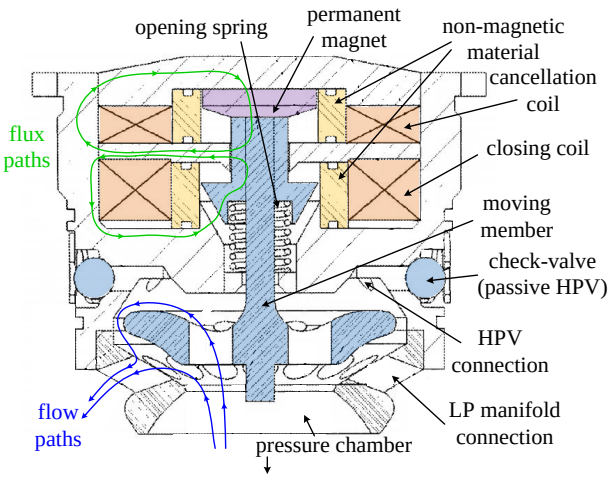

Fig. 1.12: Schematic, taken from [36] showing a LPV with embedded passive HPV.

The cancellation coil could also be used to aid the permanent magnet to extend the flow operating range of the valve. By controlling the cancellation coil such that an opening force is present during the peak flow rate (from the chamber to the low-pressure manifold leading to the maximum axial closing flow force) spontaneous valve closing can be avoided. Also, at system start-up in cold conditions, the low fluid temperature results in a much higher viscosity of the oil leading to increased valve pressure drops and axial flow forces. Similarly, the cancellation coil could be used to avoid spontaneous closing due to the increased viscosity.

A disadvantage of using variable reluctance actuators with electrically conductive cores is that eddy currents are induced which slows down the flux build up and thereby the electro-magnetic force [65]. Methods for attenuating the effect of eddy currents have been used in electric motors and other electro-magnetic applications requiring high frequency magnetic signals. Using sheets of laminated magnetic steel for the actuator core reduces the eddy current effects [12]. However, this is difficult to utilize for direct actuated valves, as the actuator core typically is integrated in the valve design and is being exposed to high pressures. Ferrite cores, made from ferrites (ceramic compounds of metals with oxygen which are ferrimagnetic) have very low conductivity reducing eddy currents effects effectively. Ferrite cores are typically used in radio frequency transformers and inductors in switched mode power supplies but are not well suited for hydraulics as the material typically is quite brittle and weak to tensile stresses.

The severity of eddy current effects in variable reluctance actuators is dependent on several design variables, such as the geometry, the actuator core

material, the temperature and the coil design and the waveform of the coil current. This makes it difficult to estimate the transient capabilities of the valve designs discussed in this section. In [79], a comparison of the capabilities of a solenoid-, a moving magnet-, and a moving coil actuator for a DDM valve was presented. Each actuator has a similar volume, is driven by the same power supply and has a steady state actuator force of approximately 250 N. Using transient electromagnetic FEA the performance of the actuator is simulated showing that the force build up of the variable reluctance actuator is much slower than for the other two actuator topologies. After 11.6 ms, 200 N was reached by the variable reluctance actuator, while the moving magnet actuator achieves 200 N in 1.7 ms and the moving coil actuator in 0.2 ms. Also, in [13] a method for calculating the magnetic diffusion times for steel cylinders assuming infinite length and constant permeability is presented. The magnetic diffusion time represents the time from a step in the magnetic field strength is given until 63.2 % of the steady-state magnetic flux is achieved and is calculated using:

$$\tau = \frac{\mu_0 \mu_\mathrm{r} \sigma r_\mathrm{cylinder}^2}{2.4048^2}, \tag{1.1}$$

where r_cylinder is the radius of the cylinder, σ is the electrical conductivity, 2.4048 is the root of the first Bessel function and μ_0 and μ_r is the permeability of vacuum and the relative permeability of the cylinder material, respectively. Using μ_r = 630, $\sigma = 1.7 \cdot 10^6$ S/m and $r_\mathrm{cylinder} = 15$ mm results in a magnetic diffusion time constant τ of 52.3 ms.

With a better established understanding of the possible influence eddy currents may have on the force build-up of solenoid actuators attention is turned to Figure 1.13 showing a comparison made by AIP [5] of the achievable revolution speed of DDMs as a function of displacement per revolution compared against conventional hydraulics. As can be seen, DDMs are capable of operating at higher speeds for all displacements, however, for displacements above 1000 cc/rev, the rotational speed is capped at approximately 1000 RPM. Possibly, the transient switching performance of the solenoid state-of-the-art AIP/MHI valves of today is pushed to the limit and could therefore be a major contributor to the limitations of the revolution speed at larger displacements. But again, since no concise performance specifications are published, it is hard to determine whether this is actually the case. Still, this has been one of the dominating motivational factors for exploring electro-magnetic actuators having better transient performance than solenoids, in this work.

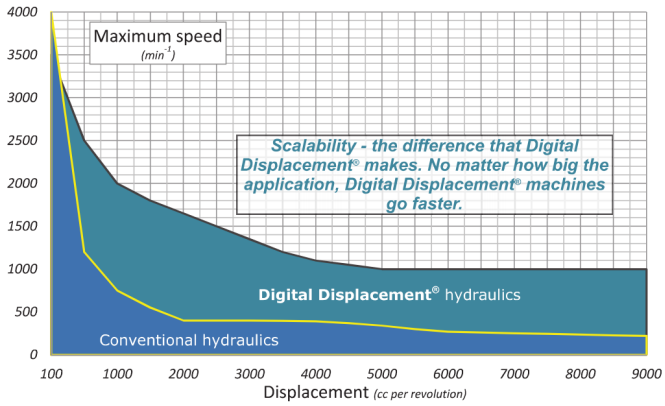

Fig. 1.13: Comparison of the possible revolution speed as a function of displacement for conventional fluid power machines. Illustration is taken from [5].

Possible Switching Valves for DDMs

This section discusses several existing valve and actuators which could be of relevance to high speed, high power DDMs. First attention is turned to the on-shelf components and then to prototype developments.

A switching valve that already have been introduced and comes relatively close to meeting the requirements for high-speed, high-power DD operation is the Bosch Rexroth WES valve [11]. According to the data sheet, the valve has an opening/closing time below 5 ms and a flow rate of 45 l/min at 5 bar pressure difference. But, the maximum switching frequency is maximum 10 Hz (possibly due to thermal limitations) capping the maximum revolution speed at 600 RPM. The rated power consumption is 25 W, corresponding to 2.5 J per closing/opening. Furthermore, the valve is of spool type which typically is associated with some leakage. An advantage is that the valve is able of opening against pressure differentials up to 350 bar.

A seat type valve recently introduced to the market having several desirable characteristics for DD operation is the LCM FSVi4.1 [103]. It is a direct solenoid actuated poppet valve (normally closed) capable of opening against large pressure differentials, which offers the advantages of no leakage and full chamber controllability. Measured results shows switching times below 3 ms and is capable of switching frequencies up to 200-500 Hz. At 5 bar the flow rate is 5 l/min, which is considered too small for high-speed, high-power DDMs, as is the case for most commercial switching valves. Also worth mentioning is that the moving armature of the solenoid benefits from a fluid-mechanical damping mechanism, referred to as cushioning groves [83], reducing both induced noise and wear.

In [31] a direct actuated on/off valve is developed with a rated flow of 33 l/min at 5 bar pressure difference and a switching time of 1 ms and an energy consumption per switching cycle of approximately 1.4 J. These specifications seem promising for high-speed operation for smaller scale DDMs, however, the valves are not leakage tight deteriorating the efficiency.

In [101], a fast switching seat type valve for large flow rates is developed. The valve utilizes a Hörbirger plate principle which has several annular rings at two opposite valve plates to form multiple metering edges. This enables obtaining large flow areas when only having small actuator stroke lengths. The developed valve is pilot operated using a 3/2 valve, making the valve capable of opening against high pressures. The pilot stage leads to a delay around 1.6 ms and the main stage is capable of transition times below 2 ms when having a high pilot pressure. The main stage valve has a measured flow rate of 90 l/min at 5 bar valve pressure drop. As discussed, normally seat/poppet valves are typically leakage free, however, utilizing the Hörbirger plate sets strict requirements to the quality of the valve plate and seat as sealing must be provided at several edges. For the prototype developed in [101] some leakage was experienced across the main-stage. The performance specifications of the valve developed in [101] satisfies several of the requirements for DDMs, such as relatively large flow capacity and fast switching, however the valve being pilot operated is considered disadvantageous since this typically implies more complicated, expensive and bigger designs. Finally, the valve does not have check-valve capability leading to increased demands to valve timing as discussed in Section 1.3.

A more recent valve with similar capabilities was introduced in [100]. The main stage valve is again being controlled by pilot stage 3/2 switching valve but instead of the Hörbirger plate, a novel concept based on multiple small poppet's is used. Similarly, measurements show flow rates of 85 l/min at 5 bar valve pressure and switching times of the main stage valve about 1 ms. A disadvantage of such valve design is that the relatively small poppet's may be sensitive to oil contamination.

A proportional valve which comes relatively close to meeting the performance requirements of high-speed DDM is the Parker DFplus proportional valve. It is a 4/3 two-stage valve where the pilot stage is controlled using a moving coil actuator leading to total switching times of 10 ms and a rated flow of 120 l/min, according to the data sheet [64]. A drawback of this valve is that both the main stage and pilot stage are spool types typically associated with leakage. Also, the valve, incl. pilot stage and power electronics is relatively large (384 mm $\times$ 274 mm $\times$ 116 mm) making it difficult to realize compact DDMs using such valves without major redesign.

Table 1.1 summarizes the valves relevant for high-speed, high-power DDMs discussed throughout this introduction. Last in the table, the specifications

of the moving coil- and moving magnet actuated valve prototypes developed during this research are shown.

For more information on switching valves and digital hydraulics, [102] gives a recent overview of other fast switching valves along with a summary of recent advancements in digital hydraulic components and applications.

Table 1.1: Comparison of valve candidates for DD operation. Kilder til papers indsaettes til sidst.

Commercial Valves	T_s [ms]	Q @ 5 bar [l/min]	leak free	valve symbol
Rexroth WES	< 5	45	no	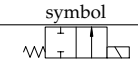
Rexroth SEC6	$7 - 10$	7	yes	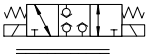
Parker DF+NG10	10	120	no	
Parker DF+NG12	13	200	no	
Sun Hydraulics DTDAXCN	50/8-20[1]	38	almost	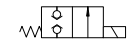
Hydac WS08W-01	50/5*	19	yes	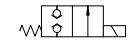
LCM FSVi4.1	< 3	5	yes	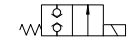
Prototype Valves	T_s [ms]	Q @ 5 bar [l/min]	leak free	valve symbol
Sturman et. al 2001 [31]	1	33	no	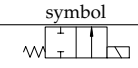
Winkler et al. 2007 [101]	<3	90	no	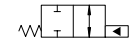
Winkler et al. 2010 [100]	<3	85	no	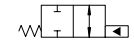
Roemer et al. 2011 [73]	2.7	100*	-	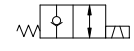
Wilfong et al. 2011 [99]	2.5-10	35	no	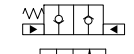
Roemer et al. 2014 [76]	1.8-2.9	1900*	-	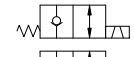
Noergaard et al. 2017 (MCA) [**D**, **I**]	2.5-3.5	400*	yes	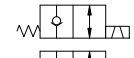
Noergaard et al. 2017 (MMA) [**J**, **K**]	3-6	510*	yes	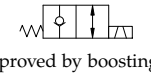

*Estimate, [1]Improved by boosting

Electromagnetic Actuators

This section discusses a few linear actuator topology candidates for DDMs. The previously discussed solenoid topology is by the far the most widespread electro-magnetic actuator for hydraulic valves due to its simple and durable design. But as discussed, inherent delay due to eddy currents and non-linear force characteristics possibly limits the potential of DDMs based

on solenoids. This is motivating for investigating other electro-magnetic actuator topologies for switching the valves.

Actuators which use permanent magnets in the design are attractive since the delay and the associated losses with the flux build up can be partially avoided. The, also mentioned, moving coil actuator (MCA) topology takes advantage of permanent magnets for generating flux which links with the movable coil placed in an air gap. The force is generated based on the Lorentz force law leading to superior transient performance since no delay exists between the coil current and the electro-magnetic force as shown in [79]. Furthermore, the force characteristics are typically linear and the stroke length is not limited. MCAs are also widely used, especially for applications requiring high-bandwidth frequency response and accurate servo control. MCAs are often referred to as voice coils due to its usability for audio speakers. However, in spite of these advantages, MCAs are not widely used in hydraulic valves. A possible explanation for this is the more fragile moving member which leads to more complicated design compared to solenoids. Furthermore, a durable connection for supplying the current to the moving coil is essential, which may be difficult to realize. Especially if considering direct actuated valves where the moving coil is exposed to the full system pressure.

Besides the mentioned Parker DF+, the MTS 257 hydraulic servo valve series also deploy the moving coil actuator principle for actuating a pilot stage. Similarly to the Parker, both stages are spool based and leaking, and the valve also appears quite bulky. In academia, moving coil actuators have been studied for valve applications requiring fast control [49, 59, 97] and as mentioned have been studied for DDMs in [72]. In this work, a moving coil actuated valve for high-speed DD operation have been designed which is introduced in Paper **D** & **I**.

In [94] a bi-stable valve with a novel actuator is introduced which also uses permanent magnets in the core. The moving member is, similarly to the valve discussed in Figure 1.10, composed of two parts which can move relatively to each other: one part is the armature and another is the hydraulic part controlling the flow through the valve. By accelerating the armature and then impacting the hydraulic part, fast transition times are achieved. This is also the reason why the authors have dubbed the concept a hammer valve. Bi-stability is achieved by using a permanent magnet in the stationary actuator core making the armature latch to both the opened and closed position. Furthermore, a novel method [38] for reducing the axial flow forces acting on moving member was utilized in the valve design and the design was leakage free. Even though this concept has several attractive properties it is not well suited for DDMs as the flow capacity of the valve is much too small (3.3 l/min @ 10 bar).

As shown in [79], linear actuators which uses permanent magnets attached to the moving member may also be well suited for DDMs. Coils

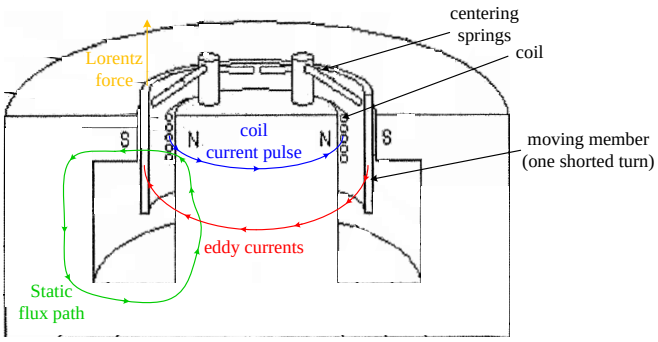

Fig. 1.14: Illustration of the working principles of the actuator disclosed in patent [14].

are incorporated in the stationary housing and is used for generating magnetic fields which oppose or assist the permanent magnet field dependent of the coil current direction. Studies on moving magnet actuators are published in [25,39] which demonstrate fast response and long stroke capabilities. Also, in Paper **J** & **K** a moving magnet actuated valve for high-speed DD operation is proposed.

A novel electro-magnetic actuator concept which could possibly be well suited is disclosed in the patent [14]. As discussed, if using normally opened valves, electro-magnetic actuation is only required for short periods of time during closing of the valve. This could possibly be achieved using the actuator concept of [14] which has been illustrated in Figure 1.14. The actuator armature is a shorted cylinder situated in a DC magnetic field (generated using permanent magnets, or an additional coil increasing the controllability). As shown, a coil is situated closely to the shortened armature which is used to induce eddy currents. As the armature is situated in a DC magnetic field, eddy currents leads to a transient Lorentz force. The behavior of the eddy currents, and thereby the actuator force, can to some extent be controlled by the current of the stationary coil. However, since eddy currents are a transient phenomenon, this actuator concept is only capable of generating force in the same direction for short periods of time making it unsuitable for normally closed valves. But, in case of normally opened valves, such a actuator concept could be well suited for DDMs since a remarkably fast response could obtained. However, it is not known whether electro-magnetic forces of proper magnitudes or durations are achievable using this concept — this is left for future studies.

1.4 Aims & Focus of Research

The overall aim of this research is design and testing of novel valve concepts for DDMs. Especially, the electro-magnetic valve actuator is in focus.

As pointed out in the introduction, DDMs have remarkable potential for improving the efficiency of variable displacement fluid power machinery. The fast switching valves are key components, and in order for the technology to succeed the valves must induce very low flow and electrical losses while enduring billions of operation cycles. The objectives being multiple and conflicting makes these valves relatively complex to design. The aims and focus of the research is listed below:

- A major research objective is to formulate optimization problems which considers all phenomena dominating the losses and the transient switching performance of the valve and actuator. The favored approach is to use a dynamic simulation model of a single pressure chamber including valves for evaluation of said quantities. To perform optimization, the models must be fast executable and generic. Suitable models do not always exist and a substantial task is to develop the required models that enable evaluating objectives accurately and rapidly when varying different parameters (geometric, material, etc.).
- The research has primarily focused on actuator topologies which are relatively new to hydraulics and certainly to digital pumps/motors. As discussed, a possible limitation of the revolution speed of state-of-the-art DDMs could be related to the achievable switching performance using solenoid actuators. Improving the switching performance of DDM valves could therefore possibly increase the revolution speed and the potentials of DDMs even further. This has motivated the exploration of untraditional electro-magnetic actuators for switching the valves.
- To properly verify the performance and viability of proposed valve concepts, extensive prototyping and testing is required. Therefore, it has been a goal to build prototypes and laboratory set-ups facilitating carrying out the desired tests. To establish proof-of-concept, a test-rig has been built which enables performing different variants of DD operation using a single piston and two prototype valves.
- Finally, a research objective was to study and develop methods to indirectly to estimate the behavior switching valve as such information is useful for monitoring and diagnostics purposes.

In Figure 1.15, the main tasks of the present work, the work flow, and which publications relate to which tasks are visualized. As the figure show,

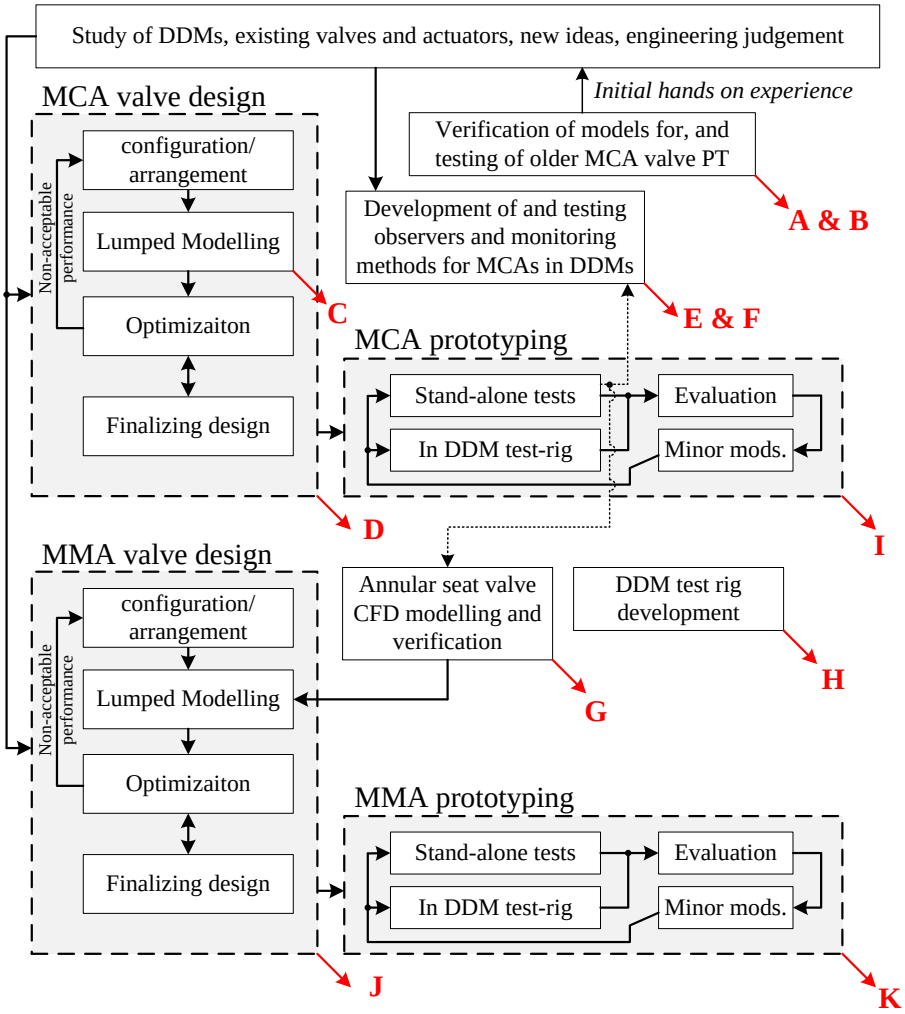

Fig. 1.15: Illustration of the main task, the work flow, and the publications of the present research. A few explanatory notes to ease interpretation of the figure: the capital letters reference to the list of publication given on page v and the dashed black lines indicate that experimental tests have been used in the study.

the research has primarily revolved about the development, design (incl. modeling and optimization) and testing of a MCA and a moving magnet actuated (MMA) valve prototype. Also, early in the research experimental research was carried out on an older MCA valve prototype developed in [72] with the objective of gaining further hands-on experience with DDM valves and to investigate the accuracy of models used in the valve design process.

1.5 Main Contributions

The main contributions of this research are:

- An analytical lumped model was developed for simulating the time-dependent behavior of moving coil actuated valves. Emphasis was put into inclusion of eddy current effects in the model. This work is published primarily in paper **C** and parts are summarized in paper **D**.
- A methodical study was conducted of different moving coil actuators design configurations (permanent magnet placement, orientation etc.). Using multi-objective optimization, optimal actuator designs are derived for each design configuration. The most suited design has been matured, refined and realized into a prototype valve for DDMs. A similar optimization study was carried out for moving magnet actuated valves for DDMs. The performances of both prototypes have been rigorously tested establishing proof-of-concept for both prototypes. The optimization studies are published in papers **D** and **J** for the moving coil and moving magnet actuated valve, respectively. The performance tests are documented in papers **I** and **K** which have been submitted for publication.
- A test rig has been developed and built for DD valve prototypes. A single piston/cylinder of an existing fixed displacement radial piston motor was modified to accommodate DD operation using prototype valves. Currently, three different DD valve prototypes have been tested. In the near future, more prototypes and different control strategies are to be tested. Details about the test set-up are published in paper **H**.
- Methods for estimating the movement of moving coil actuated valves in DDMs only based on measurements of the coil current and voltage have been developed. Also, a method for tracking (and monitoring) of fundamental actuators parameters of moving coil actuated valves in DDMs have been proposed. This work is published in papers **E** and **F**.

Also, in the following chapter an analysis of the general valve requirements for DDMs is presented. The analysis leads to concise requirements to the flow capacity and switching time of valves used in DDMs.

1.6 Reading Guidelines

Chapter 2 presents an analysis of performance requirements of the valves of DDMs. This analysis has not been published elsewhere.

Chapter 3 gives a review of two optimization routines for moving coil actuated and moving magnet actuated valves for DDMs. The majority of this work is based on paper **D** and **J**.

Chapter 4 presents experimental results obtained using the developed prototypes. Also, verification of the models used in the design process is in focus. The majority of this work is also documented in paper **I** and **K**.

Finally, the main conclusions are presented along with a discussion of the work that lies ahead.

Chapter 2

General Valve Requirements

The objective of this chapter is to establish general valve requirements for energy efficient DD operation. A major advantage of the DD technology is a potential increase in efficiency compared against traditional fluid power machinery, especially at part load. But what are the requirements to the valves in terms of pressure drop and switching time in order for achieving efficient DD operation? This is sought clarified through the analysis presented in this chapter.

As the DD technology still is emerging limited research has been published with the objective of establishing general requirements for the valves of DDMs. In [54] an efficiency analysis is presented comparing DDMs and conventional fluid power machinery based on valve plate designs. Requirements to the valve opening area and switching time are formulated based on a 4.3 CC chamber running DD pumping operation at 3000 RPM. The requirements derived are similar to what is presented in this chapter, however, only limited information is included in [54] making it difficult to understand where the valve losses are originating from. More recent studies are published in [77] where valve flow losses are investigated during DD operation cycles using a simple dynamic simulation model representing a single DD pressure chamber and valves. The authors derive general requirements to the valve switching time and the pressure drop coefficient for the valves. However, some of the assumptions the analysis is based on tend to overestimate the losses occurring during valve switching, especially if using seat/poppet based valves (elaborated later in this chapter). To the best knowledge of the author, besides [54, 77], no other research has been published on systematically deriving requirements to the valves of DDMs. However, in literature, several statements about general valve requirements and losses have been made, some of which have been summarized below:

- A switching time of 3 ms for the main stage spool valve used in the digital, non-electrical, pump/motor of [70] is considered *"more than fast enough for a pump/motor operation at 1800 RPM"*.
- *"The electric power consumption of the valves should be at maximum few percent of the maximum power of the pump in order to retain good efficiency"* [46].
- *"The valve throttling loss and electrical energy consumption loss makes up 96% (partial F-D) to 88% (sequential F-L) of the total losses depending on the operating strategy. This shows the need for a fast acting valve that requires low electrical consumption"* [53].
- *"The repeatability of the on/off valve needs to be less than 1 ms regardless of the pressure across the valve for high-speed operation or partial flow strategies"* [53].

The method presented in [77] is also the starting point of the analysis carried out in this chapter. Initially, the model and method of the analysis is explained further and the results of [77] are recreated. Then, the focus is briefly turned towards how well the machine is utilized, an important aspect not previously considered, to the knowledge of the author. Thereafter, attention is put on improvement of the analysis leading to more accurate valve requirements. Finally, the analysis is extended to derive valve requirements for efficient operation in case of using only partial displacement strokes.

The studies and results shown in this chapter have not previously been published. However, as pointed out, the method is based on [77]. Some of the analysis overlaps with studies published in Paper **G** which are brought into context at the end of this chapter.

2.1 Model and Method

A simple generic dynamic simulation model of a single pressure chamber is used to evaluate the flow losses during DD operation cycles. The model basis is given in Equation (2.1) and illustrated in Figure 2.1.

$$
\begin{aligned}
\dot{p}_\mathrm{c} &= \frac{\beta}{V}\left(Q_\mathrm{H} - Q_\mathrm{L} - \dot{V}\right), \\
Q_\mathrm{L} &= \frac{\overline{x}_\mathrm{L}}{k_\mathrm{f}}\sqrt{|\Delta p_{\mathrm{valve,L}}|}\mathrm{sign}\left(\Delta p_{\mathrm{valve,L}}\right) \;\; \text{where} \;\; \Delta p_{\mathrm{valve,L}} = p_\mathrm{c} - p_\mathrm{L}, \\
Q_\mathrm{H} &= \frac{\overline{x}_\mathrm{H}}{k_\mathrm{f}}\sqrt{|\Delta p_{\mathrm{valve,H}}|}\mathrm{sign}\left(\Delta p_{\mathrm{valve,H}}\right) \;\; \text{where} \;\; \Delta p_{\mathrm{valve,H}} = p_\mathrm{H} - p_\mathrm{c}.
\end{aligned} \tag{2.1}
$$

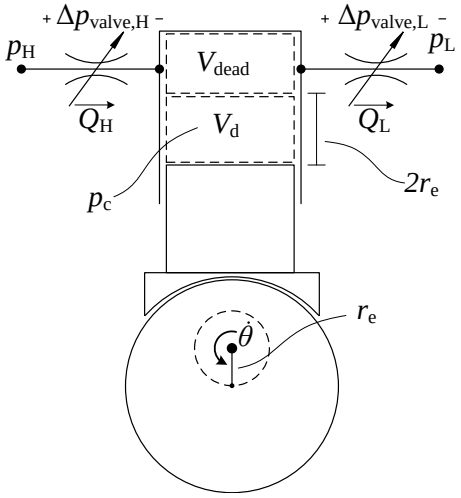

Fig. 2.1: Model of a single pressure chamber with the piston illustrated at $\theta = \pi$.

The cylinder pressure is modeled using the continuity equation and the valve flows are modeled using the orifice equation. The valves are assumed equal throughout this chapter as done in [77] [1]. The volume of the cylinder is modeled assuming a sinusoidal movement of the piston with the displacement volume V_d and the dead volume V_dead:

$$\begin{aligned} V(\theta) &= \frac{V_\mathrm{d}}{2}\left(1-\cos\theta\right) + V_\mathrm{dead}, \\ \dot{V}(\theta,\dot{\theta}) &= \frac{V_\mathrm{d}}{2}\dot{\theta}\sin\theta. \end{aligned} \tag{2.2}$$

The valve movement is normalized and modeled by prescribing a trajectory to the valves only defined by the valve switching time. In the study presented in [77] the valve movement, during closing of the valve, is modeled assuming a constant acceleration and deceleration for the first and last half of the stroke, respectively:

$$\overline{x} = \iint a\,dt \text{ where } a = \begin{cases} -\frac{4}{t_\mathrm{s}^2} \text{ for } 0 < t < \frac{1}{2}t_\mathrm{s} \\ \frac{4}{t_\mathrm{s}^2} \text{ for } \frac{1}{2}t_\mathrm{s} \leq t < T_\mathrm{s} \end{cases}, \tag{2.3}$$

where t_s is the valve switching time. For valve openings, an corresponding approach is used i.e. the first half of the switching time, the acceleration is positive and negative for the latter half. In [77] a method for calculating the shaft angles at which the closings of the valves should be initiated is

[1] As pointed out in the introduction, this is not necessarily the case and typically a larger flow area is emphasized for the LPV to retain high-efficiencies at low displacement ratios

also presented. This method is based on the valve switching sequence being completed at the dead centers. A review for the active closing of the LPV when approaching the TDC is given here, starting with the angle at which the pressurization should be completed allowing for time to open the HPV before the TDC.

$$\theta_{\text{pres, f}} = 2\pi - t_{\text{s}}\dot{\theta}, \tag{2.4}$$

where the volume at the angle $\theta_{\text{depres, f}}$ is found using Equation (2.2) and denoted $V_{\text{depres, f}}$. The chamber volume when the pressurization is initiated $V_{\text{depres, i}}$ is calculated using the continuity equation while assuming no valve flows:

$$\begin{aligned} \int_{p_{\text{L}}}^{p_{\text{H}}} \frac{1}{\beta} dp &= \int_{V_{\text{depres, i}}}^{V_{\text{pres, f}}} -\frac{1}{V} dV \\ \Rightarrow V_{\text{pres, i}} &= V_{\text{pres, f}} e^{\frac{p_{\text{H}} - p_{\text{L}}}{\beta}}. \end{aligned} \tag{2.5}$$

The angle which corresponds to the volume $V_{\text{pres, i}}$ is denoted $\theta_{\text{pres, i}}$ and also found using Equation (2.2). Similarly to Equation (2.4) the angle at which the LPV should initiate closing is found as:

$$\theta_{\text{cl, LPV}} = \theta_{\text{pres, i}} - t_{\text{s}}\dot{\theta}. \tag{2.6}$$

An analogue approach is used for calculating when to close the HPV. The openings of the valves are initiated when the chamber pressure crosses the manifold pressure level subsequent to the chamber pressure change.

To evaluate the efficiency at any displacement ratio, the model is evaluated for one idling and one motoring cycle from which the input and output energies are evaluated using:

$$\begin{aligned} E_{\text{in}} &= \int_0^{T_{\text{rev}}} Q_{\text{H}} p_{\text{H}} - Q_{\text{L}} p_{\text{L}} + \overbrace{\left(\dot{V} + Q_{\text{L}} - Q_{\text{H}}\right) p_{\text{c}}}^{P_{\text{comp}}} dt, \\ E_{\text{out}} &= \int_0^{T_{\text{rev}}} \tau_{\text{m}} \dot{\theta} dt = \int_0^{T_{\text{rev}}} \frac{V_{\text{d}}}{2} p_{\text{c}} \dot{\theta} \sin\theta \, dt, \end{aligned} \tag{2.7}$$

where τ_{m} is the torque exerted on the shaft, T_{rev} is the revolution time and P_{comp} represents the compression power. Based on the input and output energies for one cycle the efficiency is calculated using:

$$\eta = \frac{E_{\text{out}}}{E_{\text{in}}} = \frac{E_{\text{in}} - E_{\text{loss}}}{E_{\text{in}}}. \tag{2.8}$$

As pointed out in [77], the expression may be expanded to determine the efficiency at partial displacement:

$$\eta_{\alpha} = 1 - \frac{\alpha E_{\text{loss, motoring}} + (1-\alpha) E_{\text{loss, idling}}}{\alpha E_{\text{in, motoring}} + (1-\alpha) E_{\text{in, idling}}}, \tag{2.9}$$

where α is the machine displacement ratio coefficient. This is assuming all active chambers of the machine are identical and operated with the same valve switching angles. Finally, the valve flow losses are defined as:

$$E_{\text{loss, L}} = \int \Delta p_{\text{valve,L}} Q_{\text{L}} dt, \; E_{\text{loss, H}} = \int \Delta p_{\text{valve,H}} Q_{\text{H}} dt. \tag{2.10}$$

The valve flow losses $E_{\text{loss, L}}$ and $E_{\text{loss, H}}$ are not used directly in the efficiency calculations, but are defined since the valve flow losses are plotted several times this chapter.

An example of the dynamic simulation is shown in Figure 2.2 using the model parameters of Table 2.1 on page 39, a switching time t_{s} of 3.6 ms and a flow-pressure coefficient k_{f} of $2.8 \times 10^{-3} \sqrt{\text{bar}}\,\text{min/L}$ while operating a chamber of 50 CC at 800 RPM. The model is evaluated for *one* idling and *one* motoring operation cycle. The chamber pressure is seen to over-shoot after both pressurization and depressurization of the chamber. This occur due to the relatively slow opening of the valves and leads to relatively large flow losses as can be seen from the gradient of $E_{\text{loss,L}}$ and $E_{\text{loss,H}}$ at the time of the valve openings. Note that the negative chamber pressures occurring after the depressurization are not physical possible and only occur since no pressure dependent fluid-stiffness model is included in this study. This also tends to overestimate the flow losses. Considerable losses also occur during closing of the valve. This happens primarily due to the prescribed valve movement of Equation (2.3). It leads to a low velocity prior to reaching the fully closed state which in turn leads to considerable flow losses as a notable amount of flow is conducted with low valve positions. After *one* idling and *one* motoring cycling, corresponding to a machine displacement ratio of 50%, the flow losses are seen to constitute approximately 2% of the transferred energy.

By keeping the machine-related parameters i.e. β, V_{d}, V_{dead} and $\dot{\theta}$ constant while sweeping through the valve related parameters i.e. t_{s} and k_{f}, simulation data is obtained from which maps representing the efficiency at that operation point is obtained. In [77] the authors found that the results may be generalized by introducing:

$$\begin{aligned} \bar{t}_{\text{s}} &= \frac{t_{\text{s}}}{T_{\text{rev}}} \text{ where } T_{\text{rev}} = \frac{2\pi}{\dot{\theta}}, \\ \bar{k}_{\text{f}} &= \frac{k_{\text{f}}}{\frac{\sqrt{p_{\text{H}} - p_{\text{L}}}}{Q_{\text{mean}}}} \text{ where } Q_{\text{mean}} = \frac{\dot{\theta} V_{\text{d}}}{\pi}. \end{aligned} \tag{2.11}$$

This makes the results independent of the revolution speed and the nominal valve flow rate. This enables constructing a general efficiency map only spanned by $\bar{t}_{\text{s}}$ and $\bar{k}_{\text{f}}$. Figure 2.3 shows such efficiency maps for 20% and 100% displacement ratio. The results are identical to the efficiency maps

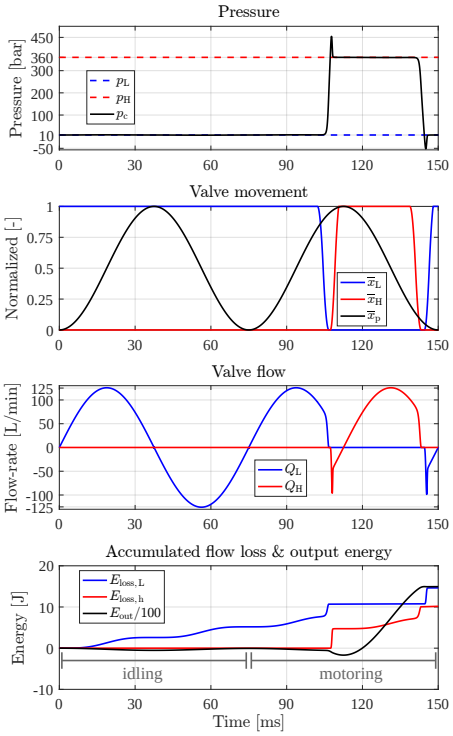

Fig. 2.2: The underlying simulation representing the highlighted point of Fig. 2.3.

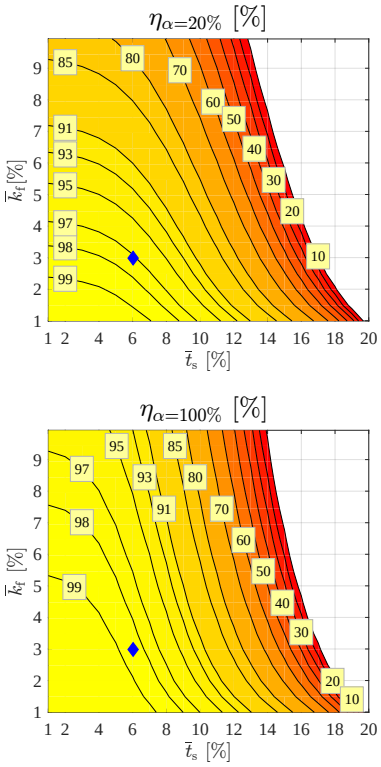

Fig. 2.3: Recreated efficiency maps of [77] at full and part displacement.

published in [72, 77] and have been generated using the model coefficients listed in Table 2.1. The normalized switching time is easy to interpret and the results show that the efficiency drops for switching times slower than approximately 5% of the revolution time. The normalized flow pressure coefficient is more difficult to comprehend and therefore a new metric is suggested. If inserting $k_f = \frac{\sqrt{\Delta p_{valve}}}{Q}$ into (2.11) and evaluating the orifice expression at the maximum flow rate the following is obtained:

$$\overline{k}_f = \frac{2\sqrt{\Delta p_{valve,\,max}}}{\pi\sqrt{\Delta p_{machine}}}, \tag{2.12}$$

where $p_{valve,\,max}$ is the valve pressure drop at the maximum flow rate. If squaring the normalized flow pressure coefficient a more intuitive metric for accessing the allowable valve pressure drop is obtained:

$$\frac{\Delta p_{valve,\,max}}{\Delta p_{machine}} = \frac{\pi^2}{4}\overline{k}_f^2. \tag{2.13}$$

To gain an understanding of this metric compared to the normalized flow-pressure coefficient, the results of Figure 2.3 are plotted again using the new metric in Figure 2.6 on page 43. The results show that in order to achieve efficiencies above 96% at full load the valve pressure drop at the peak flow rate must be below approximately 2.5-3% of the machine pressure span. However, at 20% displacement ratio, the valve pressure drop may only constitute approximately 0.5% of the machine pressure span. This demonstrates the motivation for having a larger LPV well, since the HPV is kept closed for idling cylinders and thereby not contributing to losses.

The model parameters in Figure 2.1 are used for the results presented throughout this chapter (except for Fig. 2.5). The chamber displacement volume corresponds to that to DD test rig (cf. Chapter 4). chosen oil bulk modulus corresponds to the mean stiffness of pure oil (experimentally verified in [34]).

Table 2.1: Constant parameters used in the analysis.

Parameter	Value	Description
$\dot{\theta}$	800 RPM	shaft speed
β	16000 bar	Bulk modulus
p_{L}	10 bar	Low manifold pressure
p_{H}	360 bar	High manifold pressure
V_{d}	50 CC	Displacement volume
V_{dead}	50 CC	Dead volume
$K_{\mathrm{area/mass}}$	0.2 cm^2/g	Ratio of seat area to mass

2.2 DDM Utilization

Besides obtaining high machine efficiency the energy output of each active motoring cycle should be close to the optimum energy output in the case of full stroke operation. For a conventional fluid power piston type machine with instant and ideal commutation executed at the dead centers, the energy output of one operation cycle is:

$$E_{\mathrm{con,out,ideal}} = V_{\mathrm{d}} \Delta p_{\mathrm{machine}}. \tag{2.14}$$

For DD motoring, the optimal output is less since the pressurization and depressurization of the chamber must be done prior to the respective dead centers in order for the sub-sequent passive valve opening to occur. The following presents an derivation of the maximum energy output for a DDM chamber operating in motoring mode.

The energy output during one operation cycle is calculated analytically using integration by parts of the optimal power curve shown in Figure 2.4

along with the cylinder pressure and the piston movement. The shown power curve is defined by the cylinder pressure change is completed at the dead centers and assumes infinitely fast switching. During the periods with constant chamber pressure (intervals 1 and 3 in Fig. 2.4), the mechanical power transferred to the shaft is expressed as:

$$P_{\text{out},1}(\theta) = \frac{1}{2}\, p_{\text{H}}\, V_{\text{d}}\, \dot{\theta}\, \sin(\theta)\,,$$
$$P_{\text{out},3}(\theta) = \frac{1}{2}\, p_{\text{L}}\, V_{\text{d}} \dot{\theta}\, \sin(\theta)\,. \tag{2.15}$$

The instantaneous power during depressurization and pressurization (interval 2 and 4 in Fig. 2.4, respectively) are:

$$P_{\text{out},2}(\theta) = \frac{1}{2}\left(p_{\text{L}} - \beta\, \ln\left(\frac{1/2\, V_{\text{d}}\ (1-\cos(\theta)) + V_{\text{dead}}}{V_{\text{d}} + V_{\text{dead}}}\right)\right) V_{\text{d}}\, \dot{\theta}\, \sin(\theta)\,, \tag{2.16}$$

$$P_{\text{out},4}(\theta) = \frac{1}{2}\left(p_{\text{H}} - \beta\, \ln\left(\frac{1/2\, V_{\text{d}}\ (1-\cos(\theta)) + V_{\text{dead}}}{V_{\text{dead}}}\right)\right) V_{\text{d}}\, \dot{\theta}\, \sin(\theta)\,. \tag{2.17}$$

The energy transferred to the shaft during one cycle is calculated as:

$$E_{\text{DD, cycle, motor}} = \frac{1}{\dot{\theta}} \int_0^{\theta_{\text{depres}}} P_{\text{out},1}(\theta) d\theta + \frac{1}{\dot{\theta}} \int_{\theta_{\text{depres}}}^{\pi} P_{\text{out},2}(\theta) d\theta$$
$$+ \frac{1}{\dot{\theta}} \int_{\pi}^{\theta_{\text{depres}}} P_{\text{out},3}(\theta) d\theta + \frac{1}{\dot{\theta}} \int_{\theta_{\text{depres}}}^{2\pi} P_{\text{out},4}(\theta) d\theta, \tag{2.18}$$

where θ_{depres} and θ_{pres} are the angles at which the depressurization and pressurization should initiate. Using Equations (2.2) and (2.5) these are expressed as:

$$\theta_{\text{pres}} = -\arccos\left(\left(V_{\text{d}} + 2\, V_{\text{dead}} - 2\, V_{\text{dead}}\, \text{e}^{\frac{\Delta p_{\text{machine}}}{\beta}}\right) {V_{\text{d}}}^{-1}\right), \tag{2.19}$$

$$\theta_{\text{depres}} = -\arccos\left(\left(2\, V_{\text{dead}} - 2\, \text{e}^{-\frac{\Delta p_{\text{machine}}}{\beta}}\ (V_{\text{d}} + V_{\text{dead}})\right) {V_{\text{d}}}^{-1} + 1\right). \tag{2.20}$$

Evaluating Equation (2.18) and simplifying the energy transferred to the shaft during one ideal motoring cycle is:

$$E_{\text{DD,out,ideal}} = \left(-\beta\left(\text{e}^{-\frac{\Delta p_{\text{mac.}}}{\beta}} + \text{e}^{\frac{\Delta p_{\text{mac.}}}{\beta}} - 2\right)\frac{V_{\text{dead}}}{V_{\text{d}}} - \beta\left(\text{e}^{-\frac{\Delta p_{\text{mac.}}}{\beta}} - 1\right)\right) V_{\text{d}}, \tag{2.21}$$

where $\Delta p_{\text{mac.}}$ is an abbreviation of machine pressure span $\Delta p_{\text{machine}}$.

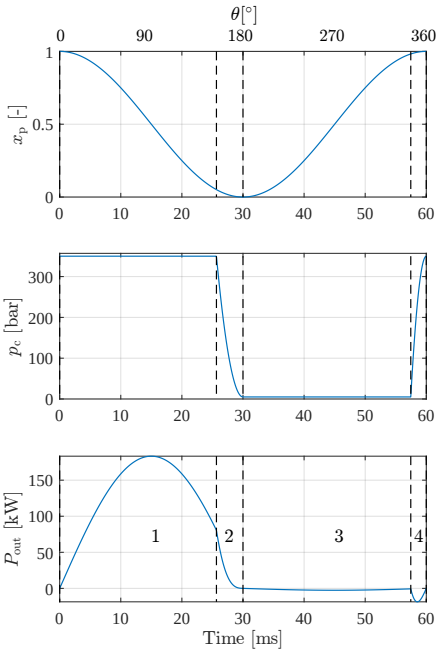

Fig. 2.4: Ideal DD motoring operation cycle for with $p_L = 5$ bar, $p_H = 350$ bar, $V_d = 100$ CC,$V_{dead} = 50$ CC, $\beta = 10,000$ bar and $\dot{\theta} = 1000$ RPM.

The analysis has also been carried out for DD pumping operation cycles. For optimal DD pumping operation, defined by initiating the pressurization and depressurization at the dead centers, the optimal energy received from the shaft during one operation cycle is identical to Equation (2.21).

Based on Equation (2.21) it is investigated how much lower the ideal output of one cycle is compared to the ideal conventional fluid power machine output defined in Equation (2.14):

$$\frac{E_{\text{DD, out, ideal}}}{E_{\text{con, out, ideal}}} = \frac{E_{\text{DD, out, ideal}}}{\Delta p_{\text{machine}} V_d} = \left(-\beta \left(e^{-\frac{\Delta p_{\text{mac.}}}{\beta}} + e^{\frac{\Delta p_{\text{mac.}}}{\beta}} - 2\right) \frac{V_{\text{dead}}}{V_d} - \beta \left(e^{-\frac{\Delta p_{\text{mac.}}}{\beta}} - 1\right)\right) \Delta p_{\text{machine}}^{-1}. \tag{2.22}$$

Figure 2.5 shows Equation (2.22) as a function of $\frac{V_{\text{dead}}}{V_d}$ and $\Delta p_{\text{machine}}$ for β equal to 5,000 bar (*left*) and 10,000 bar (*right*). The results show that the ideal output of DDMs at worst case is only approximately 84% of the ideal output power of conventional machines calculated using 2.14. This naturally occur when having a relatively large dead volume combined with low fluid stiffness and high machine pressure differences since most of the piston stroke is used

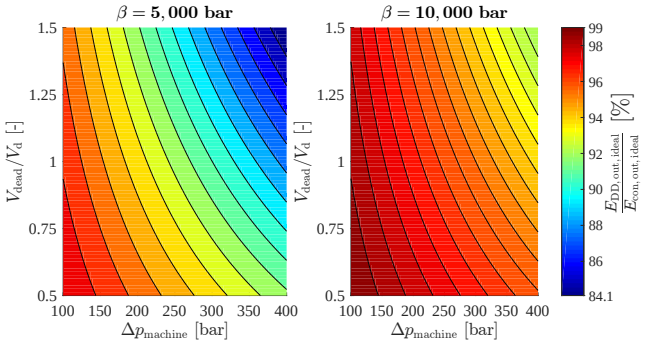

Fig. 2.5: Ideal output of DDMs vs. conventional piston machines, as a function of the ratio of the dead volume to the displacement volume and the machine pressure difference for the bulk modulus equal to 5,000 bar (left) and 10,000 bar (*right*).

for compression and decompression of the chamber. It should be noted that if none of the chamber displacement is used for pressurization or depressurization i.e. instant commutation at dead centers, large flows are required for rapid equalization of the chamber pressure which is undesirable. Therefore, conventional pistons machines of today are unlikely to utilize the chamber much better than what is possible with DD technology since some chamber displacement still is used to avoid excessive losses and pressure fluctuations in the manifolds. However, the expression of Equation (2.22) is still useful for easily determining how closely a DD chamber is operating to the optimum with respect to energy output. This is defined as the utilization factor of a DDM chamber denoted UF_{DD} and is expressed as:

$$UF_{DD} = \frac{E_{out}}{E_{DD,\,out,\,ideal}}. \tag{2.23}$$

The efficiency maps of Figure 2.3 and a map showing the DDM utilization factor is plotted in Figure 2.6 using the metric of Equation (2.13) as the vertical axis. The utilization map shows that extraordinary fast switching is required to get better values of UF_{DD} than 96%. At slower switching times, the utilization factor drops severely. This is because of the implemented timing method which is based on the valve switching sequence being completed at the dead centers. This means that a slower switching time leads to earlier pressurization and depressurization which makes the energy output decrease. The dynamic simulation results shown to the right are for the highlighted points of the contour plots which correspond roughly to the MCA valve prototype presented in this thesis when operating a 50 CC chamber at 1000 RPM.

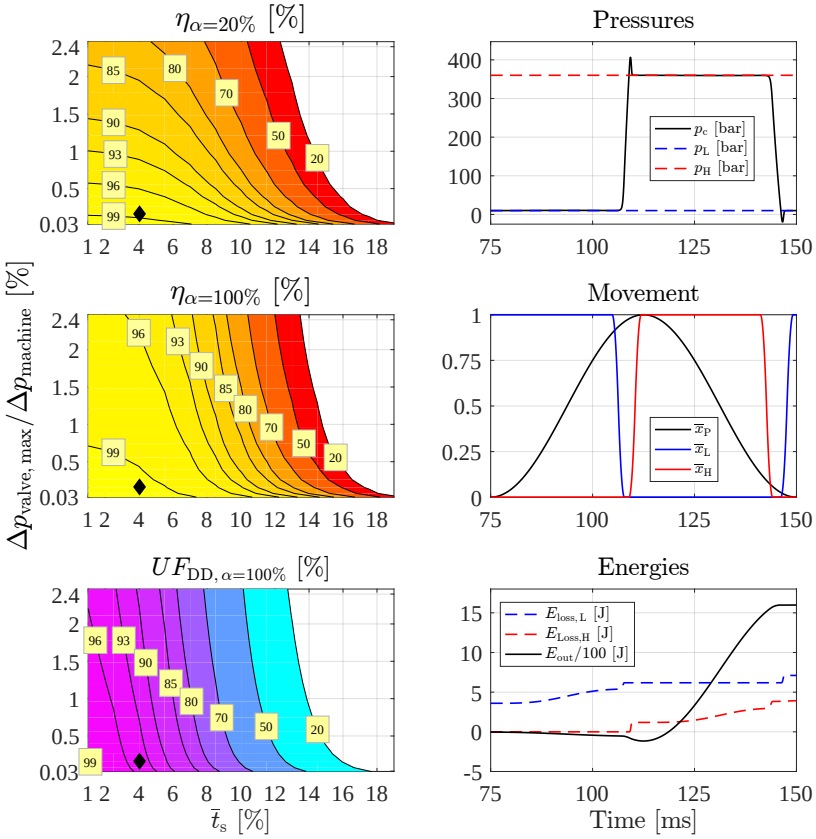

Fig. 2.6: Efficiency and machine utilization using the same assumptions as in [77]. The dynamic simulation results (*right*) corresponds to the black highlighted point. The highlighted blue point corresponds to the highlighted point in Figure 2.3. Model parameters are given in Table 2.1.

2.3 Improvement of Analysis

With the recreation of the results published in [77], the introduction of the DD utilization factor and the more intuitive metric for understanding the allowable valve pressure drop, attention is turned to improvement of the analysis. As pointed out, the assumptions made in the analysis carried out in [77] leads to excessive flow losses during valve switching and low machine utilization, both because of the prescribed valve movement and the used timing sequence. The actions made to improve it are elaborated below:

- **Valve Movement**
  At small plunger positions the plunger movement is strongly dominated by the axial forces originating from the pressure drop across the

valve seat. This means that both slow landing and slow departure of the valve seat does not necessarily occur. For a better representation of the actual valve dynamics a constant feedforward term is used along with a valve pressure dependent term:

$$\overline{x} = \iint a\,dt \text{ where } a = \begin{cases} -\frac{2}{t_s^2} + \Delta p_{\text{valve}} K_{\text{area/mass}} & \text{for closings} \\ \frac{2}{t_s^2} + \Delta p_{\text{valve}} K_{\text{area/mass}} & \text{for openings} \end{cases} \tag{2.24}$$

where $K_{\text{area/mass}}$ is defined as 0.2 cm^2/g roughly based on the MCA valve prototype presented in this thesis (when equipped with titanium plunger) and the valve pressure drop defined accordingly to Equation (2.1). Introducing the pressure dependent term means that the exact valve switching time is unknown which is a prerequisite for calculating the angles at which the valve switching sequence should be initiated. When using the constant acceleration term this effect only influence the movement vaguely during closing since the velocity is largest on impact leaving only little time to build up pressure difference. In case of the valve opening, the effect has more pronounced influence and may lead to severely reduced opening times. In spite of this, t_s is used for valve timing calculations.

- **Valve Timing**
  The timing scheme used in [77] leads to excessive valve loss and low machine utilization. The method is based on the passive valve opening being completed (the last thing of any successful DD valve switching sequence) at the dead centers. For optimal DD operation, the passive valve openings should only be initiated at the dead centers since the switchings then are performed at lower flow rates, and a smaller amount of negative work is carried out. To better represent the valve requirements in case of optimal DD operation the angle at which the valve sequence should be initiated is calculated as:

$$\begin{aligned} \theta_{\text{cl, LPV}} &= \theta_{\text{pres}} - t_s\dot{\theta}, \\ \theta_{\text{cl, HPV}} &= \theta_{\text{depres}} - t_s\dot{\theta}, \end{aligned} \tag{2.25}$$

  where θ_{pres} and θ_{depres} represent the angles at which the pressurization and depressurization should initiate given in Equations (2.19) and (2.20) respectively. The resulting difference of using this method opposed to the method of [77] is that the valves are being closed later by $t_s\dot{\theta}$.

The influence of the two proposed changes to the analysis is investigated by cross varying them, giving a total of *three* different cases yet to investigate.

2.4 Results

Figure 2.7 through 2.9 shows the results. All simulations were performed using the parameters of Table 2.1. As in Figure 2.6, the prototype design point highlighted in the presented maps corresponds to the prototype valve parameters when operating a 50 CC chamber at 1000 RPM.

From comparing Figure 2.7 against the recreated data of Figure 2.6 it becomes clear that a larger valve switching time is permitted when using the updated valve movement scheme of Equation (2.24). This significantly reduces the flow losses during closing of the valves, as can be seen from comparing the plot in the lower right of both figures. Considerable flow losses are still present during the first stage of the valve openings, even with the pressure dependent term of Equation (2.24) implemented. This occurs partly because the constant feed forward acceleration term of the Equation (2.24) is smaller than the acceleration prescribed in Equation (2.3). Figure 2.8 shows the simulated results using the valve timing of Equation (2.25) but still with the movement prescribed in Equation (2.3). This modification proves to have even bigger impact on results of the analysis. Especially the machine utilization has improved as a consequence of the pressurization and depressurization now occurring closer to the dead centers. Also, the valve switching time is seen to have much less influence on the efficiency. This is because, the valve switchings now occur at a much smaller flow rate. The flow losses during the valve openings are now very small, while the flow losses during valve closing still are considerable.

Finally, Figure 2.9 shows the results of the analysis when implementing both the updated valve movement and timing scheme. The losses during valve switchings are now close to zero leading to the vague influence on the efficiency observed. In fact, the analysis now shows that high efficient operation and a high utilization factor may be achieved even with much slower valves as long as the timing of the valve switchings is close to ideal. The requirements to the flow losses have not changed remarkably and still the valve pressure drop at the maximum flow rate should only constitute approximately 0.5% of the DDM pressure span.

2.5 Partial Flow-Diverting

The part load efficiency η_α is calculating assuming all active chambers of a DDM is operated with identical switching angles. This leads to the most efficient operation since the valves are switched as close to the dead centers as possible. However, it also only enables controlling the machine displacement in discrete steps defined by the individual cylinder displacement volumes. For DDMs having a low number of cylinders, this makes controlling the

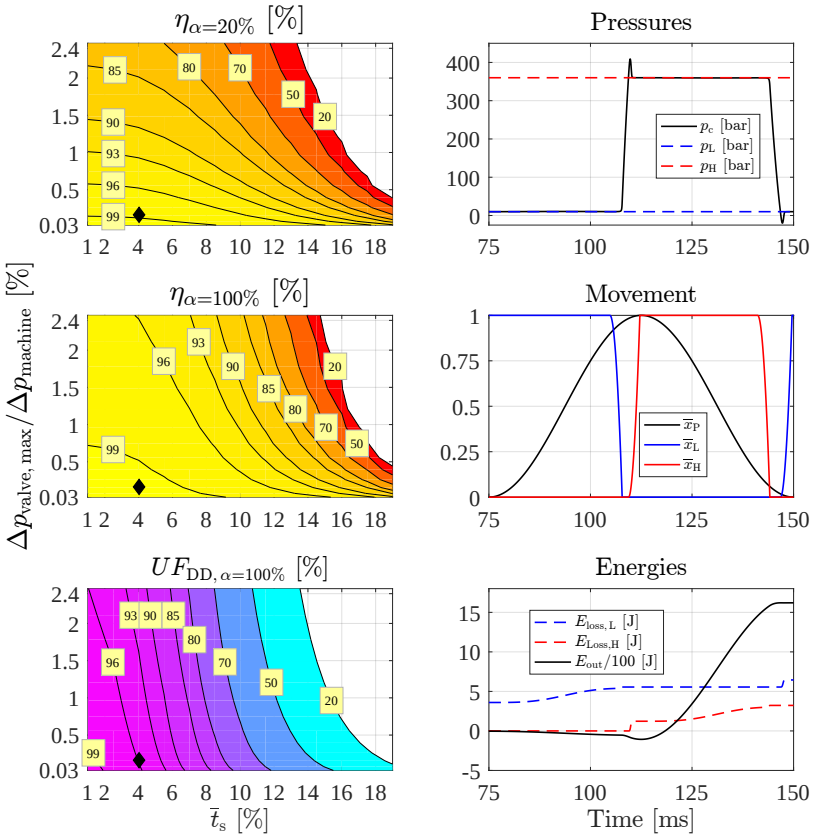

Fig. 2.7: Efficiency at 20% at 100% displacement, machine utilization and dynamic simulation results when implementing the modifications to the valve movement given in Eqn. (2.24).

displacement accurately difficult. To enhance the displacement resolution and thereby the machine controllability alternative valve switching strategies – and in particular the requirements to the valves for them to be successful – are investigated in this section.

By controlling the valves appropriately, partial motoring/pumping strokes may be obtained allowing much enhanced control of the displacement per revolution. In [55] different strategies for controlling the displacement of individual cylinders were explored. Two methods were explored i.e. partial flow-diverting (PF-D) and partial flow-limiting (PF-L). PF-L is dependent on cavitation of the cylinder without the low pressure valve passively opening due to pressure forces. This is not possible when using seat valves and the valve configuration studied in this thesis as pressure forces passively open the LPV when the chamber pressure deceeds the low pressure manifold pressure level.

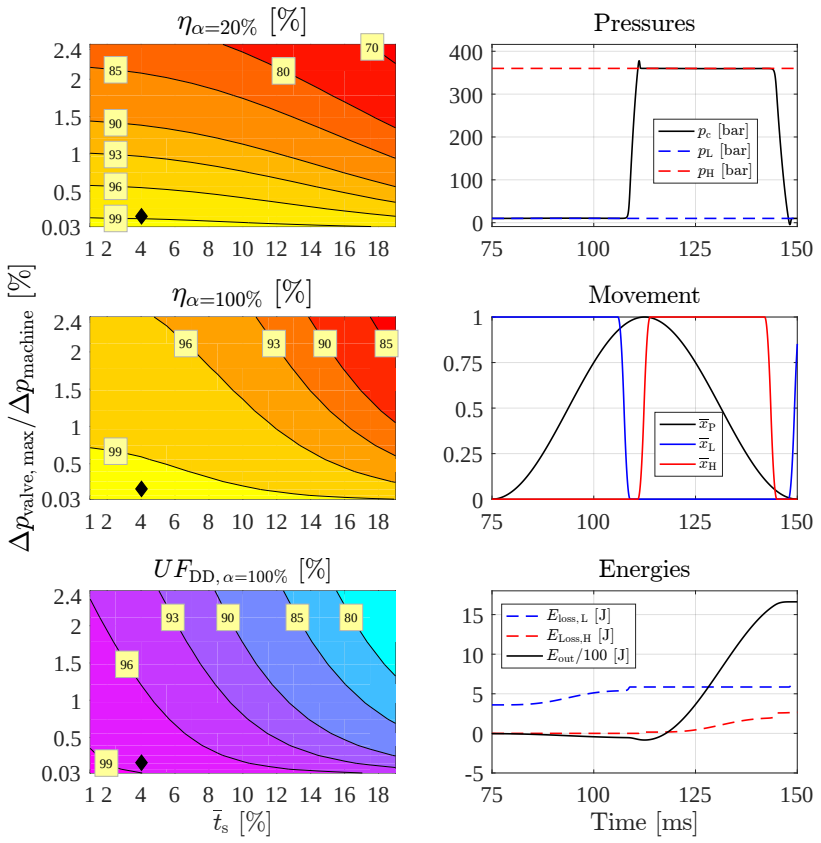

Fig. 2.8: Efficiency, machine utilization and dynamic simulation results when implementing the modifications to the valve timing given in Eqn. (2.25).

PF-D is possible using seat valves and is achieved by only pressurizing the piston parts of it's up or down stroke, for pumping or motoring cycles respectively. For motoring cycles, the pressurization should be still completed as closely to the TDC as possible. As the piston moves downwards, high pressure oil is received from the high pressure manifold until the HPV is actively closed. The chamber displacement is then controlled by the closing angle of the HPV. This approach leads to one of the valve switching sequences being performed at larger flow rates. For seat valves, this is expected to increase the valve landing speed when closing significantly, leading to both increased wear and acoustic noise. Also, switching at larger flow rates is also associated with larger flow losses. Especially the passive opening of the valves may induce considerable losses as notable pressure overshoot may occur when using valves having heavy plungers or small shadow areas (if

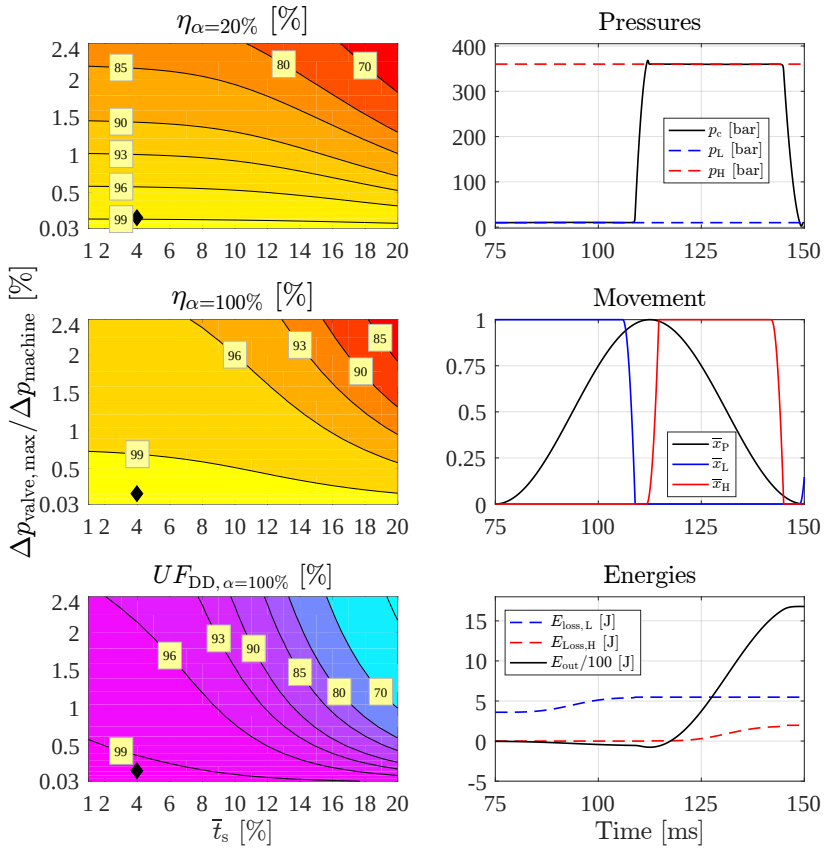

Fig. 2.9: Efficiency, machine utilization and dynamic simulation results when implementing both the suggested modifications to the analysis.

not supplying opening forces ensuring a rapid opening by other means). For motoring PF-D this means that the chamber is prone to cavitation. For pumping PF-D, the overshoot means that the chamber pressure may exceed the high-pressure manifold level which could damage the pressure chamber, if not designed for this. Therefore, both pumping and motoring PF-D cycles should be used with great care.

The efficiency of PF-D during motoring cycles has been investigated using the model of Section 2.1 with the suggested improvements of Section 2.3. The valve requirements are analyzed for three different PF-D cases i.e. 25%, 50%, 75% displacement. The closing angle of the HPV is calculated using:

$$\theta_{\mathrm{cl,HPV}} = \arccos(1 - 2\alpha_{\mathrm{PFD}}) - t_{\mathrm{s}}\dot{\theta}, \tag{2.26}$$

where α_{PFD} is the PF-D load coefficient. In the case of low values of α_{PFD} and large switching times, the HPV opening may not be completed before

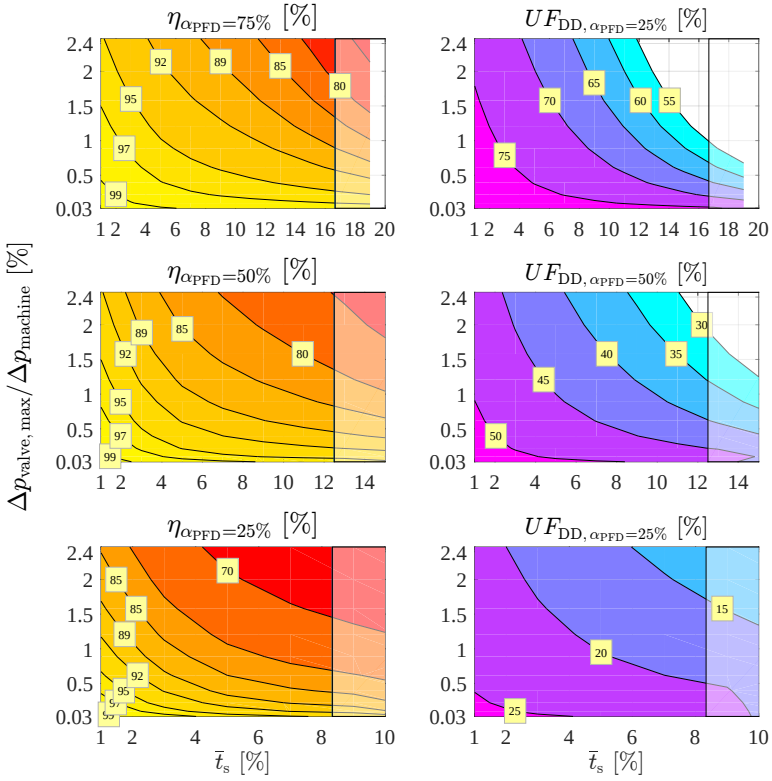

Fig. 2.10: Efficiency and machine utilization at $\alpha_{\mathrm{PFD}} = 25\%$, 50% and 75%.

the HPV closing angle $\theta_{\mathrm{cl,\,HPV}}$. Still using the valve movement of Equation (2.24) this leads to the depressurization occurring prematurely lowering the displaced fluid. For operating cycles having $\theta_{\mathrm{cl,\,HPV}} < t_{\mathrm{s}}\dot{\theta}$ this occurs and is indicated by the translucent areas of the results shown in Figure 2.10. The results show that efficient PF-D is possible for all of the analyzed values of α_{PFD} (when using $K_{\mathrm{area/mass}} = 0.2$ cm^2/g). The switching time can be observed to have more pronounced influence, occurring because the valve switchings are carried out at larger flow rates. To achieve efficiencies above 90% for all cases of α_{PFD} the valve drop should be below 0.5 % of the machine pressure span and the normalized switching time below 5%. The valve requirements for efficient PF-D are thereby stricter than in the case of the full displacement strokes considered in the previous sections, especially with respect to valve switching time.

Sensitivity Analysis of $K_{\text{area/mass}}$

The geometry dependent valve parameter $K_{\text{area,mass}}$ introduced in section 2.3 only have minor influence for full displacement strokes, but for PF-D strokes it is more important for the efficiency (or in general, when switching at larger flow rates). This is shown by calculating the efficiency as a function of k_{f} and t_{s} for different values of $K_{\text{area/mass}}$. The PF-D load coefficient α_{PFD} is set to 0.5 leading to the valve switchings being performed at instants with the largest chamber volume derivatives. The results are shown in Figure 2.11 for three different values of $K_{\text{area,mass}}$ i.e. 0, 0.1 and 0.5 cm^2/g. A value of zero corresponds to the moving member of the valve being completely pressure compensated (possible using spool valves) while a large value represents seat valves where the valve pressure difference influence the valve movement more significant. The results show that $K_{\text{area,mass}}$ influences the valve requirements considerably. For $K_{\text{area,mass}} = 0$, large switching times leads to low efficiency as large losses are induced during the opening of the LPV. As can be seen from the dynamic results, the chamber pressure is seen to be negative and at remarkable magnitudes, indicating that cavitation easily could occur. For larger values of $K_{\text{area,mass}}$ the magnitude of the negative pressure occurring during opening of the LPV is seen to decrease as the valve pressure difference makes the valve open faster leading to less throttling losses.

As pointed out earlier, when using $K_{\text{area,mass}}$ the valve switchings in the simulations are faster than prescribed switching time t_{s}. To get a better understanding of the actual switching times $T_{\text{K,area/mass}}$ is calculated which represents the switching time reduction relative to the normalized switching time:

$$T_{\text{K,area/mass}} = \frac{T_{\text{s,sim}}\dot{\theta}}{\overline{t_{\text{s}}}}, \tag{2.27}$$

where $T_{\text{s,sim}}$ is the valve switching time in the simulation. Equation 2.27 have been evaluated for the LPV for the results shown in Figure 2.11. Figure 2.12 shows the results for the closing (*left*) and the opening (*right*). Note that the $K_{\text{area/mass}} = 0$ case not is shown since $T_{\text{K,area/mass}}$ always is equal to one. The results show that the pressure forces only influence the switching time vaguely for closings but have significant more influence on the opening times.

2.6 Summary of Findings and Outlook

Based on the presented study, it is concluded that high-efficient DD operation using full displacement strokes is possible for a wide displacement range when having valve pressure drops below 0.5% of the machine pressure span.

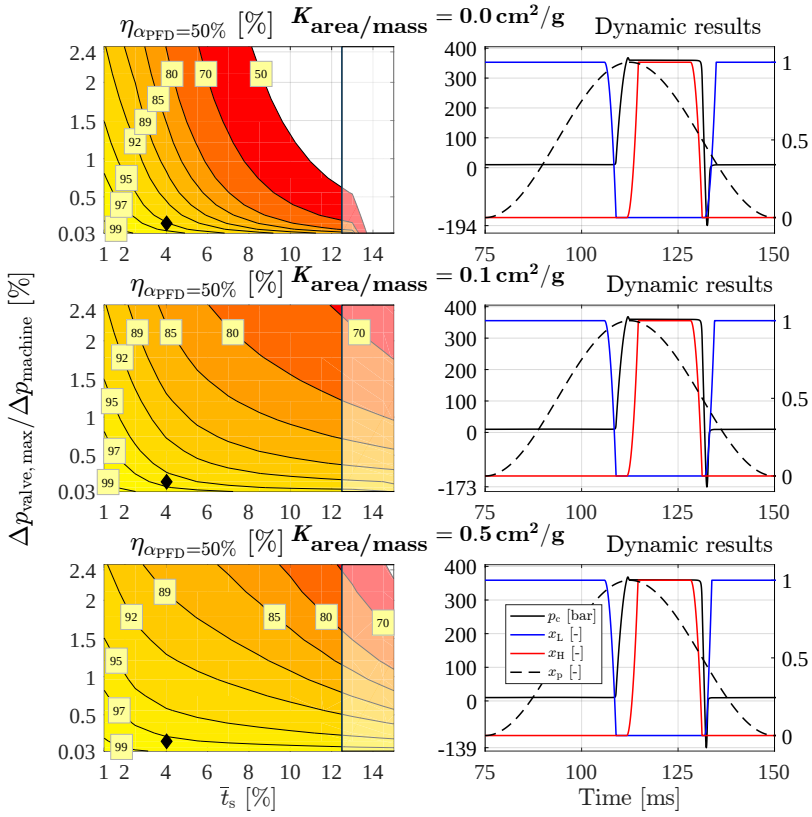

Fig. 2.11: Efficiency at $\alpha_{PFD} = 50\%$ for $K_{area/mass} = 0{,}0.1{,}0.5$ cm^2/g (left) and time-dependent results for the highlighted simulation points (right). The chamber pressure belongs to the left axis while the valve and piston position belongs to the right axis.

For full displacement strokes, the valve switching time is shown, contrary to previously published results in [77], to have minor to negligible influence on the efficiency, when using proper valve timing.

However, the valve switching time is shown to have more pronounced influence on the efficiency if using PF-D. It was shown that PF-D operation with efficiencies above 90% is possible for values of α_{PFD} as low as 25% when having $\bar{t}_s < 5\%$ and $\Delta p_{valve}/\Delta p_{machine} < 0.5\%$. Through a sensitivity analysis of the valve dependent parameter $K_{area/mass}$ it was shown that cavitation during motoring PF-D is plausible while the LPV is opening, especially for low values of $K_{area/mass}$. For pumping PF-D, similar conclusions can be drawn, only does cavitation not occur, but instead the chamber pressure may exceed the high-pressure manifold significantly and hence PF-D should be used with great care. Even if PF-D operation is not required for a particular DDM, fast

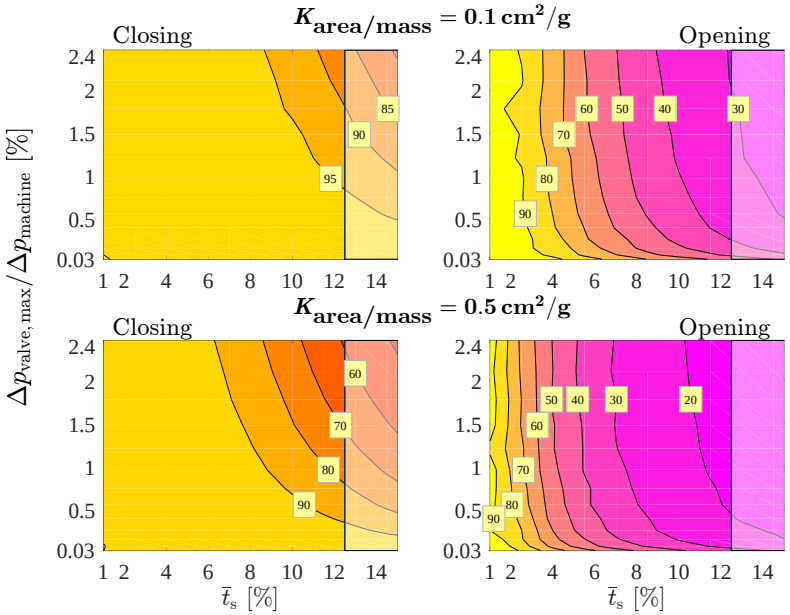

Fig. 2.12: $T_{\mathrm{K,area/mass}}$ for the $\alpha_{\mathrm{PFD}} = 50\%$ case with $K_{\mathrm{area/mass}} = 0.1$,0.5 cm^2/g.

switching valves are recommended, not necessarily to ensure high efficiency, but to make executing accurate valve switching timing easier (elaborated later in this section). Using PF-D enables refining the resolution of the machine power and displacement which is very useful, especially for DDMs having a low number of pistons, but is also suspected to increase the valve landing speed and may introduce cavitation and increased acoustic noise.

One aspect which is still not considered in the analysis is pressure chamber volume change caused by the movement of the valves. With the valve configuration tested in this thesis, the valve movement during valve closing opposes the flow induced by the movement of the piston. Therefore, the flow losses during switching are suspected to be even lower. Also, the fluid stiffness was assumed constant throughout the chapter which leads to negative cylinder pressures in the model. This tends to overestimate the valve losses and furthermore, it tends to open the LPV valve quicker than would occur (if negative pressure was not allowed). However, the fluid stiffness was kept constant and the chamber pressure was not limited by other means, to avoid loss of generality.

In Paper **G** an analysis of the flow characteristics and sizing of annular seat valves for DDMs was presented. Through static axi- symmetric CFD simulation it was found that for seat valve geometries leading to optimal energy efficiencies, the flow was primarily laminar. The simulated results were

also compared with experimental results obtained on the MCA prototype valve, also showing the flow to be laminar for the majority of the intended flow operating range. Throughout this chapter, the flow has been modeled using the orifice equation (2.1) which assumes the flow to be turbulent. This tends to underestimate the flow losses, especially at low fluid temperatures due to high fluid viscosities. Traditional fluid power control valves are primarily operated in turbulent regime, as this makes the valve pressure drop or flow rate close to independent of changes in the fluid viscosity. The study done in Paper **G** is based only on static models and does not include the increased flow losses during valve switching. In the analysis presented in this chapter, it was shown that the flow losses during valve switching are small if proper valve timing, making the results of Paper **G** more viable since this assumption have been shown possible to realize. Furthermore, the electric energy losses associated with the active closing of the valves were estimated based on the valve stroke length, the pressure/flow force acting to close the valve when fully opened and conducting the maximum flow, the mass of the moving member and the valve switching time. The results also confirms that highly efficient DD operation is possible using seat valves although the results of Paper **G** are not directly comparable with what was presented in this chapter.

The importance of executing the valve switchings precisely is studied in [53]. A 7-piston digital pump/motor with valves capable of switching in 1 ms simulated at 3000 RPM, 300 bar and 57% displacement ratio demonstrated that the valve throttling loss of 6% increases by a factor of 3 to 8 when the valve timing was off by 2 ms (corresponding to a tenth of the revolution time). The study is based on valves without check-valve capability (similarly to the analysis done in [77] and Eqn. (2.3)). In the case of using check-valves for partial strokes, the throttling losses are close to independent of the valve timing since the subsequent passive valve opening always occurs immediately after compression/decompression. However, inaccurate valve timing still leads to inaccurate control of the displaced volume. For full stroke operation when using check-valves the accuracy of the valve timing is important. As pointed out, for full strokes operation, the valves should be switched as closely to the dead centers as possible to minimize valve losses. This means that if a valve closes slightly slower than expected, the subsequent pressurization/depressurization will not complete before reaching the respective dead center and the following passive valve opening do not occur. Possibly, the closing angle of each chamber can be adjusted to compensate for any variations in the closing time, but, this requires intelligent control algorithms. To avoid this, valves with a high repeatability are needed. Therefore, fast switching capabilities are needed as the response of slow valves switched by weak actuators is more influenced by variations of the actuator force, the opposing fluid forces etc.

Chapter 3

Optimization of Actuators and Valves of DDMs

Formulations of optimization problems are proposed for deriving optimal valve and actuator designs for DDMs. The optimization is based on multiple mathematical models, which are used to evaluate the performance of the valves in DD operation. Optimal solutions are sought in terms of valve and actuator geometry and actuator parameters, such as number of turns, wire diameters etc. Both FEA and lumped models are used for evaluating a design candidate. Initially, static axi-symmetric FEA models are used for calculating steady-state actuator forces, flux distributions, flow vs. pressure characteristics etc. Based on the FEA results, lumped parameters are extracted for simulating the performance in DD operation using a single DD chamber model.

Carrying out the optimization is dependent on a number of inputs chosen by the design engineer such as choice of actuator, valve and actuator arrangement, which models to use, etc. Figure 3.1 illustrates the design procedure. The starting point is choosing an overall concept to be optimized i.e. choosing the actuator/valve class. The next step is to generate a design configuration for the chosen class e.g. magnet placement and orientation etc. Then, the models needed for evaluating the design candidate must be formulated. Dependent on the class and design configuration, tailored models are needed for accurately simulating the performance. Especially the model evaluation time is important to maintain as low as possible since a large number of evaluations are required for the optimization algorithm to converge. With the necessary mathematical framework, the formulated optimization problem is solved using the Generalized-Differential Evolution algorithm GDE3 [35] which is based on an evolutionary global optimization

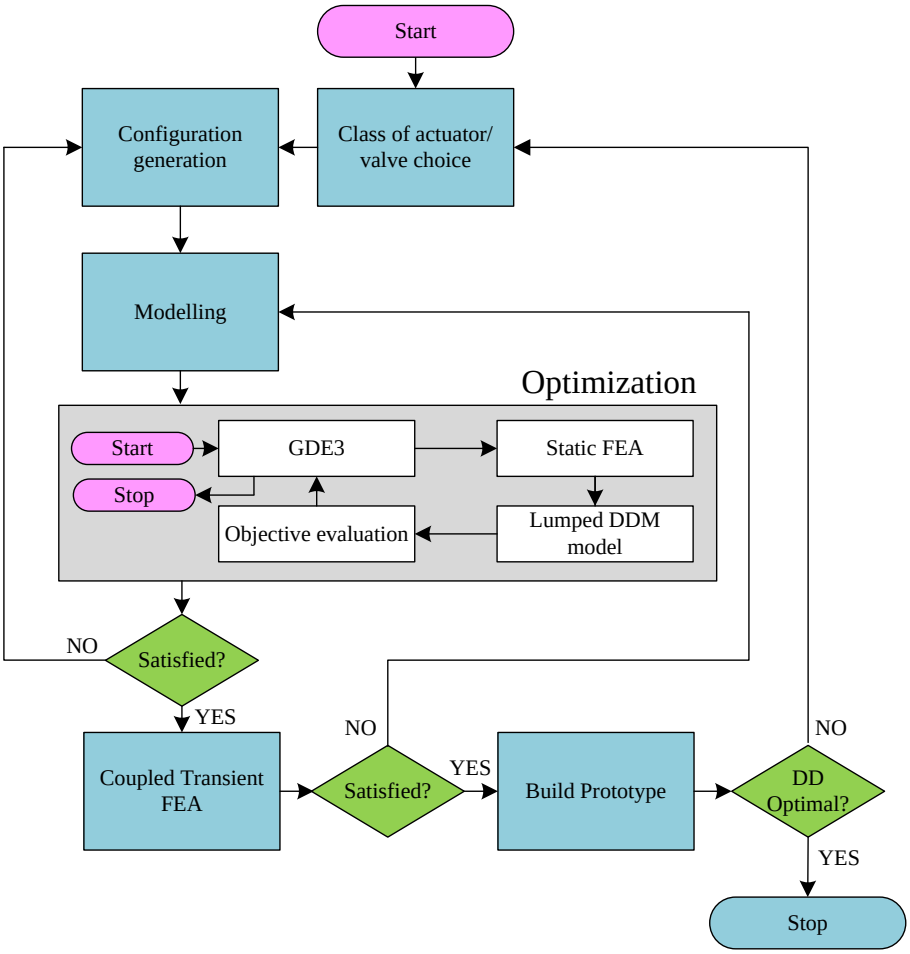

Fig. 3.1: Flow chart illustrating the design procedure and the optimization algorithm for valves and actuators of DDMs.

idea incepted by [86]. The optimization routine returns a set of optimal design candidates. If any candidates are satisfying for the design engineer, they are simulated using a more detailed model based on a coupled transient FEA. If not, the configuration is changed or modified. The more detailed, and computational expensive, coupled transient FEA simulation is carried out to assess the accuracy of the (simpler) models in the optimization. If the coherence is not adequate, the optimization models are modified and the optimization is carried out again. If the accuracy of the optimization models is satisfying, a prototype valve is build and tested. Based on the experience with the developed prototype, the process may be repeated.

The basic idea of the objective function is to initially use static FEA analysis for evaluating steady-state characteristics of the candidate. Dependent on the formulated problem, FEA can be used to solve for electro-magnetics, the fluid dynamics, the heat transfer and structural dynamics. This enables considering a wide range of physical phenomena in a single design step, possibly making deriving optimal solutions easier (opposed to more iterative methods as proposed in [72]). For the FEA analysis, the geometry of the design candidate is realized using a parametrization scheme. This is well suited for capturing the influence that minor changes in geometry impose on the performance. Emphasis is put on the use of the static case of FEA to keep the objective function evaluation time at a manageable level. To this end, lumped models must be derived which can describe the time-dependent performance of the design candidate sufficiently accurate and are relatively computational light. The necessary models for simulating a single cylinder during DD operation are combined, which facilitates evaluating the in-situ losses and performance.

The algorithm deployed for solving the multi-objective optimization problems is the Generalized Differential Evolution 3 (GDE3) [35]. The GDE3 uses Pareto optimization i.e. the algorithm returns a set of non-dominated solutions. For more details on the optimization algorithm, see [35]. Also, more details about the implementation and performance of the algorithm is published in [7]. Furthermore, in [75] the algorithm was also applied to a purely lumped model based optimization of valve parameters for large scale DDMs.

In this chapter, a review of two case studies based on the described approach is presented. First attention is turned towards the optimization of a moving coil actuator for a (predefined) valve geometry. This part is based on Paper **D**. Then, the moving magnet optimization, including optimization of the valve geometry is reviewed. This part is based on Paper **J**. Both the optimization studies are targeting a 50 CC chamber performing DD motoring (and idling) strokes for 350 bar machine pressure span and 800-1000 RPM. The valve type is in both cases a normally opened annular seat valve. Also, for both optimization problems the LPV and HPV are assumed identical.

3.1 Moving Coil Actuator Optimization

A moving coil actuator design for directly actuating the plunger of a normally opened seat valve has been derived. For this optimization problem, the plunger geometry, including the valve/actuator stroke-length was predefined. The valve plunger geometry and stroke length have been designed with the aid of CFD to ensure sufficiently low flow losses and axial flow forces

acting to close the valve during flow. Further details on the CFD models used in the design process may be found in [74].

This section is structured as follows: first the optimization problem is formulated, then the developed models are presented, and finally the results, and the MCA prototype valve designed based on the results are presented.

The Problem Formulation

To derive actuator designs which result in the smallest valve losses during DD operation, and to ensure compact solutions, three objectives are formulated which all are sought minimized simultaneously:

O1 The electrical energy consumption of the actuator.

O2 The height of the actuator. Note that the diameter of the actuator is given by the predetermined valve geometry.

O3 The valve flow losses.

Figure 3.2 shows the used parametrization and the geometry related design variables of the favored actuator configuration. In total, six design variables describe the geometry. In addition, two design variables are used for controlling when (relative to the shaft angle) a voltage step should be given to the LPV and HPV coils, and two design variables are used for controlling the duration of the voltage steps. Finally, one design variable is used for controlling the magnitude of the voltage step. In addition to the optimization objectives, a number of inequality constraints are formulated to ensure geometrical feasible designs, to ensure certain actuator characteristics, and to speed up the evaluation time in case of bad designs. Some of the constraints are listed below:

C1 The maximum electro-magnetic actuator force must exceed the opening spring force.

C2 Depending on the design point, the operation cycle may only be completed partially (too weak actuators, bad timing, etc). The violation degree is set based on the simulation time at which the operation cycle failed.

Both on the displayed constraints improve the design point evaluation time in case of bad designs. For more information on the used constraints, see Paper **D**.

Figure 3.3 shows a flow chart illustrating how a design candidate is evaluated. Based on the design vector, x, it is checked whether the geometry is feasible. If so, static electro-magnetic FEA is carried out. Based on the FEA results it is assessed whether the actuator design candidate is likely to

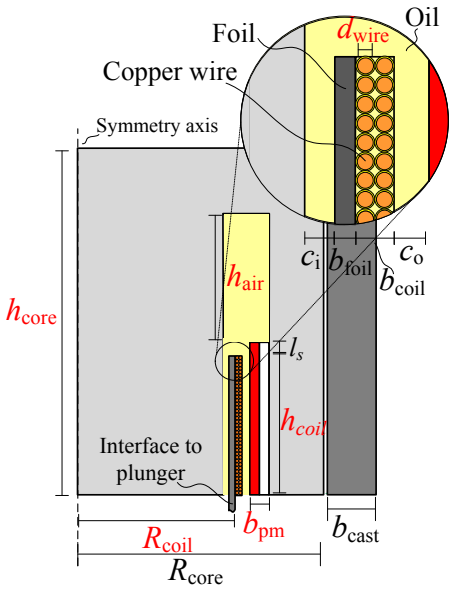

Fig. 3.2: Parametrization of one of the moving coil configurations, "*The red parameters are design variables and the black parameters are constants*". The figure is also published is Paper **D**.

succeed in switching the valve in DD operation. For instance, if the actuator at the maximum steady-state current is weaker than the opposing opening spring, the candidate is rejected i.e. constraint **C1**. If not, a single DD motoring operation cycle is simulated from which the objectives are evaluated. Likewise, the simulation is exited if the valves do not switch appropriately i.e. **C2**. For instance, the actuator may succeed in closing the valve, but it may be too late for subsequent passive valve opening to occur before the respective dead center. This results in an idling cycle which there is no need to evaluate as the actuator is not used. As indicated in the figure, the evaluation time of feasible design points typically ranges between 5-15 s when using an Intel Core i7 2.8 GHz processer and 16 GB memory.

Valve and Actuator Model

In the modeling of the time-dependent actuator current emphasis is put on inclusion of eddy current effects. As mentioned, eddy currents delay the change in magnetic flux, but this does not delay the produced electromagnetic force of the moving coil actuator due to the static field induced by permanent magnets. In fact, for moving coil actuators, eddy current are accelerating the initial force build since they lower the effective inductance of the coil. Inspired by [96], eddy current effects are included in the MCA model

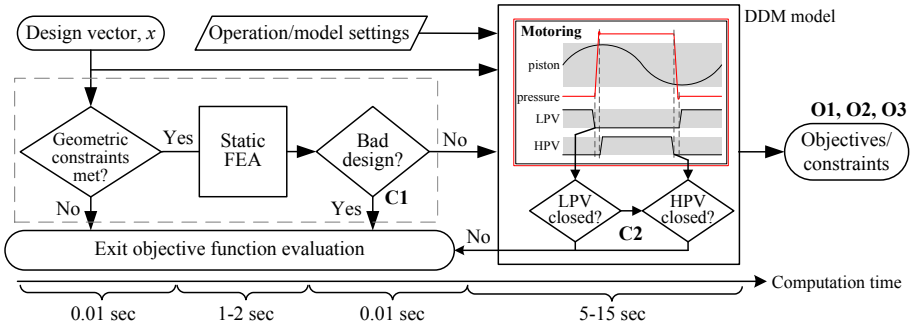

Fig. 3.3: "*Flow chart illustrating how the objective function is evaluated*". A slightly different version of this figure is published in Paper **D**.

using a two-coil transformer circuit model. The primary coil is the moving coil and the secondary coil (shorted turn) represent the eddy currents flowing in the core of the actuator. Equation (3.1) shows the transformer circuit model and Figure 3.4 illustrates the assumed flux and current paths in an axi-symmetric view (*left*) and the equivalent magnetic circuit model (*right*).

$$\begin{aligned} v_c(t) &= R_c i_c(t) + (M + L_c)\frac{di_c}{dt} - M\frac{d(i_e(t)/N)}{dt} - \overbrace{\dot{x}(t) L_{wire} N B_{gap,r}(t)}^{\epsilon(t)}, \\ 0 &= N^2 R_e(t)(i_e(t)/N) - M\frac{di_c}{dt} + (M + L_e(t))\frac{d(i_e(t)/N)}{dt}, \end{aligned} \tag{3.1}$$

Where the constants are: the coil resistance R_c, the mutual inductance linking the coil and core (i.e. the shorted turn) M, L_c is the coil self-inductance, N is the number of coil turns and L_{wire} is the length of a single coil turn. The variables are: the coil voltage v_c, the coil current i_c, the eddy current i_e, the shorted turn resistance R_e, the shorted turn self-inductance L_e, the average radial air-gap flux density $B_{gap,r}$ and the axial coil velocity $\dot{x}$.

The variables R_e, L_e and $B_{gap,r}$ are modeled based on an analytical approximation of the magnetic field diffusion depth as a function of time derived in [51] to capture the highly nonlinear behavior of eddy currents more accurately. For further details on this part of the model, see Paper **C**.

The generated Lorentz force is modeled, similarly to the back-emf voltage ϵ, as:

$$F_{mag}(t) = i_c(t) B_{gap,r}(t) L_{wire} N \tag{3.2}$$

which is used in the force equilibrium equation:

$$\ddot{x} = \frac{1}{m_{moving}} \left(F_{mov}(x, \dot{x}, \ddot{x}) + F_{flow}(x, Q, p_c) + F_{mag}(i_c, B_{gap,r}) + F_{spring} \right) \tag{3.3}$$

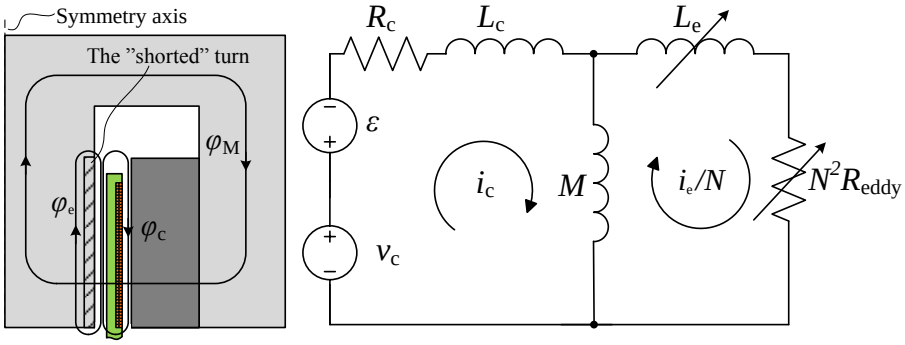

Fig. 3.4: "Transformer model applied to the MCA and equivalent magnetic circuit diagram where the shorted turn parameters are referred to the coil side". The figure is also published in Paper **D**.

Where F_{mov} represents the fluid forces induced by plunger movement, F_{flow} represents the flow induced axial forces acting on the moving member and m_{moving} is the mass of the moving member. The coefficients used for describing F_{mov} and F_{flow} are derived using CFD analysis. For further details about the mechanical model, see Paper **D** and [74]. The spring force F_{spring} is assumed constant corresponding to a relatively weak spring with a large precompression to limit the number of model parameters.

The flow vs. pressure characteristics have been modeled using:

$$\Delta p = k_{p1}(x)Q^2 + k_{p2}(x)Q \tag{3.4}$$

where k_{p1} and k_{p2} are coefficients also obtained using CFD analysis [74].

Single Cylinder DD Model

The block diagram shown in Figure 3.5 illustrates the couplings of the different sub-models. The actuator, the valve and the orifice sub-models were explained in the previous subsection, and the pressure chamber dynamic sub-model is given by:

$$\dot{p}_c = \frac{\beta(p_c, \alpha)}{V}\left(Q_H - Q_L - \dot{V}\right), \tag{3.5}$$

Where β is the bulk modulus modeled as a function of the cylinder pressure and the assumed air ration at atmospheric pressure [34], V and $\dot{V}$ is the cylinder volume and cylinder volume derivative calculated as:

$$\begin{aligned} V(\theta) &= \frac{V_d}{2}(1-\cos\theta) + V_{dead} + x_H A_{shadow} - x_L A_{shadow}, \\ \dot{V}(\theta,\dot{\theta}) &= \frac{V_d}{2}\dot{\theta}\sin\theta + \dot{x}_H A_{shadow} - \dot{x}_L A_{shadow}, \end{aligned} \tag{3.6}$$

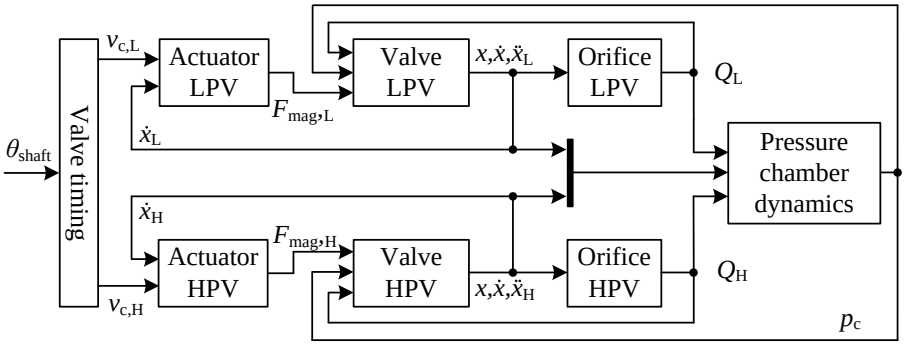

Fig. 3.5: "*Block diagram showing how the different sub-models of the lumped parameter simulation model interacts*". The figure is also published in Paper **D**.

Where A_{shadow} is the effective area which the valve pressure difference acts on. As can be seen, the cylinder model is similar to the model used for analyzing the valve requirements in Chapter 2, and the direction of the valve flows and the shaft position are defined accordingly to Figure 2.1 on page 35. However, this time, the valve movement is coupled with the cylinder volume.

Results

As indicated in Figure 3.1, it is not immediately apparent which arrangement/configuration leads to the best performing solution. To this end, the formulated optimization problem was applied to four different arrangements. Figure 3.6 shows one of each of the derived optimal designs for each arrangement. Figure 3.7 compares the optimization results. Observing **O3** (*left*) it can be seen that the variance of the flow losses is small compared to the other objectives. This indicates that actuator designs which can switch the valves in a close-to-optimal manner exist for all four arrangements. Considering objective **O2** and **O1** (*right*) geometry arrangement A is seen to perform slightly better than the other arrangement also having radially magnetized magnets. The energy consumption of the Geometry C and Geometry D is seen to be significantly higher. The electrical losses of the best designs are less than 20 W per valve, corresponding to less than 0.1 % of the average machine power being approximately 22kW (at 350 bar machine pressure span and 800 RPM).

A simulation example using the lumped DD model and the highlighted prototype design point of Figure 3.7 is shown in Figure 3.8 and Table 3.1 gives the model and prototype parameters, the operating conditions and the key performance data. The valve closing time is approximately 2 ms and the opening time approximately 3.2 ms. Note that a negative force corresponds

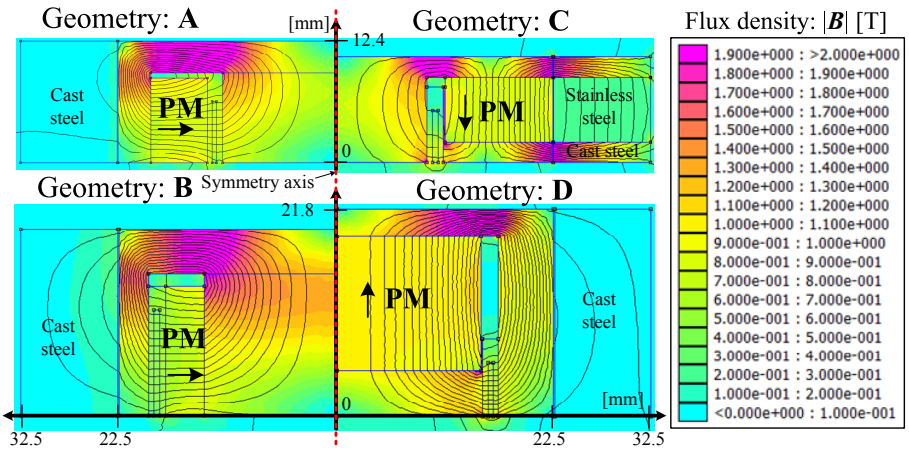

Fig. 3.6: "*Overview of the different geometries that explored in the paper. Each design is optimized and represents the highlighted points of Fig. 13 (Fig. 3.7 red.)*". This figure is also published in Paper **D**.

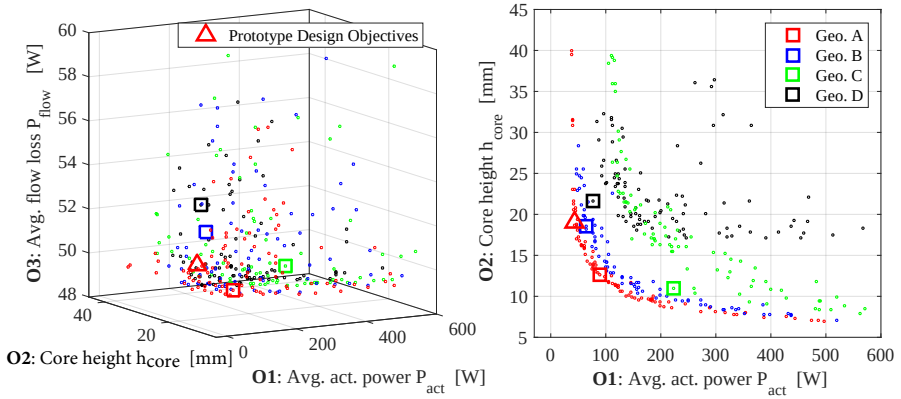

Fig. 3.7: "*Optimization results using the four different actuator geometries*". The figure is also published in Paper **D**.

to closing the valve. In Chapter 4, measurements and simulations show that the valve closing instant is easily visible from the current waveform as the back-emf voltage goes to zero on impact, leaving additional voltage to drive the current. This is not visible from Figure 3.8 since the voltage duration is shorter than the valve closing time which makes good sense from an energy perspective. The shown actuator forces $F_{\text{act,L}}$, $F_{\text{act,H}}$ is the sum of the electromagnetic actuator force and the spring force.

Based on the highlighted design point of Figure 3.7, a prototype valve has been designed and shown in Figure 3.9 and Table 3.2 on gives the key specifications. Twelve radially magnetized neodymium magnets with nickel-

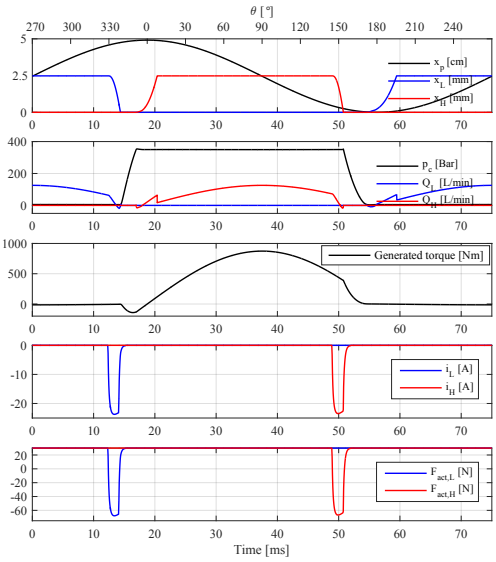

DDM parameters	**Value**
Piston stroke length	49 mm
Piston bore Ø	36mm
Cylinder dead volume	62 CC
Displacement, V_d[1]	50 CC/rev
Prototype valve parameters	
Stroke length, l_{stroke}	2.5 mm
Shadow area, A_s	4.9 cm^2
spring preload, L/H	(30/30)N
Coil layers	2
Operating conditions	
Shaft speed	800 RPM
Supply pressure, L/H	(5/350) bar
Supply voltage	80 V
Performance data	
Avg. act. power, L/H	(21/21)W
Avg. flow loss, L/H	(25/25)W
L/H closing time	(2.1/1.9) ms
L/H opening time	(3.1/3.3) ms
Avg. power[1]	22 kW
Cycle efficiency[2]	99.4%

[1]one cylinder considered.
[2]only chamber losses considered.

Fig. 3.8 & Table 3.1: Simulation example using the prototype actuator design and DDM parameters and operation conditions given in the table.

copper-nickel coatings are used for producing the static air-gap field. The valve plunger is composed of titanium (stainless steel plungers, sufficient for testing at low pressure, have also been used) and the aluminum coil former is fastened to the plunger using adhesive. A coil of two layers has been wound onto the coil former. The actuator core and the upper valve housing is composed of low-carbon steel characterized by a relatively high magnetic saturation level. The bottom valve part is made from Impax supreme which is a high strength steel alloy. Both the bottom valve part and the plunger have been surface hardened to increase the resistance to wear induced by impacts when closing during switching.

In Figure 3.9, the electrical connection to the moving coil is realized using current carrying springs. Testing of this concept proved it to be unsuccessful. Due to the ohmic resistance of the springs, heat is dissipated and the spring temperature increases which changes the structural properties of the material and the spring loses its original shape. Further, assembling the valve with this concept proved to be extremely difficult. Other methods have also been tested including an insulated Litz wire which bends with every valve switching. However, the connection fails at the soldering points after a number of valve switching (maximum number of switchings before failure using this concept is approximately 1 million). Similar problems are well known in the audio-speaker industry. Also, this concept was also difficult to assemble.

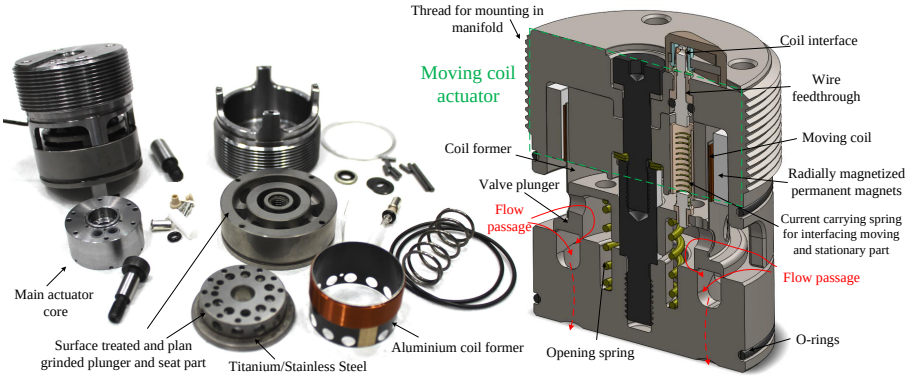

Fig. 3.9: Picture of moving coil actuated prototype parts (left) and a sectional view from a CAD-model (*right*). This figure is also published in Paper **D**

The current and favored solution is based on gold-plated spring connectors, typically used supplying constant and reliable connections between vibrating parts. This concept has been successful so far and also enables assembling and disassembling the valve much easier.

Table 3.2: Key specifications of the MCA valve prototype.

Description	Value
Valve dimensions	45 mm x 60 mm
Stroke length of actuator	2.5 mm
Effective shadow area	4.9 cm^2
Rated supply voltage	48 V
Δp @ nom. flow (125 L/min)	$\approx$ 0.5 bar
Valve closing time	2-3 ms
Opening spring force	30-35 N
Mass of moving member	19 g
Static air gap flux density	0.7-0.8 T

3.2 Moving Magnet Actuated Valve Optimization

A moving magnet actuated (MMA) valve has also been optimized. Likewise, the valve type is a normally opened annular seat valve. Instead of using a spring for generating the passive opening force, this valve concept relies on magnetic attraction forces to latch to the opened position. This is advantageous from an actuator energy view point, as the passive opening force decays as the valve is being closed, contrary to spring based solutions where the force increases when closing the valve. For this optimization problem

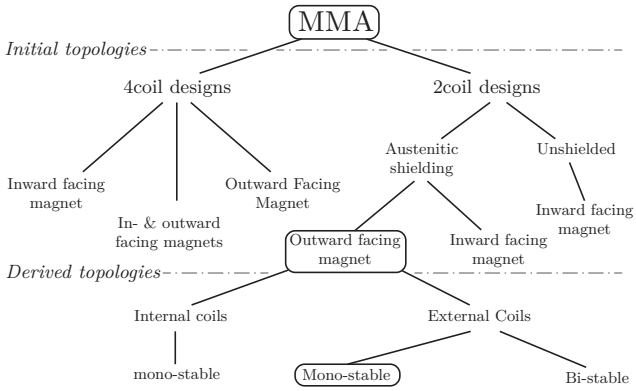

Fig. 3.10: "*Categorization of initial and derived topologies*". The figure is also published in Paper **J**.

the plunger geometry and the stroke length was included in the optimization using static axi-symmetric CFD. The outer dimensions of the valve is predefined[1].

As for the MCA valve, it is not immediately apparent which actuator topology[2] leads to the best performing design candidates. To this end, a number of systematically generated actuator topologies have been investigated as shown in Figure 3.10. Initially, a total of six actuator topologies are optimized using a simpler lumped model only considering the actuator part. Based on the most promising initial topology, three sub-topologies, shown in Figure 3.13 on page 70, have been derived where practical considerations are taken into account (manufacturability, assembly etc.). The second optimization round is done using the more elaborate single cylinder DD model explained earlier for the MCA optimization (Equations (3.5) & (3.6)). Table 3.3 gives an overview of which models are used for the initial and derived topology optimization.

This section gives a brief review of the MMA valve optimization and is structured as follows: first the optimization models are reviewed, then the optimization concerning the derived topologies is reviewed (*lower part of Fig. 3.10*). Finally, the MMA prototype valve designed based on the optimization is presented. For more thorough information, see Paper **J**.

[1]At the time the MMA valve optimization was carried out, the custom made valve manifold, shown in Figure 4.12 on page 82, had already been designed which sets forth the outer dimensions along with position of the flow ports and the o-rings used for sealing.

[2]In Paper **J** the term *topologies* is used instead of *configuration/arrangement* as primarily done in this chapter. The term *topologies* has been adopted throughout this section to comply with the displayed figures.

Table 3.3: Models used in the two phases of the MMA valve optimization.

	Initial Topologies	Derived Topologies
Mech. Motion Eqs.	✓	✓
Magnetostatic FEA	✓	✓
Electric Circuit Eqs.	✓	✓
Thermal Model		✓
Fluid Force Eqs.		✓
DDM Eqs.		✓

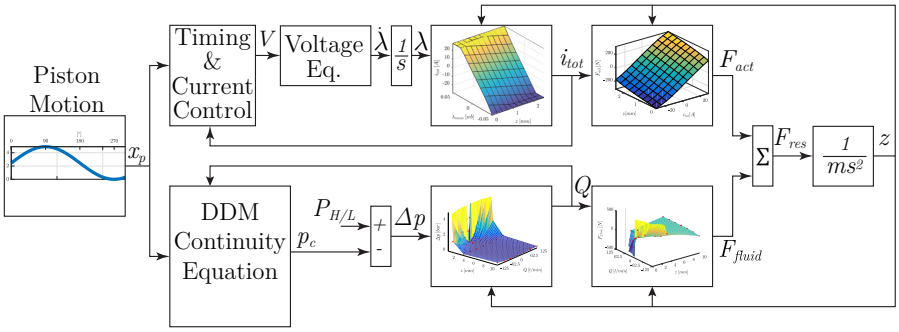

Fig. 3.11: "*Overall model block diagram for one valve*". This figure is also published in Paper **J**.

Moving Magnet Modeling

The overall model for one valve is illustrated in the block diagram of Figure 3.11. Voltage equations are formulated and solved for the flux linkage. Based on maps generated by sweeping the current and position in an axi-symmetric magnetostatic FEA, the current and subsequently the electro-magnetic force is obtained. Opposed to MCAs, and similar to solenoids, eddy currents delay the force build up. This has not been considered in the MMA models used in the optimization. Instead, as indicated in Figure 3.1, a coupled transient FEA model is used for evaluating the influence of eddy currents. Note that this step is not part of the optimization problem, but is done subsequently. The DDM continuity equation is identical to the model given for the MCA optimization in Equations (3.5) and (3.6).

The valve pressure drop and the fluid forces are mapped throughout the design and operation space using static axi-symmetric CFD analysis. See Figure 3.12 for illustrations of the flow geometry, the parametrization and solution examples. The used geometry is simplified considerably and parametrized by three parameters: the stroke length ztr, the seat width w_{sv} and the height of the inlet at the side of the valve h_{in}[3]. Designs having large

[3]In Paper **G** studies of the flow characteristics of annular seat valves are published also using axi-symmetric CFD.

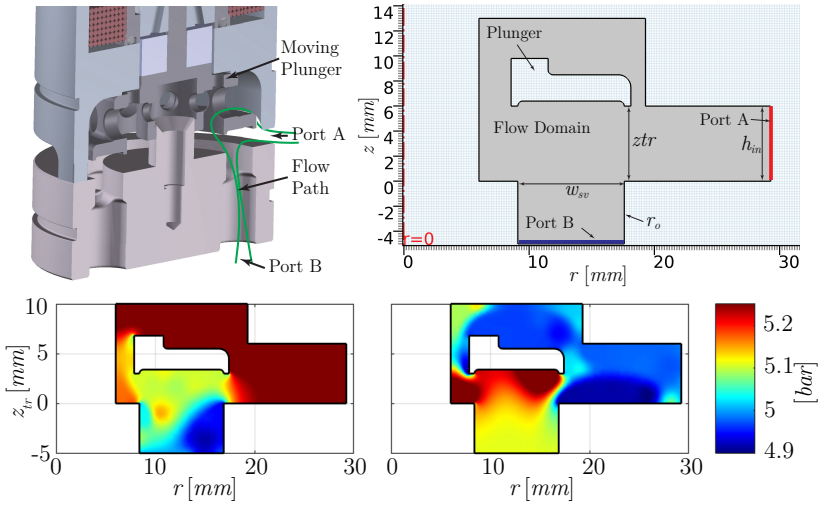

Fig. 3.12: The MMA prototype valve flow region in a sectional view (*top, left*), the parametrization of the flow domain (*top, right*), and examples of the pressure distribution for a flow rate of 125 l/min (*bottom, left*) and -125 l/min (*bottom, right*). This figure is also published in Paper **J**.

stroke lengths relative to the side inlet height are in Paper **J** demonstrated to reduce the axial flow forces acting to close the valve. This lowers the requirements to the magnetic latching keeping the valve open and thereby also lower the force requirements to the actuator[4]. As indicated in Figure 3.11, the force characteristics of the moving magnet actuator design candidates are position dependent (measured force characteristics are shown for the MMA valve prototype in Figure 4.9 on page 80). Since the force generation is based on the magnetic field(s) of the coil(s) repel or attract the moving magnet, the stroke-length is limited, especially for topologies with only one coil. By incorporating the overall valve geometry, such as the stroke length and seat width, parameters in the optimization loop, it is possible to optimize the described design trade-off and others. Due to the typical non-linear force characteristics of the MMA actuator design candidates, it is considered especially important to include the overall valve design parameters in the optimization.

Additionally to flow induced fluid forces, movement induced fluid forces are also included, again based on the results published in [74] (not indicated in Fig. 3.11).

Furthermore, as shown in Table 3.2, a thermal model is used in the derived topologies optimization phase. The temperature distribution is mapped as a function of the heat dissipated in the coil using static axi-symmetric heat flow FEA for a typical actuator design. This enables incorporating the tem-

[4]A similar mechanism was discussed in the Chapter 1 i.e. the "flow shield" of Figure 1.11 on page 20.

perature dependence of the coil in the optimization loop as will be showed in the following sub-section.

Derived Topology Optimization

For the derived topologies optimization phase two objectives are formulated:

O1 Minimize the valve closing time defined as the time from the closing signal is given until the valve is closed.

O2 Maximize the average DDM efficiency over a wide range of displacement ratios. A mean efficiency η_{mean} is obtained by integrating η_α of Equation (2.9) (cf. page 36) over a range of displacement ratios α. The electrical actuator powers are included in the machine losses.

By maximizing the DDM efficiency, both the flow losses and the electrical losses are minimized indirectly. In order to evaluate the machine efficiency at partial displacements, both a motoring and an idling cycle are simulated.

The switching time is sought minimized as a faster switching valve is associated with a higher repeatability (considering different operating speeds), as discussed in Chapter 2. In addition to the objectives, a number of constraints are formulated to ensure feasible geometries and to ensure some certain characteristics of the actuator and valve:

C1 The magnetic latching force must be larger than the flow force at the maximum flow rate. A safety margin of 10 N was used to account for model inaccuracies.

C2 In the opened (initial) position, the maximum actuator force must be sufficient for ensuring a reasonable acceleration. The minimum force is determined using $F_{\text{min}} = 2 \cdot ztr \cdot m / t_{\text{max}}^2$ where m is the mass and t_{max} is set to 5 ms.

C3 The actuator must be capable of generating a closing force at all positions.

The derived actuator topologies are illustrated in Figure 3.13. The actuator geometry is parametrized using four to six design variables (dependent on the topology). For the derived topology optimization, the maximum number of the design variables is 17, including design variables for controlling the switching sequence.

Figure 3.14 illustrates how the objective function is evaluated. As can be seen an inner loop is incorporated in the objective function evaluation because the dissipated heat of the coil heat initially is unknown (or the temperature could be estimated by other methods). The computation time of the electro-magnetic FEA simulation is seen to be much more than for the MCA

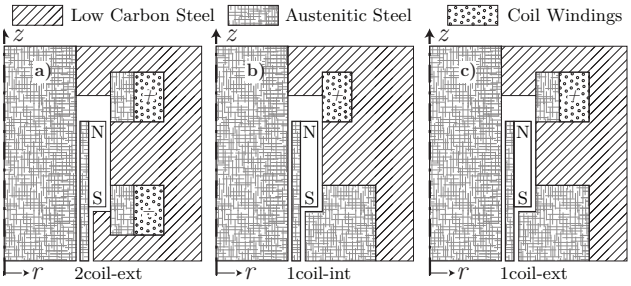

Fig. 3.13: "*Axisymmetric view of derived topologies, actuator volume only*". This figure is also published in Paper **J**.

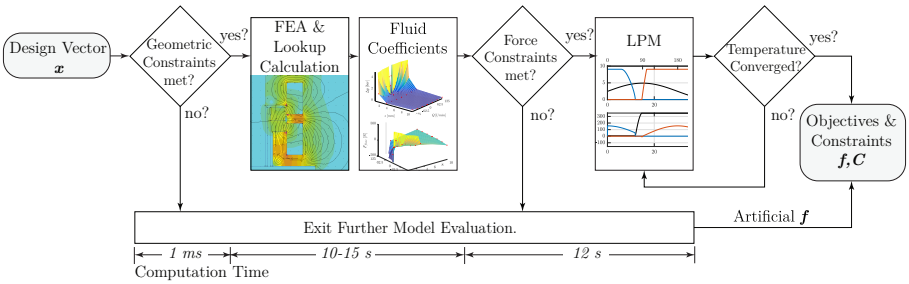

Fig. 3.14: "*Objective function evaluation flow chart*".This figure is also published in Paper **J**.

problem. This is because much more FEA model evaluations are required due to the non-linear force and flux characteristics.

The optimization results are shown in Figure 3.15. The results show that the choice of topology does not influence the Pareto front solutions significantly. The highest mean efficiencies for displacement ratios from 10 to 100% are above 98.9 (note that only valve related and compression losses are considered). With all the described constraints satisfied, the preferred topology may be chosen based on practical considerations. On this basis, the design point highlighted in the figure is chosen amongst the 1coil-ext candidates, as this design only has one coil which, in contrary to the MCA design, is outside the pressure chamber.

Based on the highlighted design point, a prototype valve is designed, manufactured and assembled as shown in Figure 3.16. Key-specifications are given in Table 3.4. Low-carbon steel is again used for the actuator part (upper part) and Impax supreme for the bottom valve part. The non-magnetic material used for the separator ring (excluding the coil from the coil) and the plunger is grade 5 titanium in order to obtain sufficient mechanical strength. A single axially magnetized zink coated neodymium magnet is glued to the plunger using adhesive. Compared against the MCA valve prototype, the

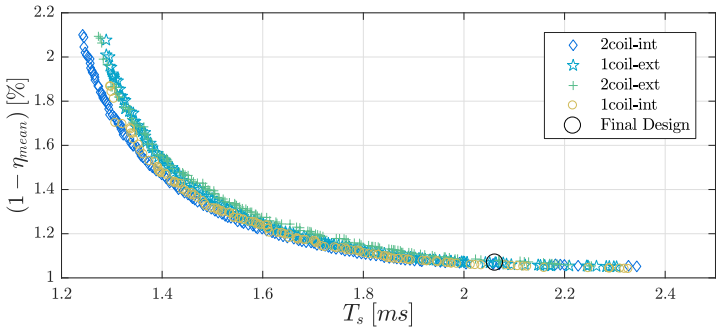

Fig. 3.15: "*Derived topologies optimization results*". This figure is also published in Paper **J**.

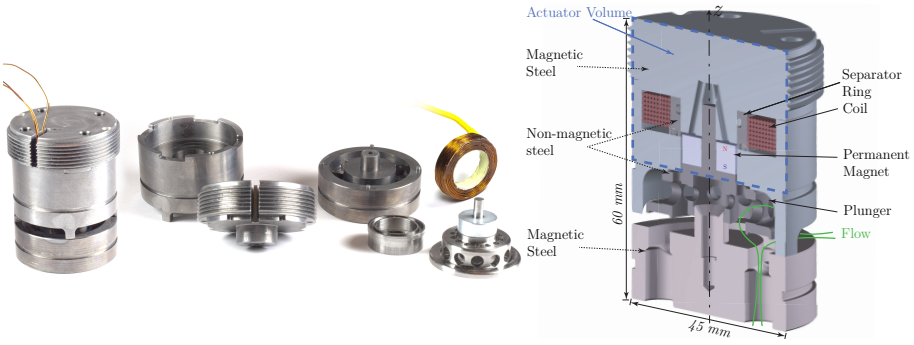

Fig. 3.16: Manufactured MMA valve prototype (*left*) and sectional CAD-model view (*right*). This figure is also published in Paper **J**.

MMA prototype consists of much fewer individual parts and is easier both to manufacture and assemble. Key performance specifications are provided for the MMA valve prototype in the following chapter.

Table 3.4: Key specifications of the MMA valve prototype.

Description	**Value**
Valve dimensions	45 mm x 60 mm
Stroke length of actuator	3 mm
Effective shadow area	5.8 cm^2
Δp @ nom. flow (125 L/min)	$\approx$ 0.3 bar
Valve closing time	4-6 ms
Mass of moving member	26 g

Chapter 4

Testing and Model Validation

The developed MCA and MMA prototype valves have been rigorously tested to verify the simulated performance. Both stand-alone tests, and tests with the valve prototypes installed in a custom built DD test rig have been carried out. This chapter reviews some of the measurements obtained for the prototype valves and compares measured results against corresponding simulations. First, attention is turned to stand alone testing of the MCA valve prototype and validation of models. Then, experimental results from standalone tests are shown for the MMA valve prototype. Finally, results are shown for both the MCA and MMA valve prototypes installed in the test rig. This chapter is primarily based on Paper **G**, **H**, **I** & **K**.

4.1 MCA Valve Stand Alone Tests and Model Validation

A series of stand-alone tests have been carried out to verify the simulated valve performance. Measurements and comparison with corresponding simulations, of the following quantities are reviewed in this section:

- ***A*** static radial flux density in the air gap,
- ***B*** transient radial flux density in the air gap,
- ***C*** static electro-magnetic actuator force as a function of current and plunger position,
- ***D*** voltage, current and position during switchings,
- ***E*** valve pressure drop during flow,
- ***F*** axial flow/pressure forces acting in the moving member during flow conduction.

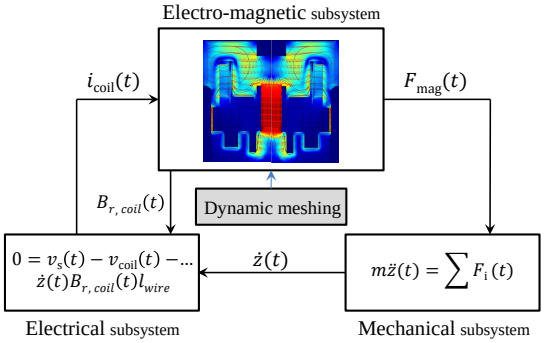

Fig. 4.1: "Coupling between the electro-magnetic, electrical and mechanical subsystems that form the whole valve switching model". This figure is also published in Paper **I**.

The mathematical models used for simulating the respective measurements are briefly reviewed. For measurement ***A*** to ***D***, the results are compared against simulations obtained using the lumped actuator model described in 3.1 and a more advanced and computationally expensive coupled time-dependent electro-magnetic FEA model. As mentioned in relation with the design procedure illustrated in Figure 3.1 on page 56, the coupled transient FEA model is used in the design process to assess the accuracy of the lumped models used in the optimization loop. The main couplings of the transient FEA model are illustrated in Figure 4.1. Dynamic re-meshing is used to facilitate moving the coil during simulations. The electrical circuit model comprises a voltage source and a distributed field coil and a manual implementation of the back-emf term. The valve movement is modeled similarly to (3.3) where the position dependent coefficients are implemented as lookup tables.

For measurement **E** and **F**, the results are compared against simulations using a steady-state axi-symmetric CFD model. See Paper **G** for details about this model.

A The measured and simulated radial flux density in the air gap is shown in Figure 4.2. The coherence of the measured and simulated results is high. The simulated air gap flux density at 15 and -15 A is also included to show the sensitivity to coil currents. At the fully opened position the average radial flux density change is 10% and -17%, respectively. Note that a negative current corresponds to a closing force.

B The time-dependent air-gap flux density has been measured when subjecting the coil to a voltage step of -30 V. This is repeated for a range of probe positions giving the measured results in Figure 4.3. For this experiment,

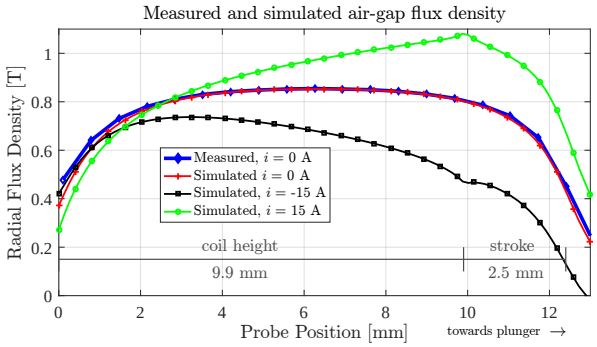

Fig. 4.2: Measured and simulated static air gap flux density.

the moving member is fixed for simplicity. In order to make room for the flux probe, one permanent magnet has been modified by grinding a groove making sufficient space for the probe. Due to the modification, the PM has

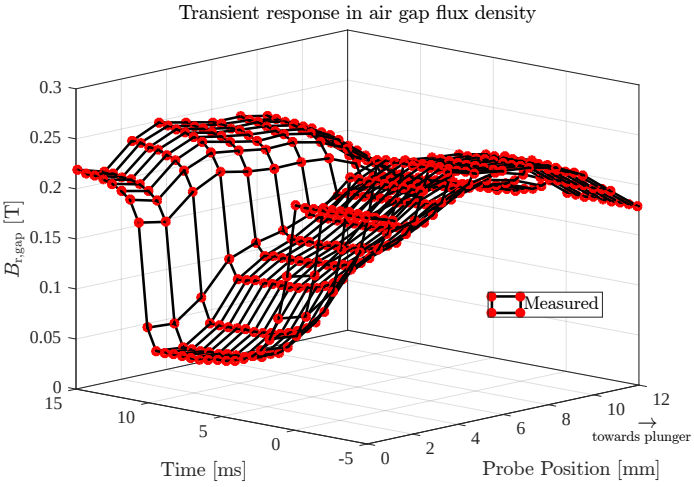

Fig. 4.3: "*Measured time-dependent air gap flux density when the coil is subjected to a voltage step*". This paper is also published in Paper **I**.

lost significant strength leading to the much lower observed radial flux density comparing against Figure 4.2. However, since the permeability of the permanent magnets is close to that of air, the change in flux density is not influenced significantly. The change in flux density is obtained by subtracting the initial flux (for each position) from the measured map. The change in flux density is shown in Figure 4.4 with corresponding simulations using the transient FEA model. Comparing the measured and simulated results, the

coupled transient model is observed to describe the time-dependent air-gap flux density quite well.

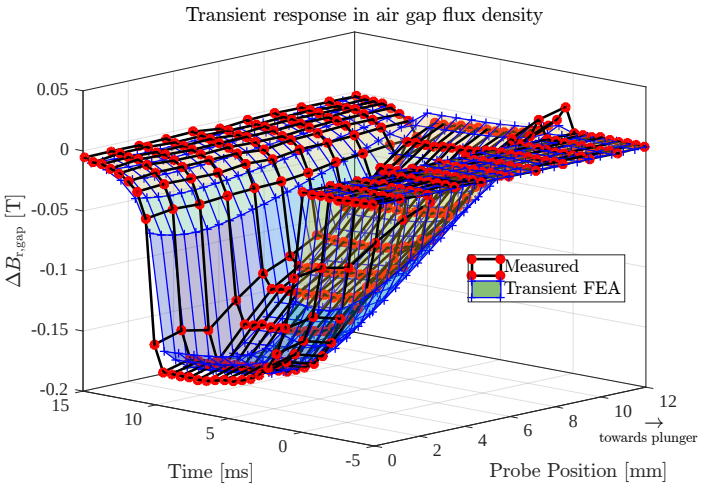

Fig. 4.4: "*Measured time-dependent air gap flux density when the coil is subjected to a voltage step*". This paper is also published in Paper **I**.

C The steady-state electro-magnetic actuator force has been measured as a function of current and position. The results are shown with corresponding simulations in Figure 4.5. The measured and simulated results primarily show good coherence, although at the extreme positions notable discrepancy is present, especially at larger (absolute) currents, as indicated by the red arrows. This occurs due to limitations of the test-setup, and the steep gradients of the measured map do not represent the actual electro-magnetic force.

D The position, the coil voltage and the coil current is measured during closing the valve. The experiment is performed with the valve situated in air and with the valve completely submerged in hydraulic oil (at atmospheric pressure) to assess the influence of the movement induced fluid forces. The measured results, for a voltage step of approximately 40 and 50 V with corresponding simulations using the coupled transient FEA model, are shown in Figure 4.6. For simulation of the air-case, the movement- and flow-induced fluid forces are set to zero.

The measured and simulated results show good coherence. For 50 V, the valve is seen to close in approximately 1.7 and 2.6 ms for the air and oil case, respectively. This shows that the movement induced fluid forces have significant influence and are important to accurately include in the model. For the

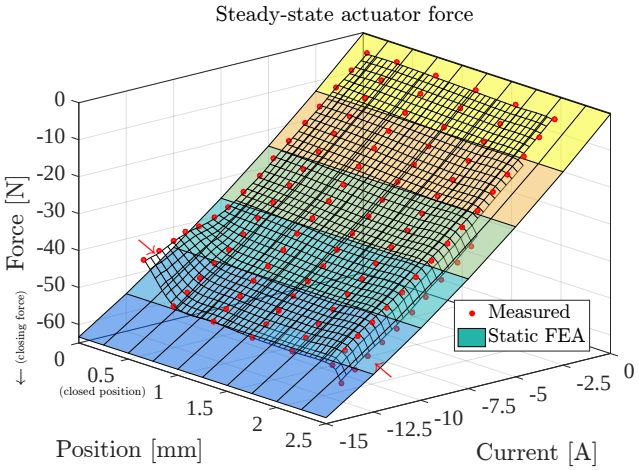

Fig. 4.5: "*Measured and simulated static actuator force vs. current and position*". This figure is also published in Paper **I**.

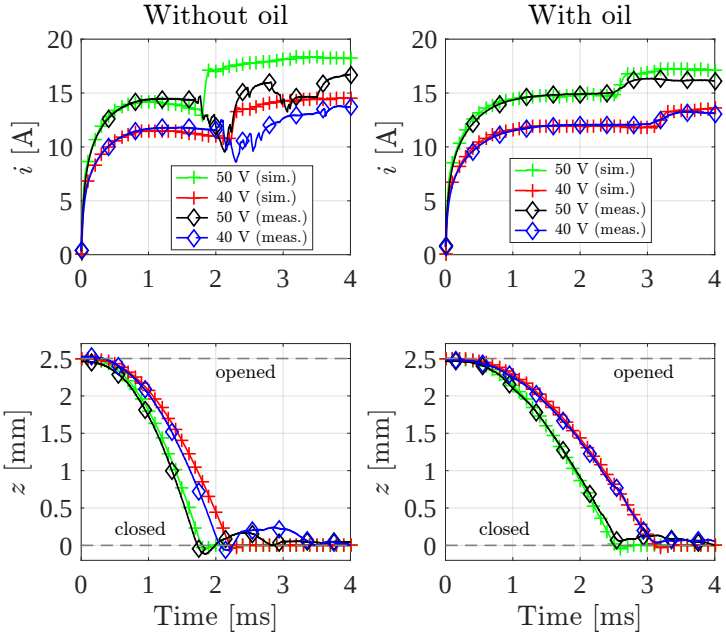

Fig. 4.6: Measured and simulated switching performance in air (*left*) and submerged in hydraulic oil (*right*). This figure is also published in Paper **I**.

air case after the valve is closed, the measured current waveforms are highly irregular. This happens because of mechanical chattering in spring connec-

tors used for the electrical interface. In oil, however, the spring connectors function quite well without chattering.

E The flow versus pressure drop characteristics have been measured at different plunger positions using a differential pressure transducer. Figure 4.7 shows the measured results with corresponding simulations. For the fully opened position ($z = 2.5$ mm), the measured pressure drop is +0.18/-0.48 bar for flow rates of $\pm$ 120 l/min. For negative flow rates (in Paper **G**, positive flow is defined as entering the bottom flow port, opposed to Figure 2.1 on 35), the coherence is satisfying when considering the simplified representation of the geometry used in the axi-symmetric models.

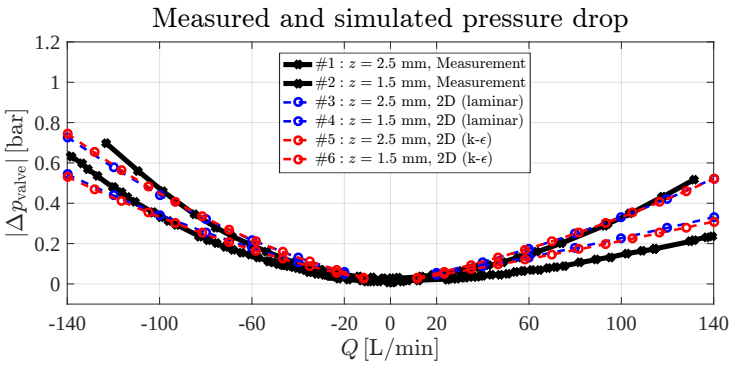

Fig. 4.7: "*Simulated and measured valve pressure drops as a function of flow rate for different plunger positions*". A slightly different version of this figure is also published in Paper **G**.

F The axial flow induced fluid forces acting to close the valve also been measured. The flow force was indirectly measured, by increasing the valve flow, until the axial flow forces exceeds the opening spring force making the valve close. By using different springs, and spacers for shortening the stroke of the valve, different initial positions and spring forces can be realized. A total of six flow force measurements have been obtained. The measured results are shown in Figure 4.8 along with corresponding simulations. The resemblance is considered satisfying considering the simplified valve geometry used for the simulations.

4.2 MMA Valve Stand Alone Testing

As for the MCA valve, a series of experiments have been carried out to investigate the performance of the valve. This section reviews experimental results for the following cases:

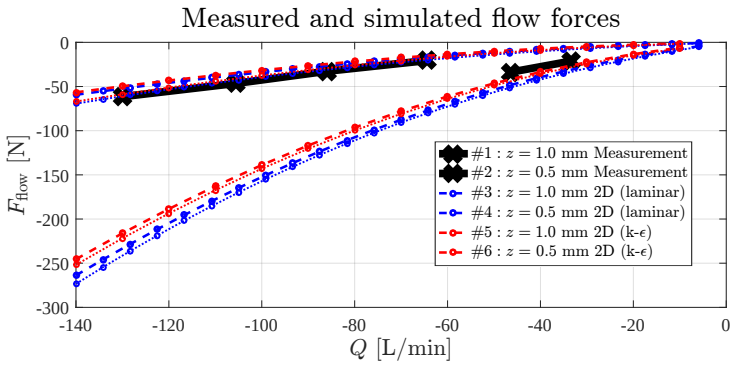

Fig. 4.8: "*Estimated and simulated steady-state axial flow induced forces (sign convention in Fig. 3). The dotted blue and red line represent the approximation based on the pressure difference i.e.* $\Delta p_{\text{valve}} A_{\text{shadow}}$ *using the Laminar and k-ϵ results respectively*". A slightly different version of this figure is also published in Paper **G**.

- ***A*** static electro-magnetic actuator force as a function of current and plunger position,
- ***B*** voltage, current and position during switchings,
- ***C*** valve pressure drop as a function of flow,

These results, and more, are also published in Paper **K**.

A As for the MCA valve, the steady-state electro-magnetic actuator force is measured as a function of current and position. The results is shown in Figure 4.9. Considering the force at zero current, a positive latching force towards the opened position is observed for all positions. A current of approximately 6-8 A is needed to drive the force to zero. At the maximum current tested (15 A) the actuator is capable of generating closing forces in the range of 20 N to 53 N depending on the position. The largest forces are present at the largest positions since the magnetic coupling between the permanent magnet field and the coil field is better at larger positions. The stroke length of the MMA valve is 3 mm, but as can be seen the maximum recorded position is approximately 2.2 mm. Similarly as for the MCA steady-state force measurement, the test-setup does not permit measuring the force for the entire stroke.

B As for the MCA valve, the switching performance has been measured with the valve in air and completely submerged in hydraulic oil. The measured results are shown in Figure 4.10. A current step of 18 A is supplied to the coil using closed-loop current control. For the air case, the closing time is observed to be 3.3 ms after the step is given. For the oil case, the closing

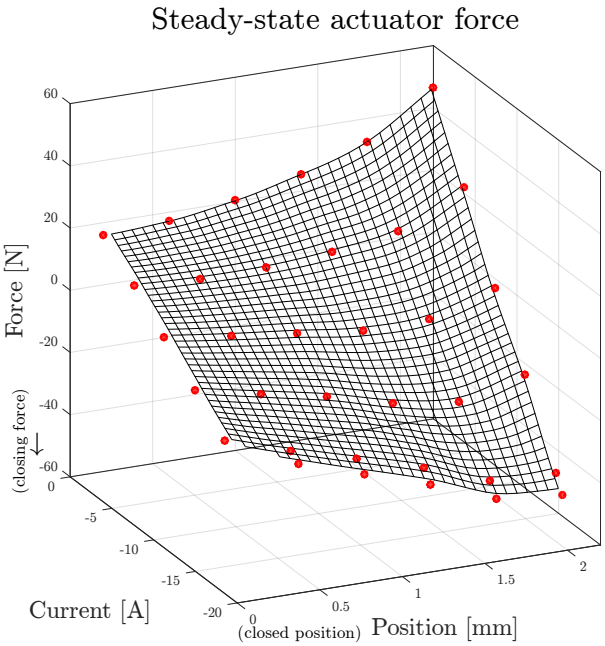

Fig. 4.9: "*Steady-state actuator force versus position and current. The red dots represent the measurements; the grid is interpolated from these data points*". This figure is also published in Paper **K**.

time increases to 5.2 ms due to the movement induced fluid forces. The delay, defined as the time between the signal is given until movement is initiated is for the air case approximately 1.1 ms and slightly more for the oil case due to stiction effects and inertia of the oil. The consumed electrical energy at the instants the moving member impact with the mechanical end-stop at the closed position is 1.4 J and 1.9 J for the air and oil case respectively.

C The measured pressure drop as function of flow rate is shown in Figure 4.11 for two different plunger positions. At the fully opened position, the measured pressure drop at -142 l/min is 0.11 bar and 0.31 bar at 108 l/min. Comparing against the measured pressure drop of the MCA valve (cf. Figure 4.8), the pressure drop of the MMA valve is lower. This is primarily because of the MMA stroke length being 3 mm, opposed to 2.5 mm for the MCA valve.

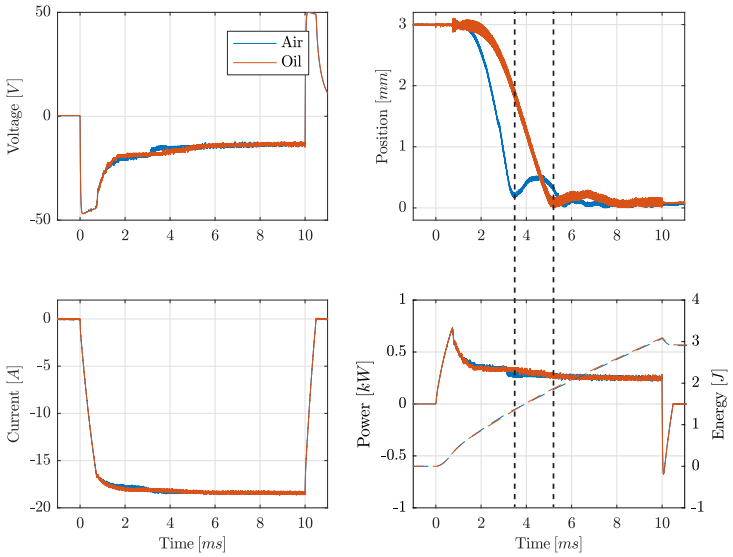

Fig. 4.10: "*Standalone test results. The dashed lines in the lower right sub-plot refers to the energy shown on the right axis*". This paper is also published in Paper **K**.

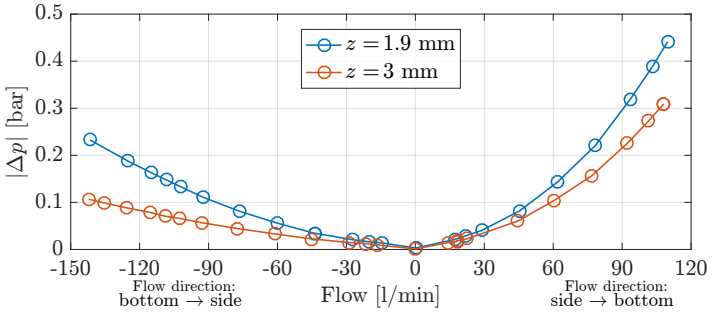

Fig. 4.11: "*Measured pressure drop vs. flow rate at two plunger positions*". Note that the flow direction of this figure is defined opposite of the results shown in Figure 4.8. This figure is also published in Paper **K**.

4.3 Test Rig for DD Operation Valve testing

A test rig for testing the valves in DD operation has been designed and built. The basis of the test rig is the Calzoni MR250 radial piston motor which has been modified to facilitate DD operation for one of the five pistons. The Calzoni machine was chosen since it has a relatively large displacement of 250 CC per revolution and can operate at relatively large speeds 800 RPM, leading to peak valve flow rates of 125 l/min. Also, the Calzoni machine

has high values of volumetric and mechanical efficiency as a consequence of the mechanism for converting the rotation of the shaft to translation of the pistons, i.e. internal piston support and a telescopic piston-cylinder mechanism [28][1]. Figure 4.12 shows the modified radial piston machine with a custom made valve block with prototype valves installed. The machine is modified by blocking the connection from the piston to the port plate and by making a connection though the piston head to the valve manifold situated on top.

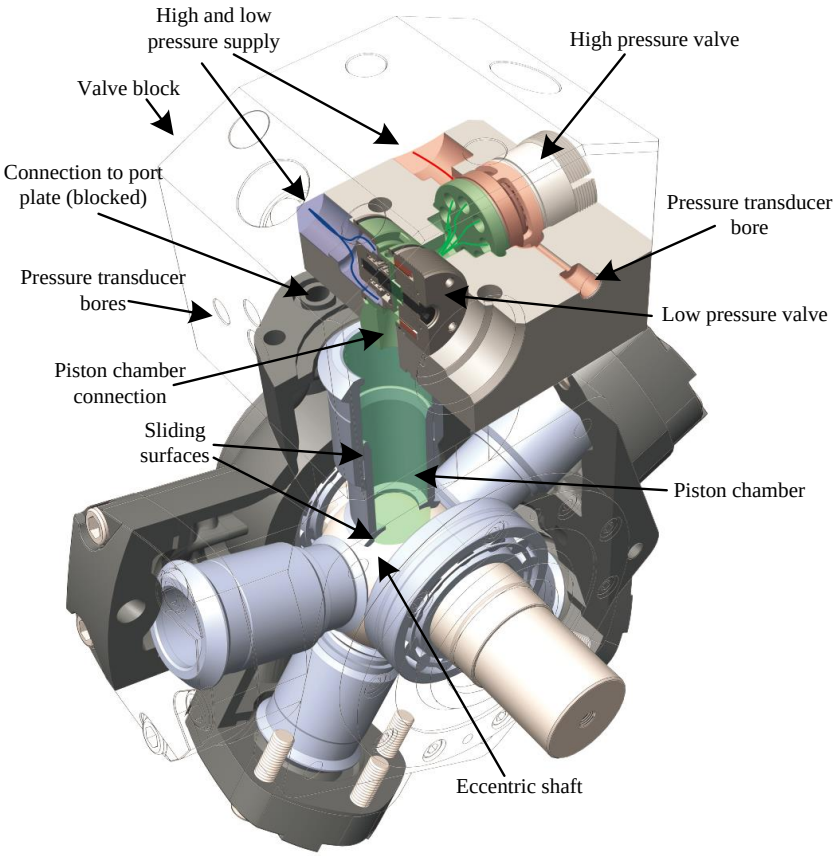

Fig. 4.12: "*CAD model showing the modified machine and the custom valve block equipped with the MCA and MMA PT valves*". This figure is also published in Paper **H**.

During tests, a permanent magnet synchronous machine is used for controlling the revolution speed by means of a four-quadrant frequency con-

[1]Previous machines of AIP also use the telescopic piston/cylinder mechanism [17]. The 3.5 MW MHI motor of the 7MW digital hydrostatic drive-train uses a crank-slider mechanism [92].

verter. The radial piston machine is fed from a hydraulic control block which is supplied from a large variable displacement pump station. Figure 4.13 shows the test rig.

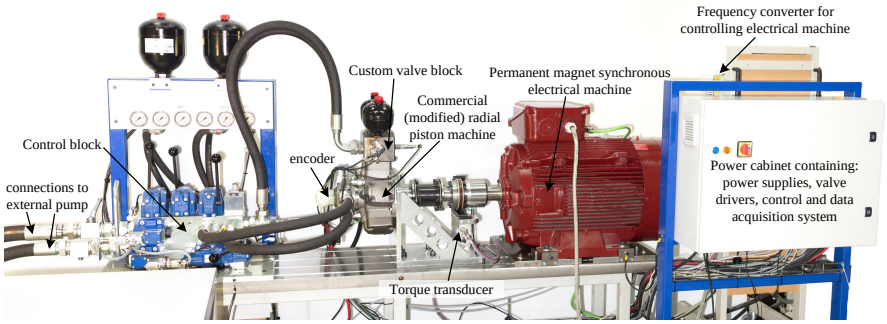

Fig. 4.13: "*Picture showing the test rig*". This figure is also published in Paper **H**.

Figure 4.14 shows a simplified schematic of the hydraulic circuit. The hydraulic control block enables both motoring and pumping DD operation cycles. For motoring, the pressure reducing valve (3) controls the pressure level, the directional valve (2) is set opposite of drawn, the gate valve (5) is open and the pressure relief valve (4) is closed (set point higher than set point of the pressure reducing valve (3). For pumping operation, the directional valve (2) is set as drawn, the gate valve (5) is closed, the pressure reducing (3) valve controls the low pressure level and the pressure relief valve (4) is used to control the pumping pressure and dissipate the hydraulic power. Accumulators are used to stabilize the pressure strings which are prone to oscillations due to the nature of DD operation. During testing, the remaining 4 cylinders of the machine are short circuited (accumulator also used here).

For more information about the test rig, see Paper **H**.

4.4 MCA and MMA valve in DD Operation

This section presents experimental results for DD motoring and pumping cycles at RPM 800 and approximately 100 bar machine pressure span. During the tests, the MCA valve was installed as LPV and the MMA valve installed as HPV. Figure 4.15 and 4.16 show the measured results for motoring and pumping, respectively. Table 4.1 summarizes key operation and performance data for both cycles. For both operation cycles, the valves are demonstrated capable of performing the necessary switching for obtaining the operation cycles. For the motoring cycle, the valve closing angles were manually tuned to maximize the machine power output (i.e. closing as late as possible). For

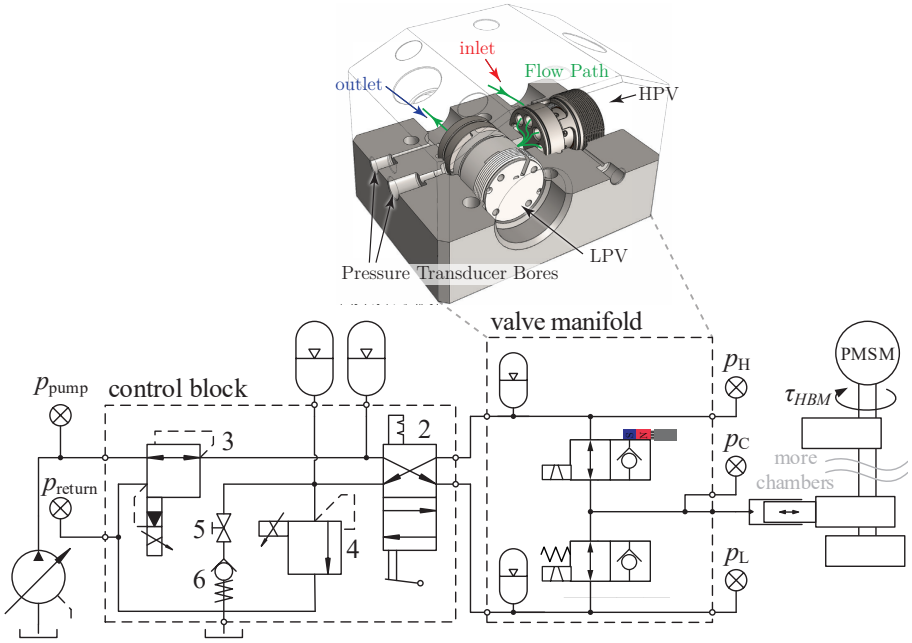

Fig. 4.14: "*CAD-drawing of valve manifold and simplified schematic of hydraulic layout used for both pressure/flow tests and DD operation tests*". This figure is also published in Paper **H**.

the pumping cycle, the valve switchings are carried out further away from the dead centers to test valve switchings at larger flow rates.

Considering the motoring cycle, the pressurization and depressurization is seen to occur close to the dead centers leading to valve switchings at the smallest possible flow rate. Based on the current wave-form, the LPV is observed to close in 3.1 ms. For the MMA closing time, the valve closing time is not directly visible from the current waveform and instead the closing time is estimated as the time from the closing signal is given until the pressurization/depressurization initiate. Using this method, the MMA valve closing time is 6.3 ms. The LPV opening time is, based on the generated back-emf voltage, 3.1 ms. The MMA valve opening time is not directly interpretable from the back-emf voltage and has therefore not been estimated. As observed subsequent to the active closings, a small voltage is supplied, long enough for the current to reach steady-state. This is used for resistance estimation which is one of the parameter tracking schemes deployed in Paper **F**. For the motoring cycle, the average electrical losses are calculated to be 44.5 W and 36.8 W for the MCA and MMA valve respectively. The flow losses for the valves cannot be directly determined from measurements since no flow sensor and no differential pressure transducer are installed during DD oper-

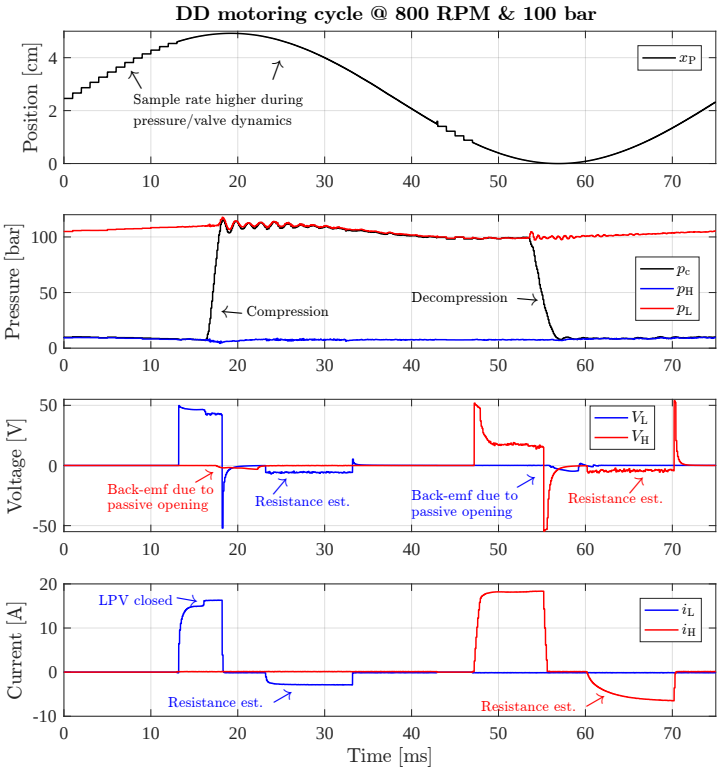

Fig. 4.15: "*DDM motoring: experimental results at 800 RPM and 100 bar*". This figure is also published in Paper **I**.

ation. Instead, the flow losses during the motoring and pumping operation cycles are estimated using:

$$Q_{\text{est}}(\theta) = \frac{V_{\text{d}}}{2}\dot{\theta}\sin(\theta)$$
$$E_{\text{flow,loss}}(\theta) = \int Q_{\text{est}}(\theta)\Delta p_{\text{valve}}(Q_{\text{est}}(\theta))d\theta\,, \tag{4.1}$$

where Δp_{valve} is based on the measured flow vs. pressure characteristics in the fully opened positions (cf. Figure 4.11) and θ is defined relative to the TDC (as in Figure 2.1). Assuming the valve switchings are performed at the dead centers, the MCA valve and MMA valve flow losses for a pumping cycle is approximately 9.90 W and 4.30 W, respectively. For motoring cycles, the flow losses are higher due to the direction dependent flow characteristics, and are calculated to be 23.8 W and 16.7 W for the MCA and MMA respectively.

For the pumping cycle, the pressurization and depressurization is observed to be further away from the dead centers, especially the pressurization. The LPV valve is, based on the current waveform, observed to close in 3.3 ms and the MMA valve is estimated to close in 5.7 ms. Comparing against the motoring cycle, the MMA valve closes in 0.6 ms less. This corresponds well with the valve being closed further away from the dead center, leading to larger flow during switching, since the flow induced forces are assisting the closing. Similarly, the opening time of the MCA valve is 2.2 ms, which is 0.9 ms faster than for the motoring case.

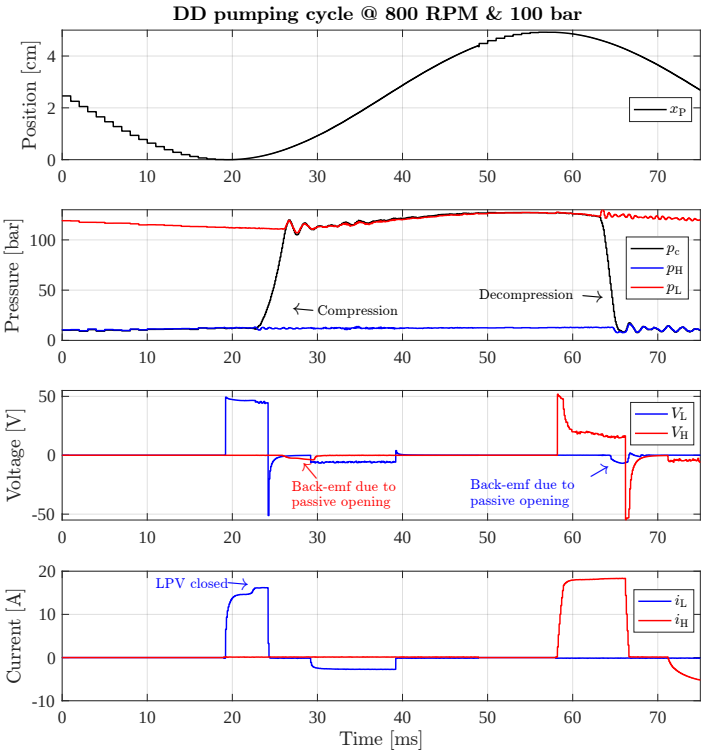

Fig. 4.16: *"DDM pumping: experimental results at 800 RPM and 100 bar."*. This figure is also published in Paper **I**.

Summary

A series of standalone tests for the MCA prototype valve was compared against a coupled transient electromagnetic FEA model demonstrating the model to be capable of simulating the actuator and valve switching performance with high accuracy. The pressure drop and the axial flow force of

the MCA valve were also experimentally determined and compared against a axi-symmetric CFD model demonstrating a satisfying coherence taking. A series of standalone test was also presented for the MCA valve to demonstrate the valve and actuator characteristics. Finally, the valves have been tested in DD operation showing both prototypes to be fully functional while only inducing losses which constitutes approximately 1% of the transferred power per valve.

Table 4.1: Parameters, operating conditions and key figures for DD operation cycles. A similar table is published in paper **K**.

DDM PARAMETERS			
Piston stroke length	24.6		[mm]
Piston bore ⌀	36		[mm]
Dead volume	62		[CC]
Displacement	50		[CC/rev]

DD MOTORING CYCLE			
Operating conditions			
Supply pressure HP/LP	≈110	≈10	[bar]
Shaft speed	800		[RPM]
Avg. mech. power	6.21		[kW]
Avg. torque output	74.2		[Nm]
MCA performance			
Avg. actuator power	44.5	0.72%*	[W]
Avg. flow loss	≈23.8	≈0.38%*	[W]
Close time	3.1		[ms]
Open time	3.3		[ms]
MMA performance			
Avg. actuator power	36.8	0.59%*	[W]
Avg. flow loss	≈16.7	≈0.27%*	[W]
Close time	≈6.3		[ms]
Open time	-		[ms]

DD PUMPING CYCLE			
Operating conditions			
Supply pressure HP/LP	≈110	≈10	[bar]
Shaft speed	800		[RPM]
Avg. mech. power	-6.23		[kW]
Avg. toque output	-74.3		[Nm]
MCA performance			
Avg. actuator power	44.7	0.72%*	[W]
Avg. flow loss	≈9.90	≈0.16%*	[W]
Close time	3.3		[ms]
Open time	2.2		[ms]
MMA performance			
Avg. actuator power	37.5	0.60%*	[W]
Avg. flow loss	≈4.30	≈0.07%*	[W]
Close time	≈5.7		[ms]
Open time	-		[ms]

*Relative to the average mechanical output

Conclusion

This thesis is concerned with the design, optimization and testing of seat valves for digital displacement machines (DDMs) operating with high piston cycle frequencies. The electrically controlled valves are key components of DDMs and strict requirements are set forth in terms of the switching time, the electrical energy consumption of the valves and the pressure drop of the valve. Based on a comparison of valve candidates it was established that on-the-shelf components which fully satisfies the strict requirements do not exist.

An analysis was carried out with the aim of determining general valve requirements in terms of switching time and valve pressure drop. The starting point of the analysis was based on valves being fully pressure compensated and a relatively conservative switching strategy as done in [77]. Analysis of the time-dependent flow losses revealed significant loses occurring during the valve switchings and in this case the switching time should be below approximately 5% of the revolution time and the valve pressure drop at the peak flow rate should be below approximately 0.5% of the machine pressure span (for 350 bar). The analysis was modified to consider seat/poppet valves by including a pressure drop dependent term representing the flow forces acting on the valve member. Furthermore, another switching strategy was deployed leading to the valve switchings being performed as closely to the dead centers as possible. With these modifications, the flow losses during valve switching are much smaller leading to much less strict requirements for the valve switching time for achieving high-efficient operation. For all full stroke cases, the valve pressure drop should be below 0.5% of the machine pressure span for achieving efficiencies of 99% and 96% at 100% and 20% displacement, respectively. The valve requirements were also investigated for partial displacement strokes. In this case, valve switchings are carried out at much larger flow rates leading to increased losses and stricter requirements for the switching time and valve pressure drop, especially if not using seat/poppet valves.

A model based optimization method was proposed for deriving optimal actuator/valve designs for DDMs. The fundamental idea of the method is to use static FEA for evaluation of steady-state characteristics from which parameters are extracted to be used in a lumped model of a single DD chamber. This enables accurately representing the influence of changes in the geometry while also assessing the in-situ performance and losses. The method was applied for developing a MCA and a MMA prototype valve which both have been tested in DD operation, proven the optimization method capable of deriving valve and actuator designs leading to high-efficient DD operation.

The prototype valves have been rigorously tested to verify the simulated valve performance and to establish proof-of-concept for the proposed valve concepts. The comparison showed that the models generally are predicting the behavior with satisfying accuracy. The MCA valve has a typical switching time of 3 ms, the MMA valve is slightly slower with a switching time ranging between approximately 4-6 ms depending on the flow rate across the valve during closing. The pressure drop was for the MCA valve measured to be +0.18/-0.48 bar at 120 l/min, dependent on the direction of the flow. The measured pressure drop of the MCA is +0.11/-0.31 bar at +142/-108 l/min. Furthermore, a custom test-rig has been designed and built for testing prototype valves in DD operation. Currently, the maximum operating conditions tested is 100 bar machine pressure difference and 800 RPM. Under these conditions, both the MCA valve and the MMA valve were shown to be fully functional with electrical losses in the region of 40 W corresponding to 0.7% of the average machine power transfer. Further, based on measured flow vs. pressure characteristics the valve flow losses during operation were estimated to be 4-24 W, dependent on the valve and operation mode, corresponding to 0.07-0.38% of the average power. These losses are indeed considered sufficiently low for high-efficient DDM operating at high-speeds. It should be noted that the valves are designed for operating with 350 bar machine pressure difference leading to an increase in the power by a factor of 3.5 and a corresponding decrease of the relative valve and actuator losses as they are close to independent of the machine pressure span.

Finally, methods for indirectly estimating the valve movement and actuator parameters of the MCA based valves in DDMs have been proposed in Paper **E** & **F**. The methods are based on measuring the coil actuator and current. The methods have been tested using experimental data demonstrating that the proposed methods are capable of estimating the valve movement relatively accurate.

Future Work

The prototype valves are still to be tested at higher pressures to ensure they perform as expected. Also, long term testing of the valves in DD operation is needed to determine and improve the reliability of the designs. Especially the moving coil actuator still exhibit weak points prone to failure when subjected to a large number of switching cycles.

Besides this, additional controllability and observability is to be built into the test rig. An imminent objective is an on-line implementation of the disturbance based observer method with the proposed parameter tracking scheme studied in Paper **F**. The estimated plunger movement is to be used for controlling the velocity of the moving valve member during the closing of the valve. The idea is to control the valve velocity so that the chamber displacement rate at the instants of valve closing is zero, leading to zero valve flow during closing. This results in very low flow switching losses and enhances the repeatability of the valve closings since fluid-induced forces are reduced.

References

[1] Artemis Intelligent Power Ltd., "Digital displacement hydraulic hybrid demonstration," 2008, www.youtube.com/watch?v=UYbilBl3GGo, accessed 2017-09-12.

[2] ——, "Products - Industrial Hydraulic Pump," April 2015, www.artemisip.com/products, accessed 2017-08-31.

[3] ——, "Digital displacement hybrid excavator - update," 2016, www.artemisip.com/digital-displacement-hybrid-excavator, accessed 2017-08-31.

[4] ——, "Edinburgh technology duo secure £2.5 million to turn wave power into electricity," 2017, www.artemisip.com/edinburgh-technology-duo-secure-2-5-million-turn-wave-power-electricity/, accessed 2017-08-31.

[5] ——, "Machinies & applications," 2017, www.artemisip.com/wp-content/uploads/2016/03/Machines-and-Applications-2015-04-03.pdf, accessed 2017-08-31.

[6] M. A. Batdorff, "Transient analysis of electromagnets with emphasis on solid components, eddy currents, and driving circuitry," Ph.D. dissertation, Purdue University, 2010.

[7] M. M. Bech, C. Noergaard, and S. Kukkonen, "A global multi-objective optimization tool for optimal design of digital fluid power components," in *Proc. of The 42nd Annual Conference of IEEE Industrial Electronics Society*. Florence, Italy: Institute of Electrical and Electronics Engineers, 2016.

[8] N. C. Bender, C. Noergaard, and H. C. Pedersen, "Experimental validation of flow force models for fast switching valves," in *Proc. of The ASME/Bath Symp. on Fluid Power and Motion Control*. Sarasota, FL: American Society of Mechanical Engineers, 2017.

[9] N. C. Bender, H. C. Pedersen, A. Plöckinger, and B. Winkler, "Reliabillity analysis of a hydraulic on/off fast switching valve," in *Proc. of The Ninth Workshop on Digital Fluid Power*, Aalborg, Denmark, 2017.

[10] Bosch Rexroth Group, "3/3, 4/2 and 4/3 directional poppet valve with solenoid actuation, type SEC," Data sheet.

[11] ——, "Directional spool valves, direct operated, with solenoid actuation, fast switching, type WES," Data sheet.

[12] J. R. Brauer, *Magnetic actuators and sensors*. John Wiley and Sons, 2006.

[13] J. R. Brauer and Q. Chen, "Alternative dynamic electromechanical models of magnetic actuators containing eddy currents," *IEEE Transactions on Magnetics*, vol. 36, no. 4, pp. 1333–1336, 2000.

[14] E. Brooks, "Eddy current inductive drive electromechanical linear actuator and switching arrangement," Nov. 30 2006, WO Patent App. PCT/US2006/019779.

[15] Cargine Engineering AB, "Actuator," Dec. 27 2011, US Patent no. US9,347,466 B2.

[16] R. E. Clark, G. W. Jewell, S. J. Forrest, J. Rens, and C. Maerky, "Design features for enhancing the performance of electromagnetic valve actuation systems," *IEEE Transactions on Magnetics*, vol. 41, no. 3, pp. 1163–1168, March 2005.

[17] M. Ehsan, W. Rampen, and S. Salter, "Modeling of digital-displacement pump-motors and their application as hydraulic drives for nonuniform loads," *Journal of Dynamic Systems, Measurement and Control*, vol. 122, no. 1, pp. 210–215, April 2000.

[18] M. Foster, "World's largest floating turbine installed at Fukushima," Wind Power Offshore, January 2015, `www.windpoweroffshore.com/article/1358221/worlds-largest-floating-turbine-installed-fukushima`, accessed 2017-08-31.

[19] FreeValve, "Qoros debuts driveable freevalve qamfree engine at 2016 Guangzhou motor show," 2016, press release, `www.freevalve.com/category/news/`, accessed 2017-09-15.

[20] M. Heikkilä and M. Linjama, "Hydraulic energy recovery in displacement controlled digital hydraulic system," in *Proc. of The 13th Scandinavian International Conference on Fluid Power*, Linköbing , Sweden, 2013, pp. 513–519.

[21] M. Heikkilä, J. Tammisto, M. Huova, K. Huhtala, and M. Linjama, "Experimental evaluation of a digital hydraulic power management system," in *Proc. of The Third Workshop on Digital Fluid Power*, Tampere, Finland, 2010.

[22] ——, "Experimental evaluation of a piston-type digital pump-motor-transformer with two independent outlets," in *Proc. of The ASME/Bath Symp. on Fluid Power and Motion Control*, Bath, UK, 2010, pp. 83–97.

[23] M. Heikkilä, J. Tammisto, and M. Linjama, "Digital hydraulic power management system - measured characteristics of a second prototype," in *Proc. of The Eighth Workshop on Digital Fluid Power*, Tampere, Finland, 2016, pp. 69–81.

[24] T. Helmus, F. Breidi, and J. Lumkes, Jr., "Simulation of a variable displacement mechanically actuated digital pump unit," in *Proc. of The Eighth workshop on digital fluid power*, Tampere, Finland, 2016, pp. 95–105.

[25] D. B. Hiemstra, G. Parmar, and S. Awtar, "Performance tradeoffs posed by moving magnet actuators in flexure-based nanopositioning," *IEEE/ASME Transactions on Mechatronics*, vol. 19, no. 1, pp. 201–212, Feb 2014.

[26] M. A. Holland, "Design of digital pump/motors and experimental validation of operating strategies," Ph.D. dissertation, Purdue University, 2012.

[27] M. A. Holland, G. Wilfong, K. J. Merrill, and J. Lumkes, Jr., "Experimental evaluation of digital pump/motor operating strategies with a single-piston pump/motor," in *Proc. of The 52nd National Conference on Fluid Power*, Las Vegas, US, 2011.

[28] P. Johansen, D. B. Roemer, T. O. Andersen, and H. C. Pedersen, "Morphological topology generation of a digital fluid power displacement unit using chebychev-grübler-kutzbach constraint," in *Proc. of The 2015 International Conference on Fluid Power and Mechatronics*, Aug 2015, pp. 227–230.

[29] P. Johansen, "Tribodynamic modeling of digital fluid power motors," Ph.D. dissertation, Aalborg University, 2014.

[30] P. Johansen, D. B. Roemer, H. C. Pedersen, and T. O. Andersen, "Asymptotic approximation of laminar lubrication thermal field at low reduced Peclet and Brinkman number," *ASME Journal of Tribology*, vol. 136, no. 4, October 2014.

[31] B. Johnson, S. Massey, and O. Sturman, "Sturman digital latching valves," in *Proc. of The Seventh Scandinavian International Conference on Fluid Power*, vol. 3, Linköping, Sweden, 2001, pp. 299–314.

[32] M. Karvonen, "Energy efficient digital hydraulic power management of a multi actuator system," Ph.D. dissertation, Tampere University of Technology, May 2016.

[33] M. Ketonen and M. Linjama, "High flowrate digital hydraulic valve system," in *Proc. of The Ninth Workshop on Digital Fluid Power*, Aalborg, Denmark, 2017.

[34] S. Kim and H. Murrenhoff, "Measurement of effective bulk modulus for hydraulic oil at low pressure," *Journals of Fluids Engineering*, vol. 134, pp. 1–10, 2012.

[35] S. Kukkonen, "Generalized differential evolution for global multi-objective optimization with constraints," Ph.D. dissertation, Lappeenranta University of Technology, 2012.

[36] O. Kuttler, S. Laird, and L. Wadsley, "Fluid distribution valve," May 19 2010, EP Patent App. EP20,080,020,083.

[37] LaunchPoint Technologies, "Electromechanical valve actuator for variable valve timing," 2014, `www.launchpnt.com/portfolio/transportation/electromechanical-valve-actuator`, accessed 2017-08-24.

[38] T. Lauttamus, M. Linjama, M. Nurmia, and M. Vilenius, "A novel seat valve with reduced axial forces," in *Proc. of The Power Transmission And Motion Control Symp.*, Bath, UK, 2007, pp. 415–427.

[39] B. Lequesne, "Fast-acting long-stroke bistable solenoids with moving permanent magnets," *IEEE Transactions on Industry Applications*, vol. 26, no. 3, pp. 401–407, May 1990.

[40] L. Li, J. Tao, Y. Wang, Y. Su, and M. Xiao, "Effects of intake valve closing timing on gasoline engine performance and emissions," *SAE International Fall Fuels & Lubricants*, 2001.

[41] W. Li, L. Xin-hui, W. Xin, C. Jin-shi, and L. Yi-jie, "Shifting strategy of digital hydraulic transmission system for wheel loader," *Journal of Jilin University (Engineering Edition)*, vol. 47, no. 3, p. 819, 2017.

[42] Y. Licheng, S. Guanglin, and L. Hongqing, "Study of the sucking and discharging process of axial piston pump with digital distribution mechanism under random low speed input," in *Proc. of The Ninth Workshop on Digital Fluid Power*, Aalborg, Denmark, 2017.

[43] P. Lindholdt and H. B. Larsen, "Digital distributor valves in low speed motors - practical approach," in *Proc. of The Ninth Workshop on Digital Fluid Power*, Aalborg, Denmark, 2017.

[44] M. Linjama, "Digital hydraulic power management system - towards lossless hydraulics," in *Proc. of The Third Workshop on Digital Fluid Power*, Tampere, Finland, 2010.

[45] ——, "Digital fluid power - state of the art," in *Proc. of The Twelfth Scandinavian International Conference on Fluid Power*, Tampere, Finland, 2011.

[46] M. Linjama and K. Huhtala, "Digital pump-motor with independent outlets," in *Proc. of The 11th Scandinavian International Conference on Fluid Power*, Linköbing , Sweden, 2009.

[47] M. Linjama, M. Paloniitty, L. Tiainen, and K. Huhtala, "Mechatronic design of digital hydraulic micro valve package," in *Proc. of The 2ndnd International Conference of Dynamics and Vibroacoustics of Machines*, Samara, Russia, September 2014.

[48] M. Linjama and M. Vilenius, "Digital hydraulics – towards perfect valve technology," *VENTIL*, vol. 2, pp. 138–148, April 2008.

[49] L. Liu and S. Chang, "A moving coil electromagnetic valve actuator for camless engines," in *Proc. of The 2009 International Conference on Mechatronics and Automation*, 2009, pp. 176–180.

[50] E. L. Madsen, J. M. Joergensen, C. Noergaard, and M. M. Bech, "Design optimization of moving magnet actuated valves for digital displacement machines," in *Proc. of The ASME/Bath Symp. on Fluid Power and Motion Control, Sarasota, FL, US*, 2017.

[51] I. D. Mayergoyz, *Nonlinear Diffusion of Electromagnetic Fields*. Academic Press, 1998.

[52] K. Merrill, M. Holland, M. Batdorff, and J. Lumkes, Jr., "Comparative study of digital hydraulics and digital electronics," *International Journal of Fluid Power*, vol. 11, no. 3, pp. 45–51, 2010.

[53] K. J. Merrill, "Modeling and analysis of active valve control of a digital pump-motor," Ph.D. dissertation, Purdue University, 2012.

[54] K. J. Merrill, M. A. Holland, and J. Lumkes, Jr., "Efficiency analysis of a digital pump/motor as compared to a valve plate design," in *Proc. of The 7th International Fluid Power Conference*, Aachen, Germany, 2010.

[55] K. J. Merrill and J. Lumkes, Jr., "Operating strategies and valve requirements for digital pumps/motors," in *Proc. of The 6th Fluid Power Net International Ph.D. Symp. on Fluid Power*, West Lafayette, US, June 2010, pp. 249–258.

[56] Mitsubishi Heavy Industries, "MHI acquires Artemis Intelligent Power, a UK venture company," 2010, url:www.mhi.com/news/story/1012031389.html, accessed 2017-08-31.

[57] ——, "Ceremony held to mark the launch of verification testing of world's first digital hydraulic drive train for offshore wind turbines at Hunterston test centre in the UK," 2015, press information, `www.mhi.com/news/story/1502051871.html`, accessed 2017-09-18.

[58] ——, "MHI hydraulic driven 7MW offshore wind turbine," December, 2016, `https://www.youtube.com/watch?v=ydupJZm_NzU&t=`, accessed 2017-08-31.

[59] L. Nascutiu, "Voice coil actuator for hydraulic servo valves with high transient performances," in *In proc. of The 2006 IEEE International Conference on Automation, Quality and Testing, Robotics*, vol. 1, Technical University of Cluj-Napoca, Romania, May 2006, pp. 185–190.

[60] T. Noguchi, H. Hirano, S. Kawabata, M. Shimizu, T. Hayashi, U. Stein, G. Voller, and W. Rampen, "Poppet valve, hydraulic machine, and power generating apparatus of renewable-energy type," Dec. 21 2016, EP Patent App. EP20,150,197,211.

[61] S. Nordaas, T. O. Andersen, and M. K. Ebbesen, "Feasibility study of a digital hydraulic winch drive system," in *Proc. of The Ninth Workshop on Digital Fluid Power*, Aalborg, Denmark, 2017.

[62] ——, "The potential of a digital hydraulic winch drive system," in *Proc. of The Ninth Workshop on Digital Fluid Power*, Aalborg, Denmark, 2017.

[63] B. Paden, O. Fiske, M. Ricci, M. Okcuoglu, D. Paden, and B. Paden, "Electromagnetic valve apparatus with nonlinear spring," Dec. 27 2013, WO Patent App. PCT/US2013/022,080.

[64] Parker Hannifin Corporation, "Direct operated proportional DC valves series D1FP," Data sheet.

[65] C. R. Paul, *Electromagnetics for Engineers with Applications*. John Wiley and Sons, 2004.

[66] N. H. Pedersen, P. Johansen, and T. O. Andersen, "Non-linear hybrid control oriented modelling of a digital displacement machine," in *Proc. of The Ninth workshop on digital fluid power*, Aalborg, Denmark, 2017.

[67] J. Quilter, "Mitsubishi to unveil 7 MW offshore turbine," November 2011, wind Power Monthly, `www.windpowermonthly.com/article/1106330/mitsubishi-unveil-7mw-offshore-turbine`, accessed 2017-09-11.

[68] Quoceant Ltd., "Quoceant partner with Artemis Intelligent Power in innovative project to provide improved power take-off for the marine energy industry," 2015, `www.quoceant.com/single-post/2015/07/31/Quoceant-partner-with-Artemis-Intelligent-Power-in-innovative-project-to-provide-improved-Power-TakeOff-for-the-marine-energy-industry`, accessed 2017-08-31.

[69] W. Rampen, "The development of digital displacement technology," in *Proc. of The ASME/Bath Symp. on Fluid Power & Motion Control*, Bath, UK, 2010, pp. 12–17, keynote adress.

[70] M. B. Rannow, P. Y. Li, and T. R. Chase, "Discrete piston pump/motor using a mechanical rotary valve control mechanism," in *Proc. of The Eighth workshop on digital fluid power*, Tampere, Finland, 2016, pp. 83–94.

[71] M. Resch and R. Scheidl, "A model for fluid stiction of quickly separating circular plates," *Proc. of The Institution of Mechanical Engineers, Part C: Journal of Mechanical Engineering Science*, vol. 228, no. 9, pp. 1540–1556, 2014.

[72] D. B. Roemer, "Design and optimization of fast switching valves for large scale digital hydraulic motors," Ph.D. dissertation, Department of Energy Technology, Aalborg University, 2014.

[73] D. B. Roemer and P. Johansen, "Design of a high efficiency valve for use in a digital displacement hydraulic pump," Master's thesis, Aalborg University, 2011, masters thesis, Aalborg University.

[74] D. B. Roemer, P. Johansen, L. Schmidt, and T. O. Andersen, "Modeling of movement-induced and flow-induced fluid forces in fast switching valves," in *Proc. of 2015 International Conference on Fluid Power and Mechatronics*, Harbin, China, August 2015, pp. 978–983.

[75] D. B. Roemer, C. Noergaard, M. M. Bech, and P. Johansen, "Valve and manifold considerations for digital hydraulic machines," in *Proc. of The 8th Workshop on Digital Fluid Power*, Tampere, Finland, May 2016, pp. 213–227.

[76] D. B. Roemer, P. Johansen, M. M. Bech, and H. C. Pedersen, *Simulation and Experimental Testing of an Actuator for a Fast Switching On-Off Valve Suitable to Efficient Displacement Machines*. Japan Fluid Power System Society, 2014.

[77] D. B. Roemer, P. Johansen, H. C. Pedersen, and T. O. Andersen, "Analysis of valve requirements for high-efficiency digital displacement fluid power motors," in *Proc. of The 8th International Conference on Fluid Power Transmission and Control*, Hangzhou, China, 2013, pp. 122–126.

[78] ——, "Method for lumped parameter simulation of digital displacement pumps/motors based on CFD," *Applied Mechanics and Materials*, vol. 397-400, pp. 615–620, 2013.

[79] ——, "Topology selection and analysis of actuator for seat valves suitable for use in digital displacement pumps/motors," in *Proc. of The 2013 IEEE International Conference on Mechatronics and Automation (ICMA)*. IEEE Press, 2013, pp. 418–424.

[80] RSSB, "RSSB funds powertrain demonstrator," January 2017, `www.rssb.co.uk/industry-news/rssb-funds-powertrain-demonstrator`, accessed 2017-09-22.

[81] S. H. Salter and M. Rea, "Hydraulics for wind," in *Proc. of The European Wind Energy Conference*, Hamburg, Germany, October 1984, pp. 534–541.

[82] M. Sasaki, A. Yuge, T. Hayashi, H. Nishino, M. Uchida, and T. Noguchi, "Large capacity hydrostatic transmission with variable displacement," in *Proc. of The 9th International Fluid Power Conference*, Aachen, Germany, March 2014.

[83] R. Scheidl, C. Gradl, and A. Plöckinger, "The cushioning groove for solenoid switching valves – concept and theoretical analysis," *International Journal of Fluid Power System*, vol. 8, no. 2, pp. 76–81, 2014.

[84] R. Scheidl, B. Manhartsgruber, G. Mikota, and B. Winkler, "State of the art in hydraulic switching control - components, systems, applications," in *Proc. Ninth Scandinavian International Conference on Fluid Power*, Linköping, Sweden, 6 2005.

[85] U. Stein, "Fluid-working machine," Jun. 24 2014, US Patent App. US12/440,371.

[86] R. Storn and K. Price, "Differential Evolution - A simple and efficient adaptive scheme for global optimization over continuous spaces," Berkeley, Cambridge, MA, Tech. report 1, May 1995.

[87] Sun Hydraulics, "2-way, direct-acting, solenoid-operated directional poppet valve," Data sheet, `www.sunhydraulics.com/model/DTDA`, accessed 2017-08-31.

[88] J. Tammisto, M. Huova, M. Heikkilä, M. Linjama, and K. Huhtala, "Measured characteristics of an in-line pump with independently controlled pistons," in *Proc. of The 7th International Fluid Power Conference*, Aachen, Germany, 2010, pp. 1–12.

[89] J. Taylor, W. Rampen, D. Abrahams, and A. Latham, "Demonstration of a digital displacement hydraulic hybrid - a globally affordable way of saving fuel," in *Proc. of The Annual JSAE Congress*, Pacifico Yokohama, Japan, 2015.

[90] J. Taylor, W. Rampen, A. Robertson, and N. Caldwell, "Digital displacement hydraulic hybrids - parallel hybrid drives for commercial vehicles," Artemis Intelligent Power Ltd., Paper presented at the annual JSAE congress, Kyoto, Japan, Tech. Rep., 2011.

[91] H. Tian, P. Y. Li, and J. D. V. de Ven, "Using an angle domain repetitive control to achieve variable valve timing for a digital displacement hydraulic motor," in *Proc. of The Ninth workshop on digital fluid power*, Aalborg, Denmark, 2017.

[92] M. Umaya, T. Noguchi, M. Uchida, M. Shibata, Y. Kawai, and R. Notomi, "Wind power generation - development status of offshore wind turbines," Mitsubishi Heavy Industries, Technical Review, 2013, vol. 50, no. 3.

[93] J.-P. Uusitalo, "A novel digital hydraulic valve package: a fast and small multi-physics design," Ph.D. dissertation, Tampere University of Technology, 2010.

[94] J.-P. Uusitalo, V. Ahola, L. Soederlund, M. Linjama, M. Juhola, and L. Kettunen, "Novel bistable hammer valve for digital hydraulics," *International Journal of Fluid Power*, vol. 11, no. 3, pp. 35–44, 2010.

[95] L. Wadsley, "Optimal system solutions enabled by digital pumps," in *Proc. of The 52nd National Conference on Fluid Power*, Las Vegas, US, March 2011.

[96] J. A. Wagner, "The shorted turn in the linear actuator of a high performance disk drive," *IEEE Transactions on Magnetics*, vol. 18, no. 6, pp. 1770–1772, 1982.

[97] ——, "The actuator in high performance disk drives: Design rules for minimum access time," *IEEE Transactions on Magnetics*, vol. 19, pp. 1686–1688, 1983.

[98] Wave Energy Scotland, "Wave Energy Scotland awards £7.5m for power take off projects," 2017, `www.waveenergyscotland.co.uk/news-events/`

wave-energy-scotland-awards-75m-for-power-take-off-projects, accessed 2017-08-31.

[99] G. Wilfong, M. A. Holland, and J. Lumkes, Jr., "Design and analysis of pilot operated high speed on/off valves for digital pump/motors," in *Proc. of The 52nd National Conference on Fluid Power*, Las Vegas, US, 2011.

[100] B. Winkler, A. Plöckinger, and R. Scheidl, "A novel piloted fast switching multi poppet valve," *International Journal of Fluid Power*, vol. 11, no. 3, pp. 7–14, November 2010.

[101] B. Winkler and R. Scheidl, "Development of a fast seat type switching valve for big flow rates," in *Proc. of The Tenth Scandinavian International Conference on Fluid Power*, vol. 2, May 2007, pp. 137–146.

[102] B. Winkler, "Recent advances in digital hydraulic components and applications," in *Proc. of The Ninth Workshop on Digital Fluid Power*, Aalborg, Denmark, 2017.

[103] T. Zehetbauer, P. Foschum, A. Plöckinger, and B. Winkler, "Advancement and demonstration of the new generation of LCM's FSVi4.1," in *Proc. of The Ninth Workshop on Digital Fluid Power*, Aalborg, Denmark, 2017.

Part II

Papers

ISSN (online): 2446-1636
ISBN (online): 978-87-7210-090-6

AALBORG UNIVERSITY PRESS